

FINAL REPORT
SPACE SHUTTLE SRM INTERIM CONTRACT

28 June 1974

By

THIOKOL/WASATCH DIVISION
A Division of Thiokol Corporation
P.O. Box 524, Brigham City, Utah 84302

Prepared For

NATIONAL AERONAUTICS AND SPACE ADMINISTRATION

George C. Marshall Space Flight Center

Contract NAS8-30754

(NASA-CR-120404)	SPACE SHUTTLE SRM	N74-32296
INTERIM CONTRACT, PART 1	Final Report	
(Thiokol Chemical Corp.)	149 p HC	
\$10.50	CSCI 22B	Unclas
	G3/31	46910

CONTENTS

	<u>Page</u>
1.0 INTRODUCTION AND SUMMARY	1
2.0 DESIGN REQUIREMENTS	5
3.0 SRM PRELIMINARY DESIGNS	19
3.1 Motor Performance	19
3.1.1 Preliminary Design Data for Space Shuttle SRM	
Configuration 1 Model TU772/40A	26
3.1.1.1 Basic Motor Description	26
3.1.1.2 Performance	27
3.1.2 Preliminary Design Data for Space Shuttle SRM	
Configuration 1-1 Model TU772/42C	33
3.1.2.1 Basic Motor Description	33
3.1.2.2 Performance	39
3.1.3 Preliminary Design Data for Space Shuttle SRM	
Configuration 1-1A Model TU772/42D	39
3.1.3.1 Basic Motor Description	39
3.1.3.2 Performance	42
3.2 Case and Structural Analysis	48
3.2.1 Case	48
3.2.1.1 Case Wall Thickness Calculation	50
3.2.1.2 Grit Blast	51
3.2.1.3 Analytical Procedure	51
3.2.1.4 Skirt Attachment Joints	55
3.2.1.5 Aft ET Attach Ring	59
3.2.1.6 Water Impact	62
3.2.1.7 Slapdown	70
3.2.1.8 Cavity Collapse	70
3.2.1.9 Penetration	78
3.2.1.10 Aft Dome	78
3.2.1.11 Nozzle	81
3.2.1.12 Aft Peaking Loads	81
3.2.1.13 Forward Peaking Loads	91
3.3 Nozzle	93
3.3.1 Nozzle Material Selection	93
3.3.1.1 Mat Tape	101

CONTENTS (Cont)

	<u>Page</u>
3.3.1.2 Hybrid Tape	102
3.3.1.3 Molding Compound	102
3.3.2 Plastic Materials Safety Factor Interpretation.	117
3.3.3 Aft Skirt and Actuation System Interface.	123
3.3.4 Nozzle Field Joint	134
3.3.5 Nozzle Cutoff	136
3.4 Propellant	140
3.4.1 Crain Design	140
3.4.2 Motor Specific Impulse	147
3.4.3 Minimum Specific Impulse	152
3.5 Insulation and Liner	156
3.5.1 Case Internal Insulation Temperature Study	156
3.5.2 Aft Case Insulation Thickness	159
3.6 SRM Design Study.	160
4.0 VIBRATION AND ACOUSTIC DATA	180
5.0 LAUNCH SITE ASSEMBLY AND STACKUP TOLERANCE	182
6.0 SRM DDT&E Schedule	188

APPENDIX A

ILLUSTRATIONS

<u>Figure</u>		<u>Page</u>
2-1	Water Impact and SRM/ET Attach Requirements	6
2-2	SRM Requirements - Geometry.	9
2-3	SRM Requirements - Performance	10
2-4	Representative SRM Performance Data	12
2-5	Residual Force and SRM Thrust Shape Data, RI Case 370 . . .	14
2-6	Residual Force and SRM Thrust Shape Data, RI Case 371 . . .	15
2-7	Residual Force and SRM Thrust Shape Data, RI Case 372 . . .	16
2-8	Residual Force and SRM Thrust Shape Data, RI Case 373 . . .	17
3-1	Case Fabrication Constraints at 146 In. Diameter	21
3-2	Case Fabrication Constraints	24
3-3	Motor Layout, Configuration 1	28-29
3-4	Thrust Versus Time Configuration 1	34
3-5	Motor Layout, Configuration 1-1.	35-36
3-6	Thrust Versus Time Configuration 1-1.	41
3-7	Motor Layout, Configuration 1-1A.	43
3-8	Thrust Versus Time Configuration 1-1A	47
3-9	Weight Versus Pressure	53
3-10	Clevis Type Attachment Mechanism for Forward Skirt (SK50183)	56
3-11	Clevis Type Attachment Mechanism for Aft Skirt (SK50184)	57
3-12	Aft Attach Ring Frame Analysis (Configuration 1-1)	60
3-13	Aft Attach Ring Results of Discontinuity Analysis (Configuration 1-1)	61
3-14	ET Attach Ring - Liftoff Condition Plus 861 psi Internal Pressure (Configuration 1-1)	63

ILLUSTRATIONS (Cont)

<u>Figure</u>		<u>Page</u>
3-15	Combined Stress Distribution in SRM Case on the Meridian Containing Strut Load "P ₂ " (Configuration 1-1)	64
3-16	SRB Cavity Collapse - STAGS Analysis Results	66
3-17	Slapdown Results, t = 0.486	71
3-18	SRM Case Buckling Parameters (Slapdown $\theta = -10$ Deg)	72
3-19	BOSOR Slapdown Results	73
3-20	SRB Slapdown - STAGS Analysis Results	74
3-21	Cavity Collapse Summary	76
3-22	Cavity Collapse BOSOR 4 Results	77
3-23	Aft Dome Buckling Calculations Summary	82
3-24	Nozzle Analysis (Max Pitch, $\theta = 0$ Deg)	83
3-25	SRM Nozzle Buckling Analysis - Configuration 0 (Max Axial Acc, $\theta = -10$ Deg - Initial Undeformed Structure)	84
3-26	Nozzle Showing Char Line	85
3-27	SRM Case Aft Peaking Loads Analysis NASTRAN Model	89
3-28	Stress Distribution (psi) - Aft Peaking Loads (Ref: S & E-ASTN-AS (74-15))	90
3-29	Effect of Forward Peaking Loads (Configuration 1-1)	92
3-30	Baseline Low-Cost Nozzle - Configuration 0	95
3-31	SRM Nozzle - Configuration 1	96
3-32	SRM Nozzle - Configuration 1-1	97
3-33	SRM Nozzle - Configuration 1-1A	98
3-34	Small Motor Firings	107
3-35	Poseidon C3 First Stage Low-Cost Nozzle (Tested 5 July 1973)	110
3-36	Low-Cost Materials Test Performance Comparison	112

ILLUSTRATIONS (Cont)

<u>Figure</u>		<u>Page</u>
3-37	Material Matrix Subscale (C3 Size) Motor Tests	114
3-38	Development Schedule	115
3-39	Plastic Material Safety Factor Interpretation	118
3-40	Baseline Low-Cost Nozzle	119
3-41	Revised Baseline Design Low-Cost Materials - NASA Safety Factors	120
3-42	Baseline Design High-Cost Materials - NASA Safety Factors	122
3-43	Submergence Comparison	126
3-44	Field Joint	135
3-45	Nozzle Cutoff Device.	137
3-46	Penetration and Cut by RDX Core Copper Sheath LSC	138
3-47	SRM Requirements - Performance	141
3-48	Comparison of Surface-Web Histories	142
3-49	Vacuum Thrust Versus Time	144
3-50	Grain Configuration (TC-526-04-01A)	145
3-51	Grain Configuration (TC-526-04-01B)	146
3-52	11-Point Star Geometry.	149
3-53	Comparison of Vacuum-Thrust Time Performance.	150
3-54	Delivered Specific Impulse Versus Nozzle Length-to- Throat Radius Ratio	153
3-55	SRB Water Entry at Splashdown (Case Insulation 1.5 In. Thick Exposed 80 Seconds)	157
3-56	Design and Optimization Program	162
3-57	Case Segment Configuration*	170
3-58	Case Fabrication Constraints	171

ILLUSTRATIONS (Cont)

<u>Figure</u>		<u>Page</u>
3-59	Comparison of Propellant Loading in Three Aft Closure Designs for Configuration 1	173
3-60	Delivered Specific Impulse Versus Nozzle Length-to-Throat Radius Ratio	174
3-61	Maximum G^* as a Function of Increased Propellant (ΔW_p) Configuration 1	175
5-1	Total Offset From True Centerline	183
5-2	Maximum Offset Due to Angularity Variation Between Segments	184
5-3	Rotational Maximum Misalignment	186
6-1	Preliminary Schedule E	189

TABLES

<u>Table</u>		<u>Page</u>
I	Dimensional, Weight, and Performance Data	3
II	Comparison of SRM Designs Generated by RI and TC	18
III	Summary of Motor Dimensions (Configuration 1)	30
IV	Weight and Center of Gravity Summary (Configuration 1). . . .	31
V	Nozzle Characteristics and Design Criteria (Configuration 1)	32
VI	Summary of Motor Dimensions (Configuration 1-1)	37
VII	Weight and Center of Gravity Summary (Configuration 1-1) . .	38
VIII	Nozzle Characteristics and Design Criteria (Configuration 1-1)	40
IX	Summary of Motor Dimensions (Configuration 1-1A).	44
X	Weight and Center of Gravity Summary (Configuration 1-1A). .	45
XI	Nozzle Characteristics and Design Criteria (Configuration 1-1A)	46
XII	SRM Buckling Summary - Water Impact Loads	65
XIII	Slapdown BOSOR Summary Sheet	75
XIV	Cavity Collapse BOSOR Summary Sheet	79
XV	Penetration BOSOR Summary Sheet	80
XVI	Nozzle Buckling Analysis	86
XVII	Nozzle Summary Data	94
XVIII	Actuator Torque Summary	99
XIX	Material Properties From Thiokol Laboratory Tests	109
XX	Submergence Comparison	125
XXI	Results From RI Analysis of SRM Designs	148
XXII	Specific Impulse Losses	151
XXIII	Performance Interchange Summary	155

TABLES (Cont)

<u>Table</u>		<u>Page</u>
XXIV	Summary	165
XXV	Impact of Design Changes From Configuration 0 to 1	167
XXVI	Mass Properties Summary (Weight-Lb)	168
XXVII	Case Weight Change Due to Water Impact and Revised SRM/ET Attachment	169
XXVIII	SRM Configuration Comparisons	176
XXIX	SRM Configuration Comparisons	177
XXX	Angular Offset	187

1.0 INTRODUCTION AND SUMMARY

This report summarizes results of the Space Shuttle Solid Rocket Motor (SRM) Interim Contract, NAS8-30754, and is submitted in response to Section 3.3 of Contract Exhibit A.

The SRM Interim Contract was awarded to Thiokol on 14 February 1974 for the purpose of conducting essential studies and analyses required to integrate the SRM into the booster and overall Space Shuttle system. Emphasis was placed on the case, nozzle, insulation, and propellant components with resulting performance, weight, and structural load characteristics being generated. The initial award was for a 90-day period. A subsequent extension of 45 days carried the contract period through 28 June 1974.

Effort conducted during the time period of this contract included studies, analyses, planning, and preliminary design activities. Technical requirements identified in the SRM Project Request for Proposal No. 8-1-4-94-98401 (Volumes I and II) and Thiokol's proposed SRM design (designated Configuration 0) established the basis for this effort. The requirements were evaluated jointly with MSFC and altered where necessary to incorporate new information that evolved after issuance of the RFP and during the course of this interim contract. Revised water impact loads and load distributions were provided based on additional model test data and analytical effort conducted by NASA subsequent to the RFP release. Launch pad peaking loads into the SRM aft skirt were provided which also represented a change from RFP requirements. A modified SRM/External Tank (ET) attachment configuration with new structural load data was supplied by NASA, and direction was received to include a 2 percent inert weight contingency.

Impact of these changes on the SRM design were evaluated by developing preliminary SRM designs optimized for low cost. Adjustments were made in some of the RFP performance partials in order to more closely approximate the flight performance desired from the SRM. Effort was also initiated to utilize SRM residual thrust versus time as performance criteria for sizing the SRM. These criteria are

provided from simulated computer flight trajectories. These changes in performance criteria were brought about primarily by significant changes in water impact loads, launch pad loads, and the inclusion of an inert weight contingency. Considerable effort was expended evaluating the SRM case and nozzle structure in relation to the revised water impact and launch pad loads. Calculations using BOSOR, NASTRAN, and STAGS (in conjunction with MSFC personnel) were conducted to determine optimum combinations of material thickness and stiffener requirements to react the imposed loads. Modifications to Thiokol's SRM automated design program (ADP) were made to account for increased structure to react the greater loads and the inclusion of an inert weight contingency.

Motor parameters such as maximum expected operating pressure (MEOP), nozzle expansion ratio, and nozzle length-to-throat radius ratio (L/R_t) were varied to assess the impact such changes had on motor sizing and cost. Cost optimization studies were conducted in which many motor parameters were allowed to vary simultaneously in order to determine the minimum SRM project cost.

Two 146-in. diameter SRM configurations evolved which provide capability to withstand the latest water impact and launch pad loads while providing approximately 660 pounds payload margin (Configuration 1) and 1,900 pounds payload margin (Configuration 1-1). Table I summarizes dimensional, weight, and performance data for these two configurations.

During the design study a third SRM design was generated which maximized the payload margin within the dimensional constraints established for Configuration 1-1. The approach used to generate this design was to use residual force versus time data developed from flight performance data rather than the RFP performance requirements. After reviewing several candidate designs, a configuration that minimized the total SRM weight while maximizing the potential payload margin was selected as a new SRM baseline. This design, Configuration 1-1A, provides a payload margin ranging from 3,000 to 4,000 pounds depending upon the shape of the thrust-time trace. The principal dimensional, weight and performance parameters for this configuration are also summarized on Table I.

TABLE I
DIMENSIONAL, WEIGHT, AND PERFORMANCE DATA

	<u>Configuration 1</u>	<u>Configuration 1-1</u>	<u>Configuration 1-1A</u>
Dome-to-Dome Case Length (in.)	1,352	1,378	1,378
Overall Motor Length (in.)	1,469	1,496	1,496
Total Inert Weight (lb)	134,200	137,800	144,560
Total Propellant Weight (lb)	1,072,300	1,090,400	1,102,000
Total Motor Weight (lb)	1,206,500	1,228,200	1,246,560
Nozzle Throat Diameter (in.)	56.6	57.3	54.4
Nozzle Expansion Ratio (initial)	6:1	6:1	7.16:1
Nozzle L/Rt (initial)	5	5	5.28
MEOP (psia)	865	876	952
Average Vacuum Specific Impulse (sec)	258.9	258.9	262.2
Total Vacuum Impulse (million lbf-sec)	277.62	282.31	288.9
Action Time (sec)	124	124	122.2
Payload Margin (provided by SRM) (lb)	660	1,890	3,000-4,000

This report is organized in six sections. Following Section I, Introduction and Summary, is Design Requirements, Section II. Details of the significant design requirement changes are provided. Section III, SRM Preliminary Designs, discusses the motor performance studies and contains subsections describing major SRM components including pertinent information generated during this contract.

Vibration and acoustic data are presented in Section IV and Appendix A. Section V contains information on the SRM stackup tolerance. SRM DDT&E schedules are presented and discussed in Section VI.

2.0 DESIGN REQUIREMENTS

Design requirements identified in Request for Proposal (RFP) 8-1-4-94-98401 were used as the basis for effort conducted during this interim contract. These basic requirements were modified to include test and analysis results available from NASA effort conducted subsequent to the RFP release and joint NASA/Thiokol effort conducted during this interim contract.

The more significant changes included water impact loads, launch pad loads, SRM/ET attach configuration and loads, inclusion of 2 percent inert weight contingency, fixed SRM diameter at 146 in., SRM length increase, and updated thrust/impulse criteria.

During the period from receipt of RFP through the end of the interim contract, there was a significant change in the loading requirements for the SRM. This load evolution was primarily a result of additional testing and analytical development by MSFC. Figure 2-1 presents a traceable summary of the design loads as they existed at four distinct time points:

1. At the time of the RFP (July 1973) when loads were defined in Volume II, Section V, Appendix H.
2. At the beginning of the interim contract when new loads were defined in loads document S & E-ASTN-ADL (73-68).
3. During the interim contract when certain load modifications and additions had been made by various means as outlined in figure 2-1.
4. At the end of the interim contract after revised water impact loads were introduced as shown in figure 2-1.

One of the most notable changes which occurred between the period from (1) → (3) above was the addition of a cavity collapse loading requirement. This condition, which was not covered in the RFP, imposes some very significant overpressures on the aft segments of the case. These pressures which are applied in

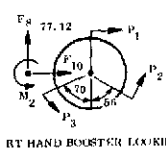
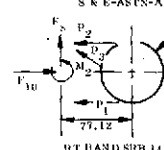
CRITERIA FOR SRM DESIGN	CONFIGURATION 0		CONFIGURATIONS 1, 1-1, AND 1-1A
DATE	RFP JULY 1973	14 FEB, START OF 99-DAY CONTRACT	30 APR 1974
LOADING EVENT	CONDITION LOAD	CONDITION LOAD	CONDITION LOAD
SLAPDOWN V_v = VERTICAL VELOCITY V_H = HORIZONTAL VELOCITY θ = ENTRY ANGLE T = TIME SEQUENCE P = PRESSURE ON SRM	$V_v = 80 \text{ FT/SEC}$ $V_H = 0$ $\theta = \text{UNDEFINED}$ $T = 2$ $P = f(\theta, Z)$ $P_{MAX} = 32 \text{ PSI}$ DISTRIBUTION PER: FIG'S 15 AND 16 APPEN II RFP 6-1-4-94-9410	$V_v = 100 \text{ FT/SEC}$ $V_H = 45 \text{ FT/SEC}$ $\theta = -10$ $T = 2.5$ $P = f(\theta, Z)$ $P_{MAX} = 36 \text{ PSI}$ DISTRIBUTION PER: FIGURE III-23 S & E-ASTN-ADL (73-68)	$V_v = 100 \text{ FT/SEC}$ $V_H = 45 \text{ FT/SEC}$ $\theta = -5^\circ$ $T = 1.5$ $P_{MAX} = 24.8$ $P = f(\theta, Z)$ DISTRIBUTION PER: FIGURE III-23 S & E-ASTN-ADL (73-68)
CAVITY COLLAPSE	NONE	$V_v = 100 \text{ FT/SEC}$ $V_H = 45 \text{ FT/SEC}$ $\theta = -10$ $P = f(\theta, Z)$ $P_{MAX} = 135 \text{ PSI}$ DISTRIBUTION PER: FIG III-10 S & E-ASTN-ADL (73-68)	$V_v = 100 \text{ FT/SEC}$ $V_H = 30 \text{ FT/SEC}$ $\theta = 5^\circ$ $P = f(\theta, Z)$ $P_{MAX} = 166 \text{ PSI}$ LOAD DISTRIBUTION PER: FIGURE 1A S & E-SRB (74-114)
PENETRATION h = PENETRATION DEPTH MEASURED FWD FROM AFT TAN POINT (TP) P = PRESSURE ON SRM	$V_v = 80 \text{ FT/SEC}$ $V_H = 0 \text{ FT/SEC}$ $\theta = 0$ $h_{MAX} = 636.1 \text{ IN.}$ $P = f(h)$ $P_{MAX} = 18.3 \text{ PSI AT TP}$ FIGURE 14 APPEN II RFP	$V_v = 100 \text{ FT/SEC}$ $V_H = 0 \text{ FT/SEC}$ $\theta = 0$ $h_{MAX} = 610.5 \text{ IN.}$ $P = f(h)$ $P_{MAX} = 22.2 \text{ PSI AT TP}$ (HYDROSTATIC PRESSURE)	← SAME
MAX AXIAL DECELERATION	$V_v = 80 \text{ FT/SEC}$ $V_H = 0 \text{ FT/SEC}$ $\theta = 0^\circ$ $P_1 = 66 \text{ PSI (NOZ)}$ $P_2 = 118 \text{ PSI (NOZ THROAT)}$ $P_3 = 72 \text{ PSI (SKIRT)}$ $P_4 = 54 \text{ PSI (DOME)}$ SEE FIG 5, APPEN II, RFP	$V_v = 100 \text{ FT/SEC}$ $V_H = 45 \text{ FT/SEC}$ $\theta = 10^\circ$ $P_1 = 260 \text{ PSI (DOME)}$ $P_2 = 170 \text{ PSI}$ $P_3 = 170 \text{ PSI}$ $P_4 = 116 \text{ PSI}$ SEE FIG III-10 S & E-ASTN-ADL (73-68)	$V_v = 100 \text{ FT/SEC}$ $V_H = 45 \text{ FT/SEC}$ $\theta = 5^\circ$ $P_1 = 253 \text{ PSI AFT CLOSURE}$ $P_2 = 160 \text{ PSI}$ $P_3 = 150 \text{ PSI}$ $P_4 = 113 \text{ PSI}$ SEE FIG III-10 S & E-ASTN-ADL (73-68)
MAX PITCH	$V_v = 80 \text{ FT/SEC}$ $V_H = 0 \text{ FT/SEC}$ $\theta = 0$ UNDEFIRED $(P = 0)$	$V_v = 100 \text{ FT/SEC}$ $V_H = 45 \text{ FT/SEC}$ $\theta = -10^\circ$ $P_1 = 68 \text{ PSI (AFT DOME)}$ $P_2 = 124 \text{ PSI}$ $P_3 = 5.1 \text{ PSI}$ $P_4 = 115 \text{ PSI}$ $P_5 = 100 \text{ PSI}$ $P_6 = 128 \text{ PSI}$ S & E-ASTN-ADL (73-68)	$V_v = 100 \text{ FT/SEC}$ $V_H = 45 \text{ FT/SEC}$ $\theta = 0$ $P_1 = 48 \text{ PSI (AFT DOME)}$ $P_2 = 112 \text{ PSI}$ $P_3 = 6.0 \text{ PSI}$ $P_4 = 148 \text{ PSI}$ $P_5 = 108 \text{ PSI}$ $P_6 = 150 \text{ PSI}$ S & E-ASTN-ADL (73-68)
AFT SKIRT PEAKING LOADS N_{MAX} = (MAX LIVE LOADS) M = BENDING MOMENT P = AXIAL LOAD - (COMPRESSIVE)	1 HR WINDS FROM ORBITER FUELED ET NO PAYLOAD (STATION 1000) $M = 3.25 \times 10^6 \text{ IN.-LB}$ $P = 1.54 \times 10^6 \text{ LB}$ NORMAL DISTRIBUTION NO PEAKING EFFECTS DEFINED SEE FIG 1-7 APPEN II, RFP	1 HR WINDS (20.9 KM/H) ORBITER SIDE FUELED ET $N_{MAX} = 5,000$ $N_{MAX} = 32,000 \text{ LB IN. (LIMIT)}$ S & E-ASTN-AS (74-15)	← SAME
FWD SKIRT PEAKING LOADS N_{MAX} = (MAX LIVE LOADS) - (COMPRESSIVE) + (TENSILE)	SUB MAX ACCELERATION (STATION = 500) $M = 118 \times 10^6 \text{ IN.-LB}$ $P = 2 \times 10^6 \text{ IN.-LB}$ NORMAL DISTRIBUTION NO PEAKING EFFECTS DEFINED TABLE 1-3 APPEN II, RFP	$N_{MAX} = 1,100$ $N_{MAX} = 26,100 \text{ LB IN. (ULTIMATE)}$ SUB MAX ACCELERATION DISTRIBUTION PER: S & E-ASTN-AS (74-15)	← SAME
ET ATTACH LOADS LOADS POSITIVE AS SHOWN	MAX SUB GIMBAL HQ BOOST $M_2 = 17.89 \times 10^6 \text{ IN.-LB}$ $F_8 = 307,300 \text{ LB}$ $F_{10} = -81,200 \text{ LB}$ $P_1 = 307,300 \text{ LB}$ $P_2 = 150,000 \text{ LB}$ $P_3 = 58,250 \text{ LB}$ TABLE 1-3 APPENDIX II, RFP 	LEFT QTY $M_2 = 21.4 \times 10^6 \text{ IN.-LB}$ $F_8 = 30,000 \text{ LB}$ $F_{10} = -72,500 \text{ LB}$ RIGHT QTY $M_2 = 11.2 \times 10^6 \text{ IN.-LB}$ $F_8 = 206,000 \text{ LB}$ $F_{10} = -88,000 \text{ LB}$ STOUT LOADS $P_1 = 171,040 \text{ LB}$ $P_2 = -237,000 \text{ LB}$ $P_3 = -20,865 \text{ LB}$ $P_1 = 75,160 \text{ LB}$ $P_2 = -102,000 \text{ LB}$ $P_3 = -214,800 \text{ LB}$ S & E-ASTN-ADL (73-74) 	← SAME ← SAME (15 APR, ADDITIONAL) ET LH2 PARTIAL FILL (S & E-ASTN-ASP 74-27) 1 DAY SIDE WIND A 0 LB $P_{MAX} = 88,521 \text{ LB (NO EFFECT)}$
*PRESSURES AS SHOWN DO NOT INCLUDE A 2 PSI ULLAGE PRESSURE WHICH WAS INCLUDED IN ALL ANALYSES			

Figure 2-1. Water Impact and SRM/ET Attach Requirements

a highly asymmetric manner present a design requirement which has significant impact on the case design.

Thiokol has identified the specific cavity collapse condition listed in figure 2-1 as the most dominant in terms of effect on the two aft cylindrical case segments.

The baseline slapdown design condition has changed from the RFP conditions of 80 ft/sec vertical velocity (V_V), and zero horizontal velocity (V_H), to $V_V = 100$ ft/sec and $V_H = 45$ ft/sec at the end of the interim contract. The entry angle (θ) also evolved from an undefined value in the RFP to -10° at the beginning of the interim contract and was subsequently reduced to -5° during the interim contract.

Configuration 0 which was evaluated under the terms of the RFP was adequate for the $V_V = 80$, $V_H = 0$ condition. As the slapdown loading conditions changed at the beginning of the interim contract, analytical investigations revealed that configuration 0 was not adequate for the new loads. During the interim contract, the entry angle design value was reduced from -10° to -5° as a result of further NASA probability studies. At this angle, all configurations considered (0, 1, 1-1, and 1-1A) were capable of withstanding slapdown loads without design modifications specifically incorporated to accommodate slapdown.

The baseline penetration conditions changed from $V_V = 80$ ft/sec, $V_H = 0$ to $V_V = 100$ ft/sec, $V_H = 0$ during the time between the RFP and the interim contract. However, this requirement is completely overpowered by the cavity collapse requirement and, consequently, is not a design driver.

Significant changes also occurred in the maximum acceleration condition pressure distributions in the aft skirt cavity between the RFP and the end of the interim contract. For instance, the maximum pressure on the aft dome increased from 54 psi to 253 psi as a result of the change. This pressure increase resulted in some relatively high aft dome membrane thicknesses early in the interim contract effort. However, an agreement between TC and NASA personnel concerning analytical evaluation techniques resulted in reduced membrane thickness

requirements. Configuration 1-1 with a maximum expected operating pressure (MEOP) of 861 psig represents the transition condition between internal pressure and external pressure critical conditions. In other words, for the specific design parameters involved (strength, size, and factor of safety requirements), if MEOP is 861 or above, the membrane thickness will be controlled by internal pressure requirements. If MEOP is less than 861 psi, the aft dome thickness will be controlled by external pressure which occurs at \ddot{Z} max during water impact. Other pressure distributions which occur during this condition are listed in figure 2-1, but are of little consequence as far as direct impact on the design of the SRM case.

The maximum pitch condition is essentially new since the RFP where pressure distributions were undefined. The final design conditions do not appear to present significant design considerations.

The RFP included a comprehensive listing of the bending, shear, and axial loads predicted for prelaunch conditions. The one-hour wind from orbiter to ET was identified by TC as the critical condition and Configuration 0 was evaluated under the effects of this loading and found to be adequate. However, at the time of the RFP these ground loads were assumed to be distributed with normal

$\frac{MC}{I}$, $\frac{VQ}{I}$, and $\frac{P}{A}$ load distributions.

As the design of the aft support skirt developed it was predicted by NASA that there would be a load peaking effect; resulting in higher case stress levels than would exist under the assumptions of normal load distributions. This new condition created the necessity for design changes in the membrane thickness of the aft skirt and aft cylindrical segment thickness of Configuration 0.

A similar load peaking effect was defined for the forward sections of the case near the thrust takeout point. Investigation revealed, however, that these forward peaking loads were not sufficiently high to have an appreciable effect on the case design.

Under the terms of the RFP the aft attach loads between the SRM and the ET were to be induced into the SRM through a load ring at three load points. These load points consisted of a shear pin and two struts with all induced loads tangential

to the ring. Subsequent loading concepts received during the interim contract reflected a two strut-sway brace configuration which induced both radial and tangential load components into the ring. A "T" section load ring which was incorporated in Configuration 0 was found to be inadequate under the effects of the new attach concept.

SRM geometry changes also occurred from the RFP to those currently used. Figure 2-2 defines the RFP values and the dimensions identified by NASA during the 90-day effort.

Figure 2-3 presents ballistic performance values defined in the RFP and modified values which evolved during the interim contract effort. These changes were made to update the SRM performance requirements to account for increases in weight caused by other requirement changes.

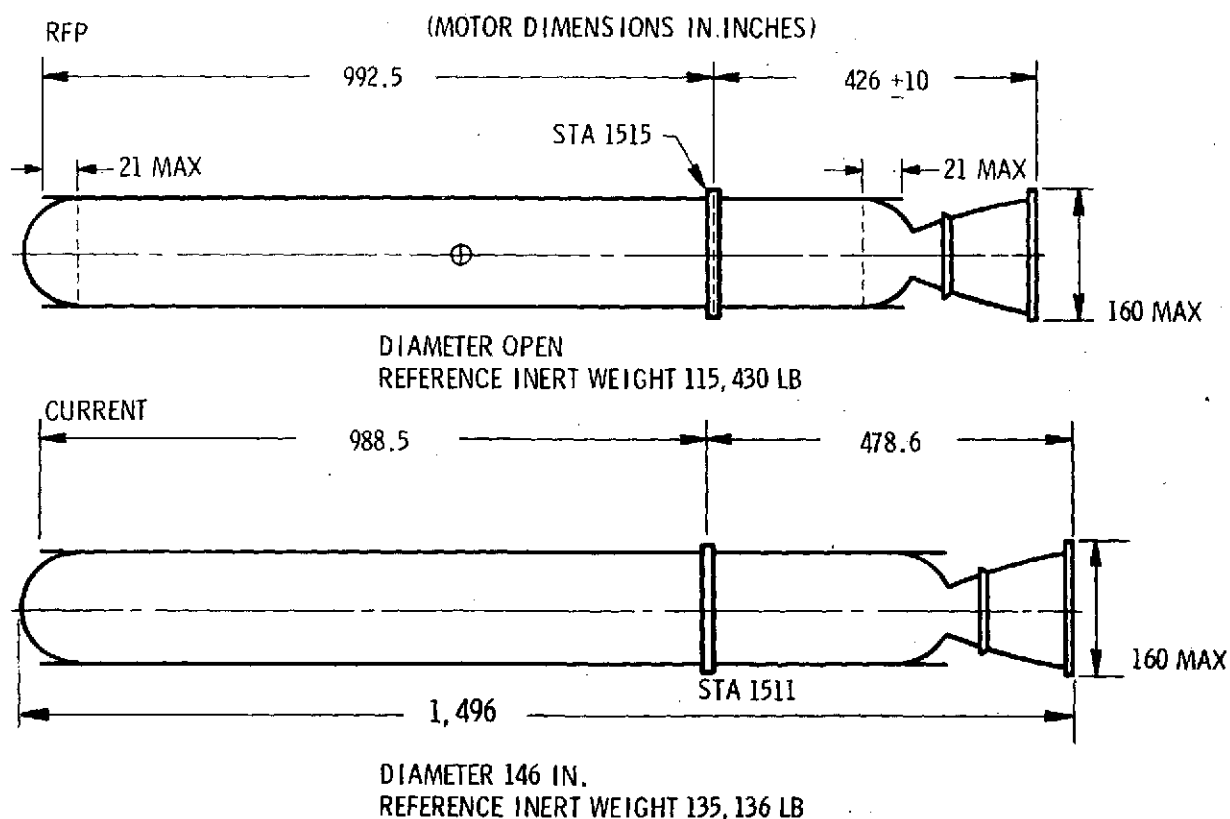
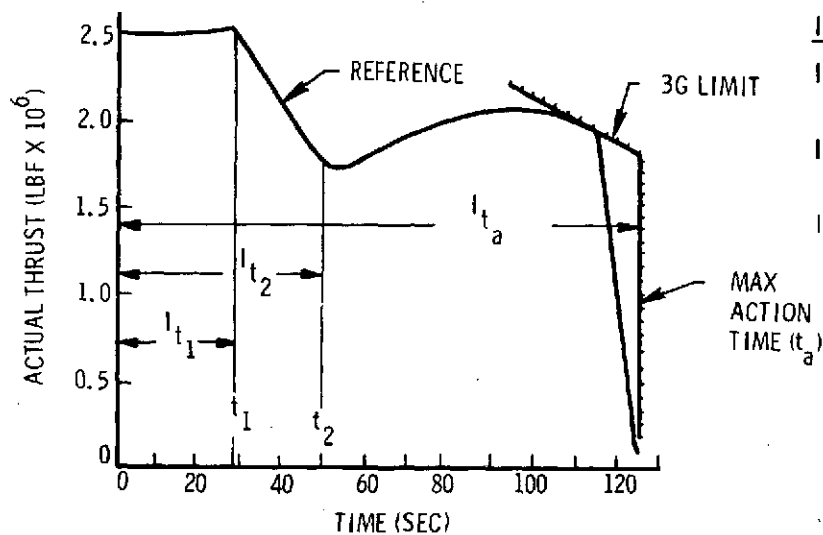


Figure 2-2. SRM Requirements - Geometry

RFPSL THRUST ($0 \leq t_F \leq t_1$)

$$F_{SL} = 2.508 (1 + \Delta W_p / W_p) \pm 2\% \text{ MLBF}$$

IMPULSE, LBF-SEC

$$I_{t_1} = 0.275 (I_{t_a}) \pm 1/2\%$$

$$I_{t_2} = 0.460 (I_{t_a}) \pm 1/2\%$$

$$I_{t_a} = 257.02 \times 10^6 (1 + \Delta W_p / W_p)$$

TIME, SEC

$$t_1 = 28$$

$$t_2 = 50$$

$$t_a \text{ MAX} = 124.6$$

$$W_{\text{INERT}} \text{ REF} = 115,430$$

INTERIM

$$F_{SL} = 2.626 (1 + \Delta W_p / W_p) \pm 2\% \text{ MLBF}$$

IMPULSE, LBF-SEC

$$I_{t_1} = 0.275 (I_{t_a}) \pm 1/2\%$$

$$I_{t_2} = 0.460 (I_{t_a}) \pm 1/2\%$$

$$I_{t_a} = 267.6 \times 10^6 (1 + \Delta W_p / W_p)$$

TIME, SEC

$$t_1 = 28$$

$$t_2 = 50$$

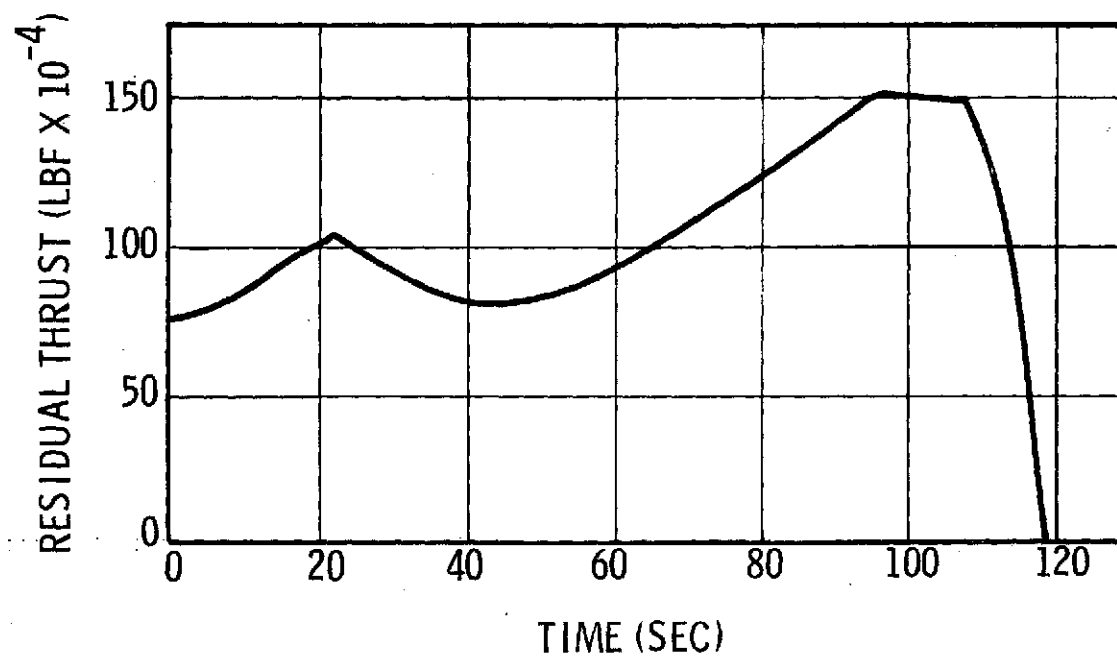
$$t_a \text{ MAX} = 124.6$$

$$W_{\text{INERT}} \text{ REF} = 135,136$$

Figure 2-3. SRM Requirements - Performance

During most of the interim contract period, SRM designs were sized using values specified for initial thrust and delivered impulse at three points in time during motor operation as shown in figure 2-3. Configurations 1 and 1-1 were designed using requirements stated in this form. Subsequent evaluation of the flight performance of these two configurations by RI revealed that the payload margin was lower than anticipated. This prompted action to use a different method for specifying SRM performance requirements. The method proposed was to establish a force-time requirement that must be supplied to the Shuttle vehicle by the SRM in order to provide a specified payload margin. This force, referred to as the "force-to-the bolts," is that required to produce a desired vehicle acceleration-time profile. By using this force data it is possible to shape the thrust time trace of an SRM to precisely match the required flight performance and thus provide the desired payload margin. This method was evaluated by Thiokol and proved to be an effective approach for generating SRM designs that deliver the required flight performance without the need for specifying specific motor parameters. As a result the method was incorporated in Thiokol's Automated Design Program (ADP) and used to establish design parameters for a new SRM Baseline referred to as Configuration 1-1A. Figure 2-4 presents the residual force and trajectory goals provided.

The design calculations introduced into the motor sizing subroutine of the ADP to determine the required SRM thrust-time trace necessitates input of residual force, vehicle acceleration, SRB inert weight, and ambient pressure all as a function of time. Using the above data the routine solves for thrust by summing the residual force and the force required to accelerate the SRB. The thrust-time data are then used to size an SRM design. Included in the sizing calculations are burning surface area versus thickness burned data for the propellant grain required to generate the specified residual force and acceleration traces. Since the SRM weight is required to determine thrust from the input data, the final design solution is arrived at by iterating several times through the routine.



TRAJECTORY GOALS

7,000 LB PAYLOAD MARGIN
(75K ET)

4,000 LB MARGIN FROM SRM

MAX q = 650 PSF

MAX g = 3.0

Figure 2-4. Representative SRM Performance Data

The residual force data for four thrust-time traces were provided by RI for SRM sizing using the ADP. Along with the residual force data, RI sent SRM designs calculated by their SHAPE program to generate the specified performance. Each design was configured to provide a total payload margin of 7,000 pounds, 3,000 pounds from the ET and 4,000 pounds from the SRM assuming an ET dry and residual weight of 75,000 pounds. The residual force data and typical SRM thrust shape data for the four cases (RI case numbers 370 through 373) are presented on figures 2-5, 2-6, 2-7, and 2-8. The thrust-time trace for Case 370 was shaped to approximate the trace of Thiokol's proposal design (Configuration 0). The other three traces were modified to reduce trajectory losses and thus illustrate (along with Table II) the effect of thrust or flight profile shaping on SRM size. Summarized on Table II are the propellant, inert and total weights for the four RI-generated designs. Notice that the weights for the SRM designs decrease from Case 370 to 373 as changes were made in the thrust-time trace. Thus, by this comparison the SRM weight can be reduced 42,900 pounds by shaping the thrust-time to meet the requirements of Case 373 rather than Case 370.

Also shown on Table II are the weights for two Thiokol ADP generated designs (case numbers 371 and 373). Since the ADP designs incorporated a higher performance nozzle and also were constrained to dimensional limits specified for Configuration 1-1A, the weights for the Thiokol designs vary somewhat from the RI weights. However, the same trend exists in that the total weight for Case 373 is significantly less than that for Case 371. The ADP could not generate a reasonable design for Case 370 within the dimensional constraints specified for Configuration 1-1A due to the relatively high total impulse requirement. Thus the thrust-time traces for Cases 371 and 373 represent performance limits for an SRM that will provide a payload margin of 3,000 to 4,000 pounds.

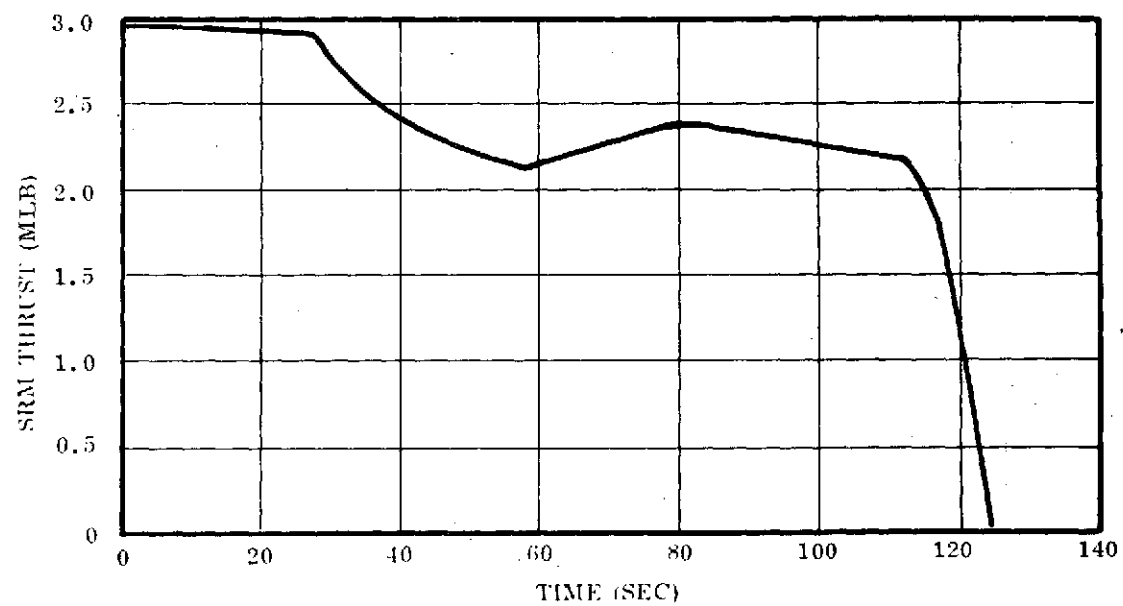
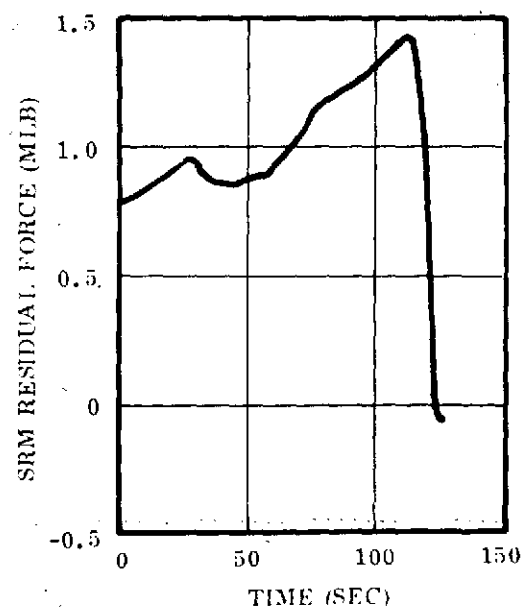


Figure 2-5. Residual Force and SRM Thrust Shape Data, RI Case 370

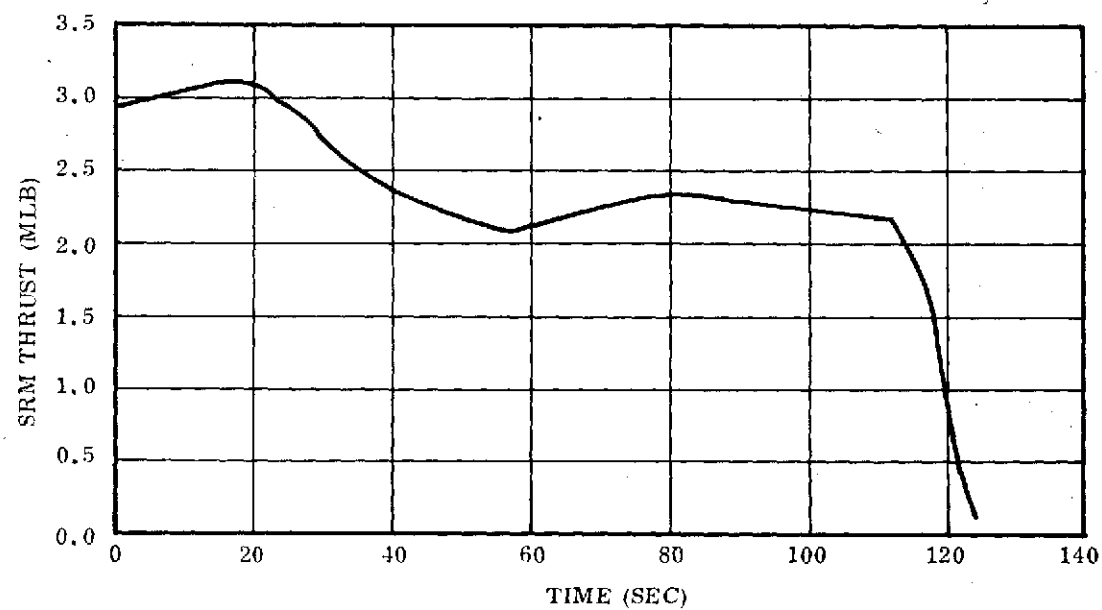
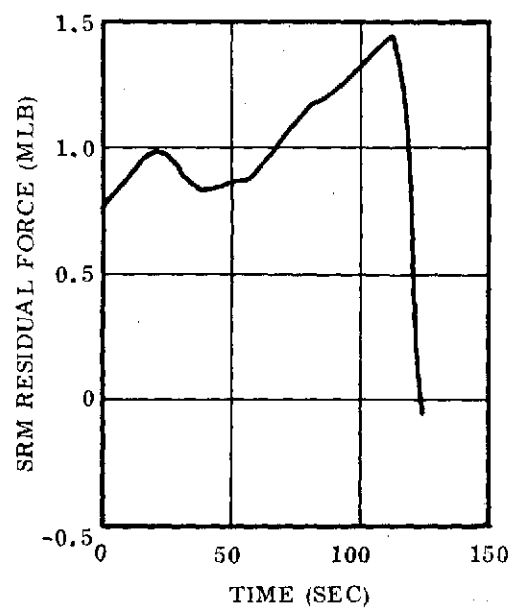


Figure 2-6. Residual Force and SRM Thrust Shape Data, RI Case 371

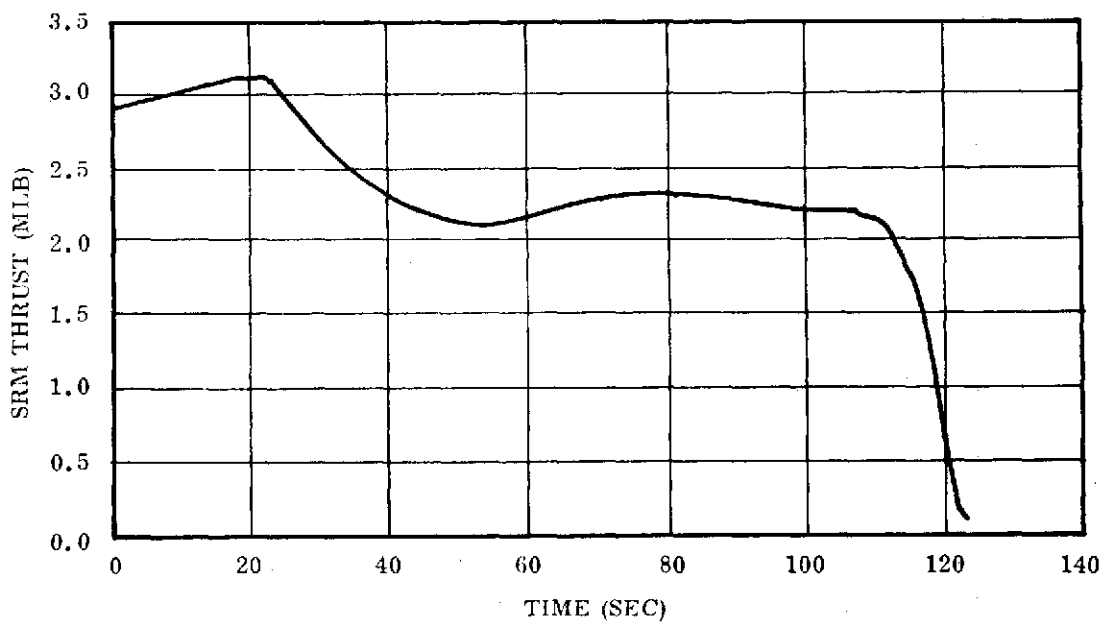
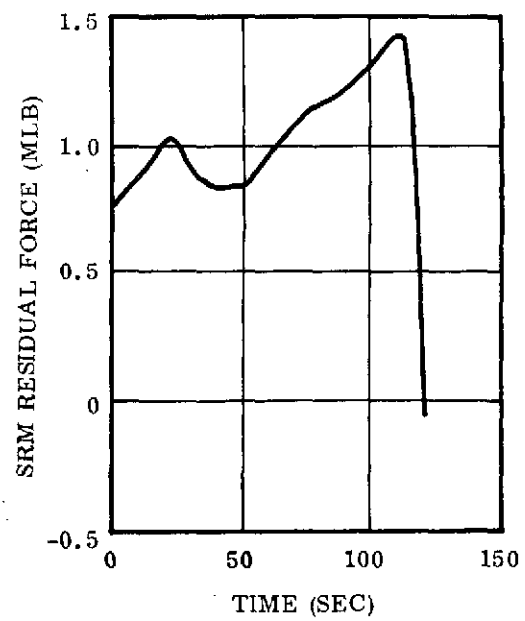


Figure 2-7. Residual Force and SRM Thrust Shape Data, RI Case 372

21

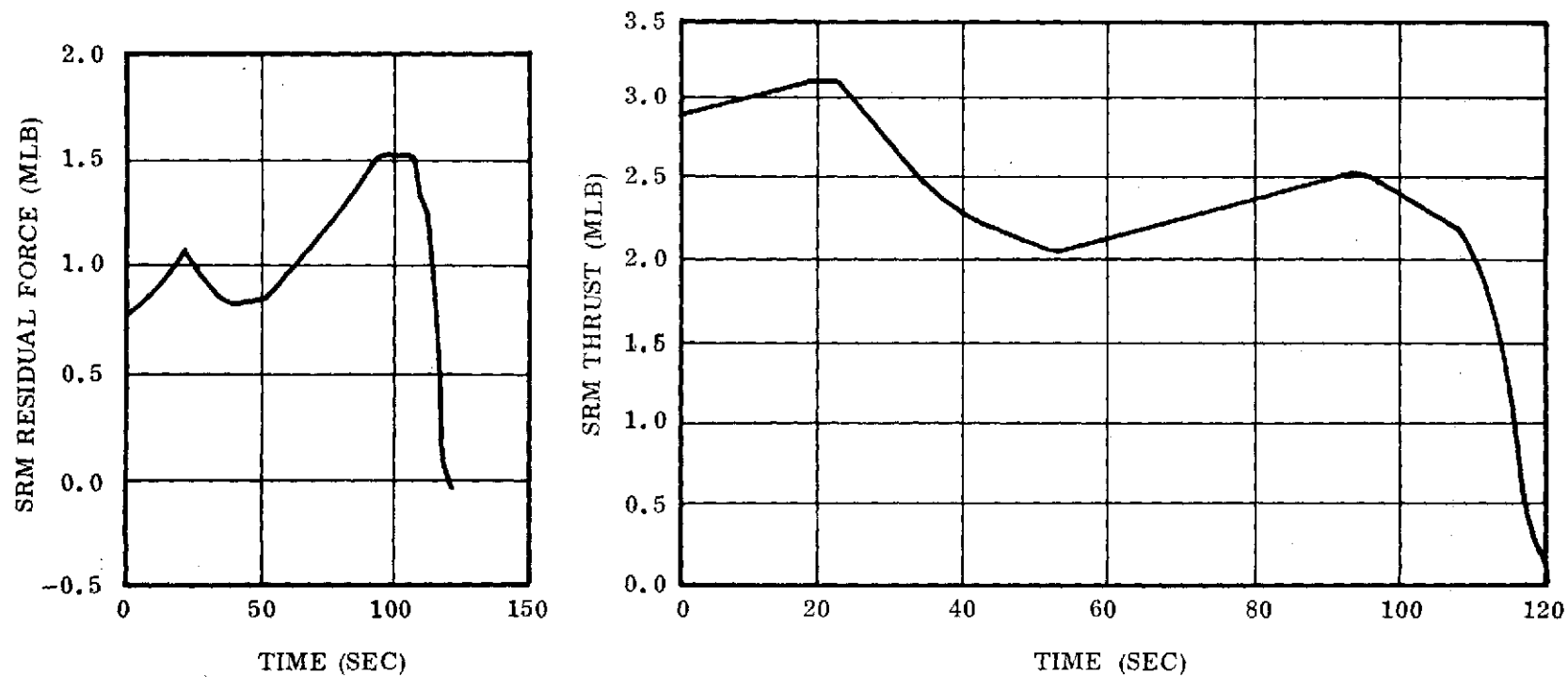


Figure 2-8. Residual Force and SRM Thrust Shape Data, RI Case 373

TABLE II

COMPARISON OF SRM DESIGNS
GENERATED BY RI AND TC

RI Case No.	RI Data ⁽¹⁾			TC Data ⁽²⁾		
	Weights, lbm			Weights, lbm		
	Prop.	Inert	Total	Prop.	Inert	Total
370	1,134,200	140,700	1,274,900			
371	1,119,800	139,100	1,258,900	1,103,100	145,100	1,248,200
372	1,112,000	138,200	1,250,300			
373	1,095,700	136,300	1,232,000	1,084,700	142,900	1,227,600

(1) Based on average delivered specific impulse of 258.9 lbf-sec/lbm

(2) Based on average delivered specific impulse of 262.2 lbf-sec/lbm

3.0 SRM PRELIMINARY DESIGNS

3.1 MOTOR PERFORMANCE

Preliminary design data for three SRM designs referred to as Configurations 1, 1-1, and 1-1A are presented in this section. The flight performance of the configurations has been evaluated by Rockwell International (RI) using their Shuttle Performance and Cost Evaluation (SPACE) Program. Configuration 1 was determined to provide a payload margin of 660 pounds and Configuration 1-1 a margin of 1,890 pounds. The payload margin for Configuration 1-1A was determined to range from 3,000 to 4,000 pounds depending upon the shape of the thrust-time trace and the loaded propellant weight.

The SRM performance requirements specified in the RFP were used in the initial sizing of an earlier version of Configuration 1; however, a flight performance evaluation of this design by RI concluded that the specified minimum delivered impulse was not adequate to provide a positive payload margin. The reasons for this deficiency were: 1) the reference SRM inert weight specified in the RFP was significantly less than that of the revised SRM design; and, 2) the delivered specific impulse was somewhat less than initially predicted due to an increase in the estimated nozzle losses. As a result, the RFP performance requirements for the baseline design were changed to the following:

$$\begin{aligned}F_{SL} &= 2.626 \times 10^6 (1 + \Delta W_p / W_p) \text{ lbf} \\I_{Ta} &= 267.6 \times 10^6 (1 + \Delta W_p / W_p) \text{ lbf-sec} \\ \text{Reference Propellant Weight} &= 1,072,300 \text{ lbm} \\ \text{Reference Inert Weight} &= \underline{135,136} \text{ lbm}\end{aligned}$$

Configuration 1 is a cost-optimized design capable of meeting the revised water entry loads, launch pad loads, and ET interface requirements while providing a small positive payload margin. An earlier version of this configuration presented at the SRM Design Review on 9 April 1974 (reference: TWR-10046) was determined by RI to have a negative payload margin. The delivered specific impulse of this earlier design was increased about 0.9 percent by modifying the nozzle. The nozzle changes included increasing the initial nozzle expansion ratio from 5.5 to 6

and increasing the initial throat-to-exit length/throat radius (L/Rt) from 4.45 to 5. With this new nozzle and the propellant weight of the earlier design the current Configuration 1 provides a 660 pound margin.

Configuration 1-1 was designed to maximize performance within a maximum length of 1,495.6 inches using RFP requirements. The design reflects the revised water entry loads, launch pad loads, and ET interface requirements and provides the maximum payload margin at a nominal increase in cost. The tangent-to-tangent case length is about the maximum possible for an eleven-piece (nine cylindrical segments and two closures) case design considering the revised loads and ET attach requirements. The cylindrical segments are divided as follows:

1. Six 156-inch long common segments
2. One 86-inch segment with double flanges for an attachment ring
3. Two common 127-inch long segments each with two flanges for stiffening rings

A length of 156 inches is the maximum for a 146-inch diameter segment with no upsets for flanges. Any case segment requiring provisions for local upsets for flanges must be shorter in length. A sketch illustrating the case fabrication constraints for 146-inch diameter segments is shown in figure 3-1. Present estimates are that the maximum length of a segment requiring a double flange positioned as specified for the attach segment is about 92 inches. The maximum length of the two aft segments requiring two flanges is estimated to be about 130 inches. Since all the cylindrical segments are at or near the maximum length, the only way the overall case length for Configuration 1-1 can be increased is to add an additional segment.

Configuration 1-1 is 26 inches longer than Configuration 1 and contains 18,000 pounds more propellant. The expansion ratio and L/Rt for the Configuration 1-1 nozzle is the same as that for Configuration 1, and, thus, the motor delivers the same specific impulse. Due to the increased propellant weight, Configuration 1-1 delivers 4.4×10^6 lbf-sec or 1.6 percent more total impulse than Configuration 1.

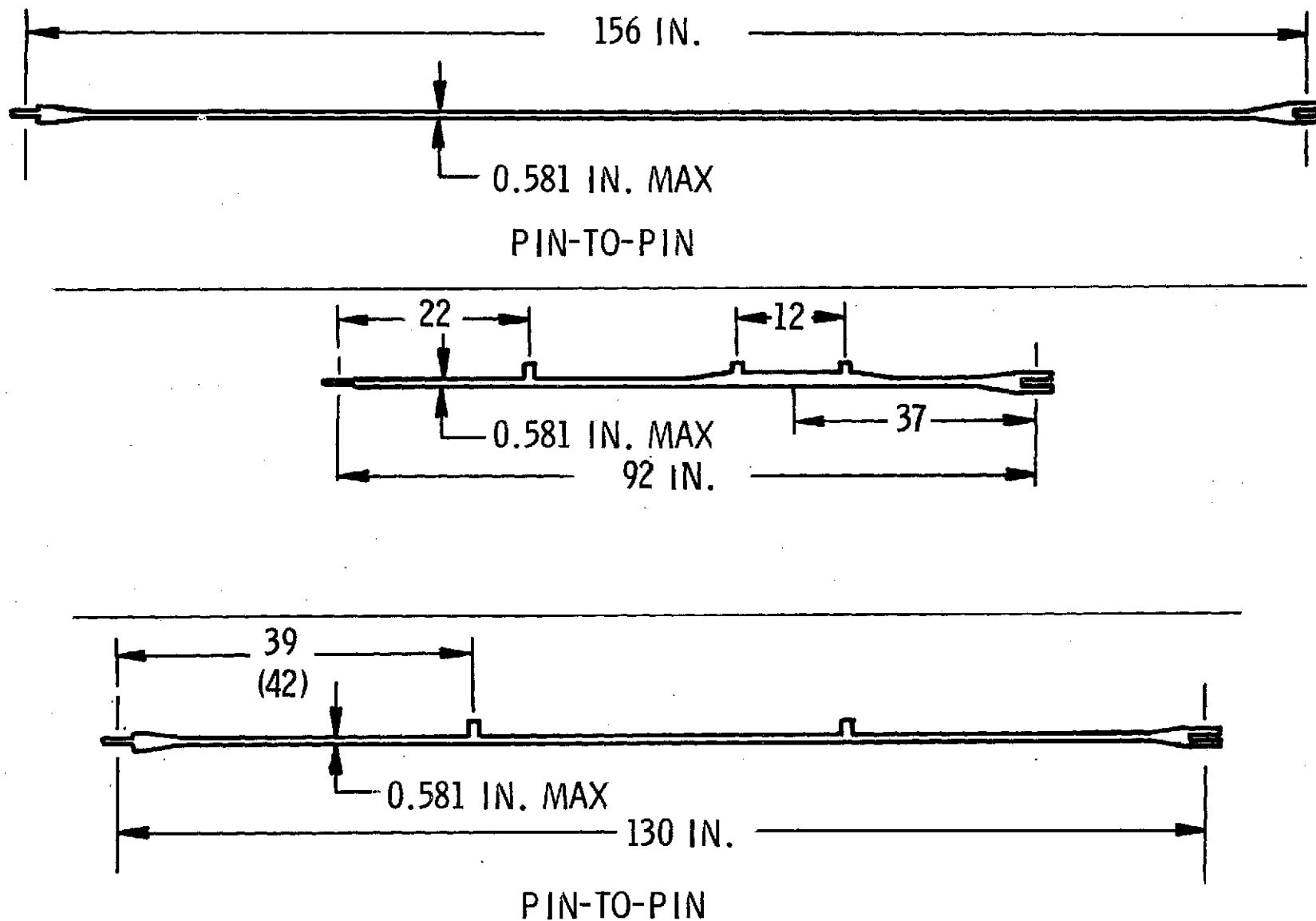


Figure 3-1. Case Fabrication Constraints at 146 In. Diameter

Configuration 1-1A was generated to provide the maximum payload margin within the geometry of Configuration 1-1. The principal differences between Configuration 1-1 and 1-1A are that Configuration 1-1A contains 11,600 pounds more propellant, incorporates a higher performance nozzle, and has a thicker case wall required to survive the latest water impact and on-pad bending loads. The Configuration 1-1A nozzle has an initial expansion ratio of 7.16 and an L/Rt of 5.28 and delivers an average vacuum specific impulse of 262.2 lbf-sec/lbm which is about 1.5 percent higher than that for Configuration 1-1.

The evolution of Configurations 1, 1-1, and 1-1A can be traced back through several stages during the interim contract period. The structural analysis of the case relative to the revised structural loads requirements set the pace during the entire study. The initial step was to evaluate the effect that the new water impact loads would have on the Configuration 0 (Thiokol proposal design) case design. The results of this early appraisal, using the BOSOR computer code, indicated that the new slapdown loads would require the wall thickness of the forward case segments to be increased to 0.576 inch. This thickness was greater than that dictated by internal pressure for ballistic performance, and, thus, established the minimum case wall for the first design iteration. This first design was referred to as a trend design and was reported to NASA on 20 February 1974 (reference TWR-10011). The weights for this trend design were as follows:

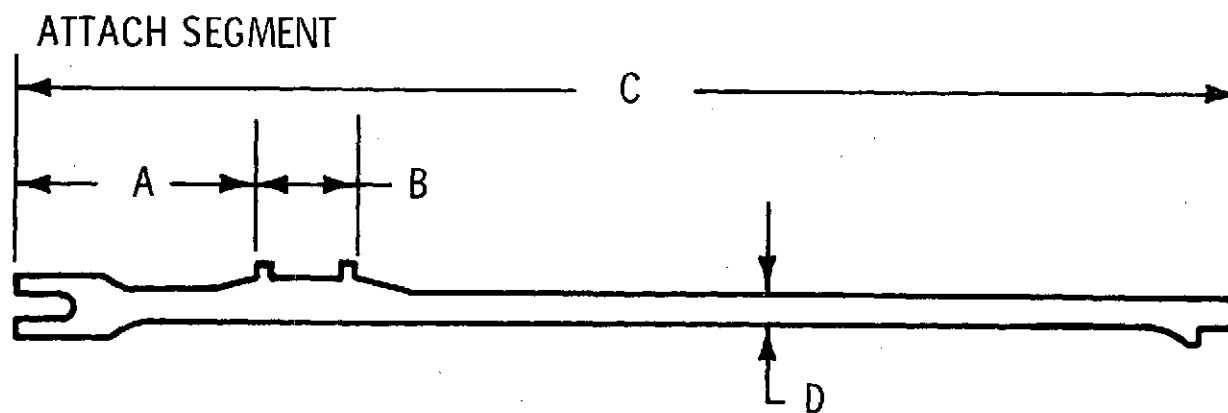
	<u>Weight (lb)</u>
Propellant	1,083,000
Case	116,120
Inert Weight	154,200

A more detailed analysis of the slapdown loads using the STAGS computer code later proved that the wall thickness considered necessary to survive slapdown as defined by BOSOR was quite conservative. This analysis showed that a minimum nominal wall thickness of 0.46 inch would be adequate for slapdown.

The next area of structural analysis activity was to determine the effect of cavity collapse on the aft portion of the case. As attention was directed toward this

region of the case, it was determined, through communications with the case fabricator, that length restrictions would have to be placed on the attach segment. This length restriction was the result of the requirement that the ET attach provision consist of a double flange, spaced about 12 inches apart. In order to manufacture this double flange on the attach segment, the segment length would have to be significantly shorter than the 142 inches incorporated in Configuration 0. The new length of the attach segment would now vary from 100 to 135 inches depending upon the location of the double flange relative to the distance from the joint as shown in figure 3-2. The impact of this reduction in the length of the attach segment was that another cylindrical segment had to be added to the case in order to load the required propellant weight. The approach taken was to incorporate the additional segment in the aft casting segment. As a result, the aft casting segment in all subsequent designs would consist of an attach segment, two short segments (ranging in length from 100 to 130 inches, depending upon propellant loading requirements), and an aft dome. This approach was taken to preserve the commonality of the 156-inch case segment length in the other three casting segments and also to retain the interchangeability of the two center casting segments. In addition, the use of two shorter case segments and an extra joint in the aft portion of the case provided additional stiffness in a region subjected to high cavity collapse loads.

During the remainder of the study effort, several design iterations were made to identify the optimum combinations of case wall thickness and local stiffening required to withstand the latest cavity collapse loads as a function of segment length. One of the design iterations was reported to MSFC at the SRM Design Review on 9 April 1974 (reference TWR-10046). At this review Configuration 1 had two 107-inch aft case segments with wall thicknesses of 0.51 inch and no stiffeners. Following this review an update by MSFC of the cavity collapse loads indicated that this design would not be structurally adequate. As a result, the design was modified to incorporate two stiffeners on each of the two aft segments, and an additional stiffener was added to the attach segment. The attach segment length had to be reduced to 86 inches to accommodate the additional stiffener. This 14-inch reduction in length was distributed between the two aft segments, increasing the length of these



<u>A</u> (IN.)	<u>B</u> (IN.)	<u>C</u> (IN.)	<u>D</u> (IN.)
6	12	135	0.581 (MAX)
13	12	112	0.581 (MAX)
36	12	100	0.581 (MAX)

Figure 3-2. Case Fabrication Constraints

segments to 114 inches. This case design with the shortened attach segment and two stiffeners on both aft segments was incorporated in both Configuration 1 and 1-1 designs presented at the MSFC SRB baseline reviews on 18 April 1974 (reference TWR-10059).

A more recent analysis of the shortened attach segment design indicates that the additional stiffener will not be required for cavity collapse. Thus, the case designs presented in this final report for Configurations 1 and 1-1 incorporate the shortened attach segment without the additional stiffener.

In addition to the requirement changes that directly affected the case structural design, the following items were introduced as design requirements:

1. Two percent inert weight allowance
2. G^* constraint
3. Nozzle exit cone cutoff device
4. MSFC nozzle safety factor interpretation
5. Use of conventional plastic materials in nozzle

The two percent inert weight allowance requested by MSFC was considered in this study as an increase in the total inert weight of the SRM. The two percent penalty applied to the total calculated inert weight, in turn, required the addition of more propellant based on the specified SRB inert weight partials. The inert weight added in this manner was assumed to have no unit cost. However, since the motor was increased in size to accommodate the burden of two percent additional inert weight, all the component costs are correspondingly higher.

An upper limit was established for the flow parameter G^* (mass flow per unit area) in order to prevent erosive burning from affecting the ballistics of motor designs generated during the interim contract period. In a meeting on 6 March 1974 with MSFC representatives, a maximum value of $3.1 \text{ lbm/sec-in.}^2$ at 90°F was the set for G^* . This is the maximum value developed in a Titan III booster without the motor experiencing an abnormal pressure rise at ignition. The effect of this limit was to restrain the cross sectional loading of propellant in a 146-inch diameter

case. As a result, when this limit was reached during a design iteration if more propellant had to be added, the port area and the motor length had to be increased.

Analysis of the water impact loads concluded that the loads can be significantly reduced if the nozzle exit cone is cut off. As a result, it was recommended that the nozzle exit cone be cut off just aft of the compliance ring and jettisoned before water impact. The current estimate is that this cutoff device will weigh approximately 50 lbm.

Designs generated during this study incorporated the use of MSFC interpretation of safety factors for determining the required thickness of nozzle plastic parts. By using the MSFC interpretation for determining nozzle safety factors, the weight of the nozzle for Configuration 1 increased about 5 percent.

Another change in the nozzle was the use of conventional plastic materials in place of the low-cost materials selected for the baseline design. Due to the difference in thickness and density of these materials the nozzle weight increased about 6.4 percent. The design philosophy was to configure a nozzle based on low-cost plastic materials but include the cost of conventional materials as an increment to the SRM program cost. This approach was selected to provide an SRM with performance capable of performing the intended mission even if the higher weight, high-cost nozzle materials are used. If the low-cost nozzle ablative materials are used (as intended), some performance margin will exist. The nozzle metal parts will be designed to accommodate either the high-cost or low-cost materials.

The basic design and performance data for the three configurations are presented in the following preliminary design documents.

3.1.1 Preliminary Design Data for Space Shuttle SRM Configuration 1 Model TU772/40A

3.1.1.1 Basic Motor Description

The Solid Rocket Motor (SRM) presented in this document has a steel case of D6AC material with a wall thickness of 0.488 inch in the cylindrical segments. The motor is nominally 146 inches in diameter with a slightly larger dimension over the

external joint structure. The boss-to-exit motor length is 1,468.5 inches, and the case boss-to-boss length is 1,352 inches. The case is comprised of 11 pieces; a forward closure, six common 156-inch segments, an 86-inch attach segment, two 114-inch segments with stiffeners, and an aft closure.

The motor is divided into four casting segments; a forward segment with igniter boss and a grain structure composed of an 11-point star configuration that blends into a cylindrical bore section, two interchangeable cylindrical segments that have tapered bore grain configurations, and an aft segment with a tapered bore. The aft segment grain is cut back to accept a submerged flexible bearing nozzle and incorporates the necessary nozzle mounting boss. The overall motor layout is presented in figure 3-3.

Table III presents a summary of the principal motor dimensions. Table IV presents a weight summary and center of gravity locations for the SRM before and after firing.

The motor contains 1,072,300 lbm of propellant and is to operate at an MEOP of 850 psig. Total burn time is approximately 124.4 seconds. Inhibiting is used on some slot faces to achieve thrust shaping.

The nozzle has a 17.8 percent throat submergence and is capable of being moved 8 degrees in any direction. Expected nozzle driving rate is 3 degrees per second. Nozzle throat diameter is 56.6 inches, and the initial expansion ratio is 6.0 to 1. The pivot point is located aft of the nozzle throat. The exit cone is of the contoured type with initial and final angles of 23.6 and 13.8 degrees, respectively. Table V summarizes the pertinent nozzle design data.

3.1.1.2 Performance

The following list of performance parameters apply to this motor design.

Average Stagnation Pressure (psia)	530
MEOP (psig)	850
Web Burn Time (sec)	114.5
Average Vacuum Thrust (lbf) (total time)	2,230,000
Vacuum Specific Impulse (lbf-sec/lbm) (at average expansion ratio of 5.82:1)	258.9

Page intentionally left blank

TABLE III
SUMMARY OF MOTOR DIMENSIONS
(CONFIGURATION 1)

<u>Dimension Description</u>	<u>Value (in.)</u>
Aft Segment	372.0
Cylindrical Segment (2 required)	312.0
Forward Segment	356.0
Assembled Case	1,352.0
Forward Dome-to-Nozzle Exit	1,468.5
Total Nozzle	165.5
Nozzle Flange-to-Exit	116.5
Nozzle Throat Diameter	56.6

TABLE IV

WEIGHT AND CENTER OF GRAVITY SUMMARY
(CONFIGURATION 1)

<u>Item</u>	<u>Fwd Segment (lb)</u>	<u>Cylindrical Segment (2 required) (lb)</u>	<u>Aft Segment (lb)</u>	<u>Total (lb)</u>	<u>\bar{X} (in.)*</u>
Case	25,215	21,303	28,372	96,193	
Insulation, Liner, and Inhibitor	4,901	1,632	5,563	13,728	
Raceway	60	58	58	234	
Propellant	288,637	259,417	264,829	1,072,300	
Subtotal	318,813	282,410	264,822	1,182,455	
Nozzle				20,578	
Igniter				649	
Attach Provisions				190	
Contingency				2,631	
Total Inerts				134,203	
Total Motor (Prelaunch)				1,206,503	1,162.6
Expended Inerts				4,488	
Total Motor (Burnout)				129,715	1,274.9
Propellant Mass Fraction				0.889	

*CG reference plane is 493.7 inches forward of forward dome igniter flange

TABLE V
NOZZLE CHARACTERISTICS AND DESIGN CRITERIA
(CONFIGURATION 1)

Throat Diameter, initial (in.)	56.6
Throat Area, initial (in. ²)	2,516
Exit Diameter, initial (in.)	138.64
Exit Area, initial (in. ²)	15,096
Expansion Ratio, initial	6 to 1
Exit Cone, contoured	
Initial Angle (deg)	23.6
Exit Angle (deg)	13.8
Submergence (%)*	17.8
Pressure, average web (psia)	530
MEOP (psig)	850
Safety Factors	
Ablatives	2.0 on erosion +1.25 x char
Thermal Protection	1.0
Structure	1.4
Nozzle Weight (lb)	20,578
Length, throat-to-exit (in.)	141.5
Length/Throat Radius (initial)	5

*Submergence, % = $\frac{\text{Length, Throat-to-Flange}}{\text{Length, Throat-to-Exit}} \times 100$

Burning Rate at 1,000 psia (in./sec)	0.408
Total Vacuum Impulse (million lbf-sec)	277.62
Initial Expansion Ratio	6.0:1

Figure 3-4 presents the thrust-time history for this motor.

3.1.2 Preliminary Design Data for Space Shuttle SRM Configuration 1-1 Model TU772/42C

3.1.2.1 Basic Motor Description

The solid rocket motor (SRM) presented in this document has a steel case of D6AC material with a wall thickness of 0.494 inch in the cylindrical segments. The motor is nominally 146 inches in diameter with a slightly larger dimension over the external joint structure. The boss-to-exit motor length is 1,496 inches, and the case boss-to-boss length is 1,378 inches. The case is comprised of 11 pieces; a forward closure, six common 156-inch segments, an 86-inch attach segment, two 127-inch segments with stiffeners, and an aft closure.

The motor is divided into four casting segments; a forward segment with igniter boss and a grain structure composed of an 11-point star configuration that blends into a cylindrical bore section. Two interchangeable cylindrical segments in the center of the motor that have tapered bore grain configurations, and an aft segment with a tapered bore. The aft segment grain is cut back to accept a submerged flexible bearing nozzle and has the necessary nozzle mounting boss. The overall motor layout is presented in figure 3-5.

Table VI presents a summary of the principal motor dimensions. Table VII presents a weight summary and center of gravity locations for the SRM before and after firing.

The motor contains 1,090,400 lbm of propellant and operates at an MEOP of 861 psig. Total burn time is approximately 124.4 seconds. Inhibiting is used on some slot faces to achieve thrust shaping.

The nozzle has a 17.6 percent throat submergence and is capable of being moved 8 degrees in any direction. Expected nozzle driving rate is 3 degrees per second. Nozzle throat diameter is 57.3 inches, and the initial expansion ratio is

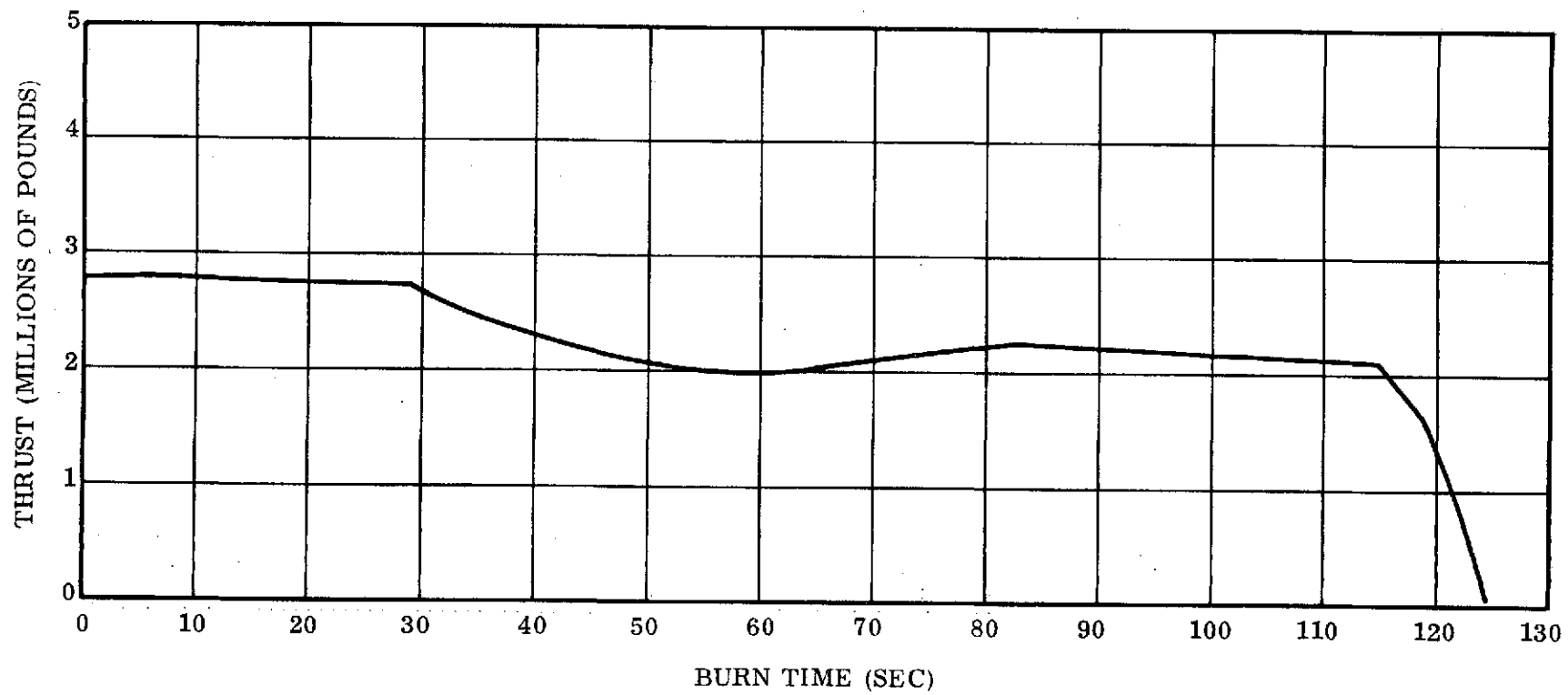


Figure 3-4. Thrust Versus Time Configuration 1

Page intentionally left blank

TABLE VI

SUMMARY OF MOTOR DIMENSIONS
(CONFIGURATION 1-1)

<u>Dimension Description</u>	<u>Value (in.)</u>
Aft Segment	398.0
Cylindrical Segment (2 required)	312.0
Forward Segment	356.0
Assembled Case	1,378.0
Forward Dome-to-Nozzle Exit	1,496.0
Total Nozzle	167.2
Nozzle Flange-to-Exit	118.0
Nozzle Throat Diameter	57.3

TABLE VII

WEIGHT AND CENTER OF GRAVITY SUMMARY
(CONFIGURATION 1-1)

<u>Item</u>	<u>Fwd Segment (lb)</u>	<u>Cylindrical Segment (2 required) (lb)</u>	<u>Aft Segment (lb)</u>	<u>Total (lb)</u>	<u>\bar{X} (in.)*</u>
Case	25,496	21,545	30,197	98,783	
Insulation, Liner, and Inhibitor	4,901	1,632	5,881	14,046	
Raceway	60	58	64	240	
Propellant	287,646	258,525	285,704		1,090,400
Subtotal	318,103	281,760	321,846	1,203,469	
Nozzle				21,192	
Igniter				649	
Attach Provisions				190	
Contingency				2,702	
Total Inerts				137,802	
Total Motor (Prelaunch)				1,228,202	1,176.0
Expended Inerts				4,578	
Total Motor (Burnout)				133,224	
Propellant Mass Fraction				0.888	1,289.4

*CG reference plane is 493.7 inches forward of forward dome igniter flange.

6.0 to 1. The pivot point is located aft of the nozzle throat. The exit cone is of the contoured type with initial and final angles of 23.6 and 13.8 degrees, respectively. Table VIII summarizes the pertinent nozzle design data.

3.1.2.2 Performance

The following list of performance parameters apply to this motor design.

Average Stagnation Pressure (psia)	526
MEOP (psig)	861
Web Burn Time (sec)	114.4
Average Vacuum Thrust (lbf) (Total Time)	2,268,000
Vacuum Specific Impulse (lbf-sec/lbm) (at average expansion ratio of 5.82)	258.9
Burning Rate at 1,000 psia (in./sec)	0.408
Total Vacuum Impulse (million lbf-sec)	282.31
Initial Expansion Ratio	6.0:1

Figure 3-6 presents the thrust-time history for this motor.

3.1.3 Preliminary Design Data for Space Shuttle SRM Configuration 1-1A Model TU772/42D

3.1.3.1 Basic Motor Description

The solid rocket motor (SRM) presented in this document has a steel case of D6AC material with a wall thickness of 0.521 inch in the cylindrical segments. The motor is nominally 146 inches in diameter with a slightly larger dimension over the external joint structure. The boss-to-exit motor length is 1,496 inches, and the case boss-to-boss length is 1,378 inches. The case is comprised of 11 pieces; a forward closure, six common 156-inch segments, an 86-inch attach segment, two 127-inch segments with stiffeners, and an aft closure.

The motor is divided into four casting segments; a forward segment with igniter boss and a grain structure composed of a 9-point star configuration that blends into a cylindrical bore section. Two interchangeable cylindrical segments in the center of the motor that have tapered bore grain configurations, and an aft

TABLE VIII

NOZZLE CHARACTERISTICS AND DESIGN CRITERIA
(CONFIGURATION 1-1)

Throat Diameter, initial (in.)	57.3
Throat Area, initial (in. ²)	2,579
Exit Diameter, initial (in.)	140.34
Exit Area, initial (in. ²)	15,469
Expansion Ratio, initial	6 to 1
Exit Cone, contoured	
Initial Angle (deg)	23.6
Exit Angle (deg)	13.8
Submergence (%)*	17.6
Pressure, average web (psia)	526
MEOP (psig)	861
Safety Factors	
Ablatives	2.0 on erosion + 1.25 x char
Thermal Protection	1.0
Structure	1.4
Nozzle Weight (lb)	21,192
Length, throat-to-exit (in.)	143.2
Length/Throat Radius (initial)	5

*Submergence, % = $\frac{\text{Length, Throat-to-Flange}}{\text{Length, Throat-to-Exit}} \times 100$

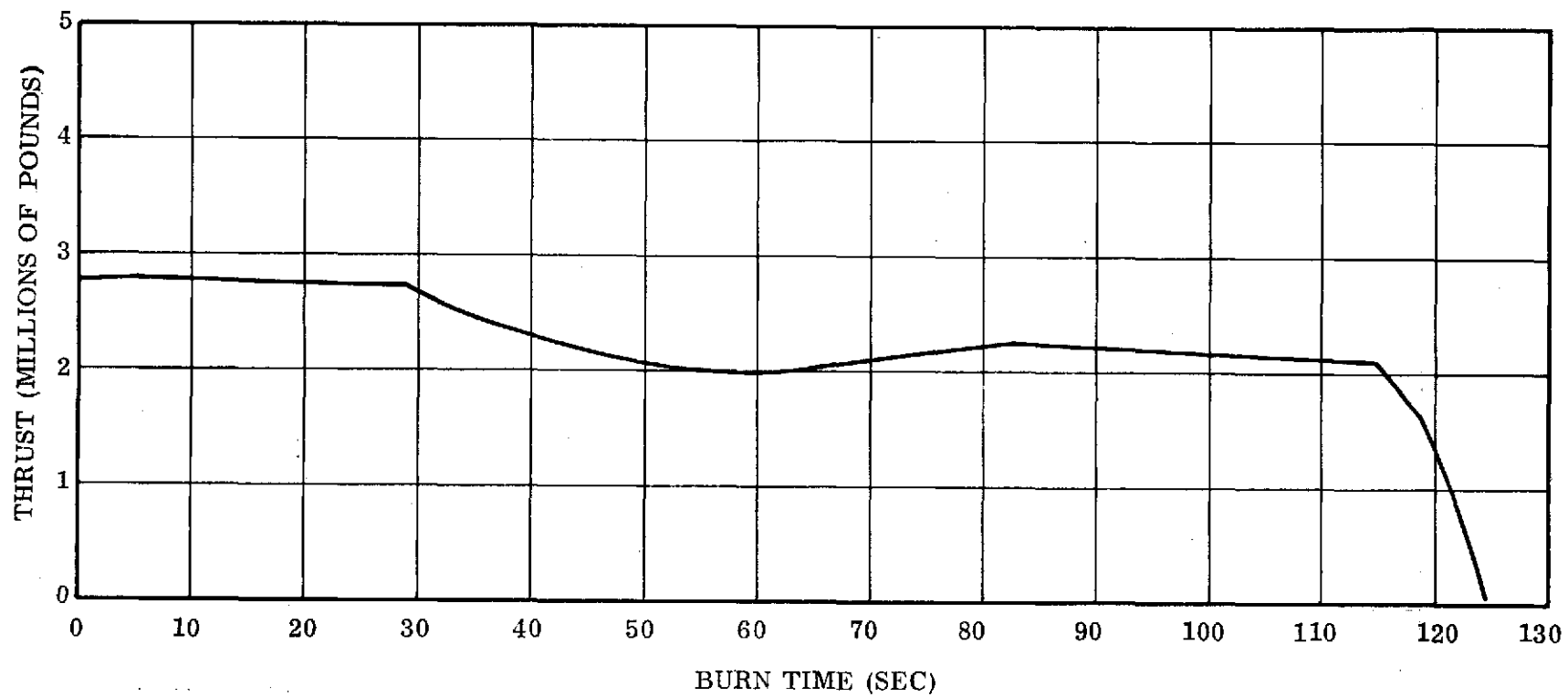


Figure 3-6. Thrust Versus Time Configuration 1-1

segment with a tapered bore. The aft segment grain is cut back to accept a submerged flexible bearing nozzle and has the necessary nozzle mounting boss. The overall motor layout is presented in figure 3-7.

Table IX presents a summary of the principal motor dimensions. Table X presents a weight summary and center of gravity locations for the SRM before and after firing.

The motor contains 1,102,000 lbm of propellant and operates at an MEOP of 937 psig. Total burn time is approximately 122.2 seconds. Inhibiting is used on some slot faces to achieve thrust shaping.

The nozzle has a 17.9 percent throat submergence and is capable of being moved 8 degrees in any direction. Expected nozzle driving rate is 3 degrees per second. Nozzle throat diameter is 54.4 inches, and the initial expansion ratio is 7.16 to 1. The pivot point is located aft of the nozzle throat. The exit cone is of the contoured type with initial and final angles of 24.6 and 13.25 degrees, respectively. Table XI summarizes the pertinent nozzle design data.

3.1.3.2 Performance

The following list of performance parameters apply to this motor design.

Average Stagnation Pressure (psia)	764
MEOP (psig)	937
Web Burn Time (sec)	114.4
Average Vacuum Thrust (lbf) (Total Time)	2,320,440
Vacuum Specific Impulse (lbf-sec/lbm) (at average expansion ratio of 6.94)	262.2
Burning Rate at 1,000 psia (in./sec)	0.3995
Total Vacuum Impulse (million lbf-sec)	288.94
Initial Expansion Ratio	7.16:1

Figure 3-8 presents the thrust-time history for this motor.

Page intentionally left blank

TABLE IX
SUMMARY OF MOTOR DIMENSIONS
(CONFIGURATION 1-1A)

<u>Dimension Description</u>	<u>Value (in.)</u>
Aft Segment	398.0
Cylindrical Segment (2 required)	312.0
Forward Segment	356.0
Assembled Case	1, 378.0
Forward Dome-to-Nozzle Exit	1, 496.0
Total Nozzle length	167
Nozzle Flange-to-Exit	118.0
Nozzle Throat Diameter	54.43

TABLE X

WEIGHT AND CENTER OF GRAVITY SUMMARY
(CONFIGURATION 1-1A)

<u>Item</u>	<u>Fwd Segment (lb)</u>	<u>Cylindrical Segment (2 required) (lb)</u>	<u>Aft Segment (lb)</u>	<u>Total (lb)</u>	<u>\bar{X} (in.)*</u>
Case	26,769	22,643	32,925	104,980	
Insulation, Liner, and Inhibitor	6,114	1,620	5,246	14,600	
Raceway	60	58	64	240	
Propellant	290,707	261,275	288,743	1,102,000	
Subtotal	323,650	285,596	326,978	1,221,820	
Nozzle				20,892	
Igniter				649	
Attach Provisions				365	
Contingency				2,834	
Total Inerts				144,560	
Total Motor (Prelaunch)				1,246,560	1,175.3
Expended Inerts				5,006	
Total Motor (Burnout)				139,702	1,285.5
Propellant Mass Fraction				0.884	

*CG reference plane is 493.7 inches forward of forward dome igniter flange.

TABLE XI

NOZZLE CHARACTERISTICS AND DESIGN CRITERIA
(CONFIGURATION 1-1A)

Throat Diameter, initial (in.)	54.43
Throat Area, initial (in. ²)	2,327
Exit Diameter, initial (in.)	145.65
Exit Area, initial (in. ²)	16,661
Expansion Ratio, initial	7.16 to 1
Exit Cone, contoured	
Initial Angle (deg)	24.6
Exit Angle (deg)	13.25
Submergence (%) *	17.9
Pressure, average web (psia)	764
MEOP (psig)	937
Safety Factors	
Ablatives	2.0 on erosion +1.25 x char
Thermal Protection	1.0
Structure	1.4
Nozzle Weight (lb)	20,892
Length, throat-to-exit (in.)	143.7
Length/Throat Radius (initial)	5.28

*Submergence, % = $\frac{\text{Length, Throat-to-Flange}}{\text{Length, Throat-to-Exit}} \times 100$

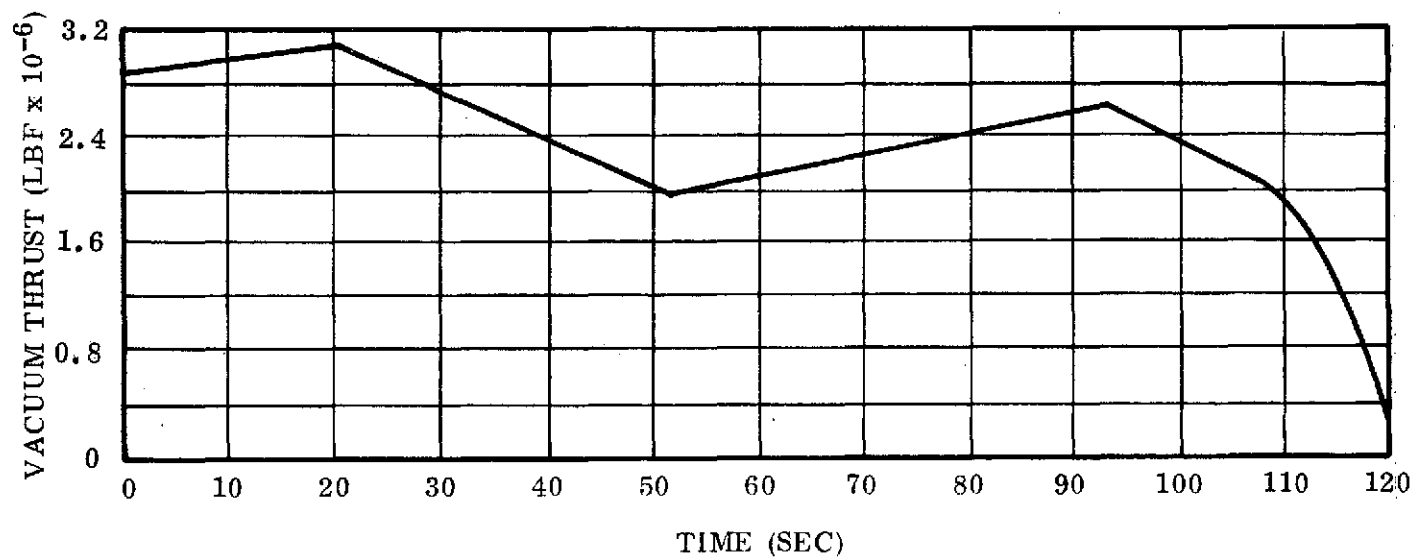


Figure 3-8. Thrust Versus Time Configuration 1-1A.

3.2 CASE AND STRUCTURAL ANALYSIS

Major changes in SRM structural loading affecting the case and nozzle design, evolved subsequent to the RFP and during the interim contract. In general these changes, due to water impact, ET attach, and pad loads, required an increase in the structural capability of the case which increased the inert weight of the SRM. NASA Report S & E-ASTN-ADL (73-68), "Updated Water Impact Loads for the Space Shuttle Solid Rocket Booster (SRB), 4-11-73 Configuration," was provided to Thiokol at the initiation of the interim contract.

The following sections present a summary of the impact of the revised loading conditions on the design of the basic case and nozzle. The effort described is the work accomplished during the interim contract which was primarily in support of performance studies. The analyses which were involved were general in nature and were intended to assess the general impact of such design considerations as water impact, ET attach, pad loads, and basic design philosophy. Analyses such as detailed discontinuity and refined stress analyses were not performed due to the transient nature of the designs involved.

3.2.1 Case

One of the principal areas of concern is the basic cylindrical wall of the case and in particular the case wall thickness required to fulfill all design requirements. A technique is developed which establishes the minimum wall thickness requirement of the case with consideration given to fracture toughness, crack growth rates, proof test, flight test pressures cyclic life requirements, and grit blast removal. The development of this procedure is outlined in the case wall thickness section. It was determined under the terms of the RFP that fracture mechanics (cyclic life) requirements are dominant over factor of safety requirements.

It should be pointed out that about a 3 percent overdesign is required in the case wall due to the dominance of cyclic life requirements. If certain RFP requirements are relaxed slightly, basic strength considerations will dominate. Most notable of the rather severe RFP requirements is the requirement for a subsequent proof test before each use at a pressure level 1.2 times the case MEOP.

Configuration 1-1A does provide a cylindrical case thickness based on a safety factor of 1.4 as agreed on with MSFC. Discussions are continuing to modify structural design requirements so that cyclic life requirements do not dominate.

Typical designs of clevis joints for both forward and aft SRB skirt attachments are presented. These designs are adequate to accommodate the current forward and aft peaking loads. Fabrication considerations affecting the attachment design need further investigation. An additional area of interest was the ET attach ring where a change from the RFP attach concept resulted in the need for a redesign of the ring cross section. A new design was developed and analyzed which bolts to the case on two stub flanges which are 12 in. apart and are provided in a special attach segment of the case. The most severe loading condition was found to occur during liftoff, and the results of an analysis of this condition are presented.

A major area of concern is the effect of the water impact loads on the design. The cavity collapse requirement is of particular importance, in that it creates a need for two additional circumferential ring stiffeners in each of the two aft segments (Configuration 1-1). No additional wall thickness (over the 0.51 in. required for the aft peaking loads) will be required according to preliminary indications from BOSOR and subsequent supporting analysis on STAGS. A recommendation is made for further support analysis on STAGS. The slapdown loads under the terms of the present requirements (see figure 2-1) do not affect the case design as long as nominal case wall thickness is above 0.461 in. This value is based on one STAGS point extrapolated by BOSOR results. We understand that NASA results based on several STAGS points indicate that this value can go as low as 0.41 in.

The requirements of cavity collapse are more severe than the requirements of penetration, and, therefore, penetration does not affect the design.

The aft dome thickness requirement for external pressure is based on the requirements of NASA TND-1510 per agreement between NASA and Thiokol. The thickness requirement for the aft dome under the effects of internal pressure was determined using the same technique as developed for the case wall, considering the stress reduction for a hemisphere. In Configurations 0, 1, 1-1, and 1-1A, the internal

pressure requirements were dominant over the external pressure requirements which occur at maximum axial deceleration. Configuration 1-1 was then subjected to a BOSOR analysis with all aft skirt cavity pressures acting and the resulting factor of safety was 1.25 (using a KDF of 0.75). The only configuration verified on BOSOR was Configuration 1-1; however, Configuration 1-1A will provide an even greater safety factor due to its 8.7 percent greater membrane thickness.

The nozzle was also evaluated under the effects of maximum axial acceleration (\ddot{Z} max), and maximum pitch ($\ddot{\theta}$ max). The \ddot{Z} maximum condition had very little significance to the nozzle, and Configuration 1-1 was found to be adequate for maximum pitch when the uncharred ablative material was included in the analysis. The stress analysis of the nozzle shell for the $\ddot{\theta}$ maximum condition shows factors of safety less than 1.25 but does not include the ablative material. It remains for future effort to evaluate the effect of ablatives on the nozzle stress levels during the $\ddot{\theta}$ maximum sequence.

The aft cylindrical segment of the case must be increased in thickness to accommodate the aft peaking loads. It is ultimately shown by NASTRAN computer analysis that a final nominal thickness of 0.51 in. is adequate to sustain these loads and exhibit a factor of safety over the required value of 1.4. The results of the analysis are presented.

The forward peaking loads are not critical, and it is shown from simplified conservative analysis techniques that they are not deleterious to the design.

3.2.1.1 Case Wall Thickness Calculation

The basic case wall thickness requirement is determined from the complex interaction of internal pressure, fracture mechanics, and grit blast considerations. During the interim contract period, a procedure was developed to determine the case wall thickness requirements on the basis of stress-time history as related to flaw growth and the successive removal of material due to grit blasting during the refurbishment process. In conjunction with this effort, a further review of Minuteman grit blast experience was conducted and applied to all designs included in this effort. A summary of the results of each phase of the effort follows.

3.2.1.2 Grit Blast

In 1971 a detailed study of three reclaimed Minuteman, Stage I, motor cases was conducted. The material was D6AC steel. One-two mils of epoxy-polyamid avcoat primer was removed from the outside surface and a grip clad vinyl primer from the inside with 100-200 grit zirconium silicate abrasive. Six hundred and seventy-six individual points were measured on each of the three cases before and after grit blast with the following results:

<u>Case</u>	<u>Decrease in Total Wall Thickness (Average 676 Points)</u>
1	0.00055 in.
2	0.00028 in.
3	0.00061 in.

Average Removal 0.00048 in. (2 sides)

Average Removal Per Side, Per Use = 0.00024 in.

or for 20 uses (19 removal processes) the total material removed is

$$19 (0.0048) = 0.0091 \text{ in. / 19 reuses}$$

This value was used in all basic wall sizing work for this effort.

3.2.1.3 Analytical Procedure

The general procedure for determining case wall thickness requirements is based on standard principles of linear fracture mechanics as they interact with the case stress-time history.

The essence of the approach is as follows:

1. Establish the maximum depth flaw which can exist in the case by an initial high level proof test.
2. Allow this initial crack to grow through the effects of a specified number of use cycles consisting of:
 - a. One flight at MEOP
 - b. One grit blast
 - c. One proof test at a pressure higher than MEOP

Both time dependent \dot{a} and cycle da/dn flaw growth are considered in the analysis as well as the increase in stress levels for each subsequent cycle due to the loss from grit blast.

3. The wall thickness requirements to complete N cycles are iteratively determined
4. The output of the program includes such useful information as:
 - a. Initial factor of safety
 - b. Final factor of safety (after grit blasts)
 - c. Critical flaw size
 - d. Initial wall thickness requirements
 - e. Final wall thickness requirements
 - f. Pressure level of initial proof

The program input and mathematical development are as follows; all the input constants listed are those which were used in the development of figure 3-9 which shows thickness as a function of internal case pressure.

INPUT DATA

Given:

K_{IC}	=	Plant Strain Fracture Toughness = 90,000 psi $\sqrt{\text{in.}}$
$\frac{da}{dn}$	=	Cyclic Crack Growth Rate = $1.32 \times 10^{-16} (K_I)^{2.48}$ in./cycle
\dot{a}	=	Time Dependent Crack Growth Rate = 5.833×10^{-8} in./sec
P	=	Internal Case Pressure, MEOP (psi)
φ	=	Proof Factor = 1.2
Δt	=	Thickness Removed Per Use = 0.0048 in./use
N	=	Number of Uses = 40
T_2	=	Time at Proof Pressure Sec (120 sec)
T_1	=	Time at Service Sec (100 sec)
R	=	Radius of Case (73 in.)
F.S.	=	Initial Factor of Safety (1.4)

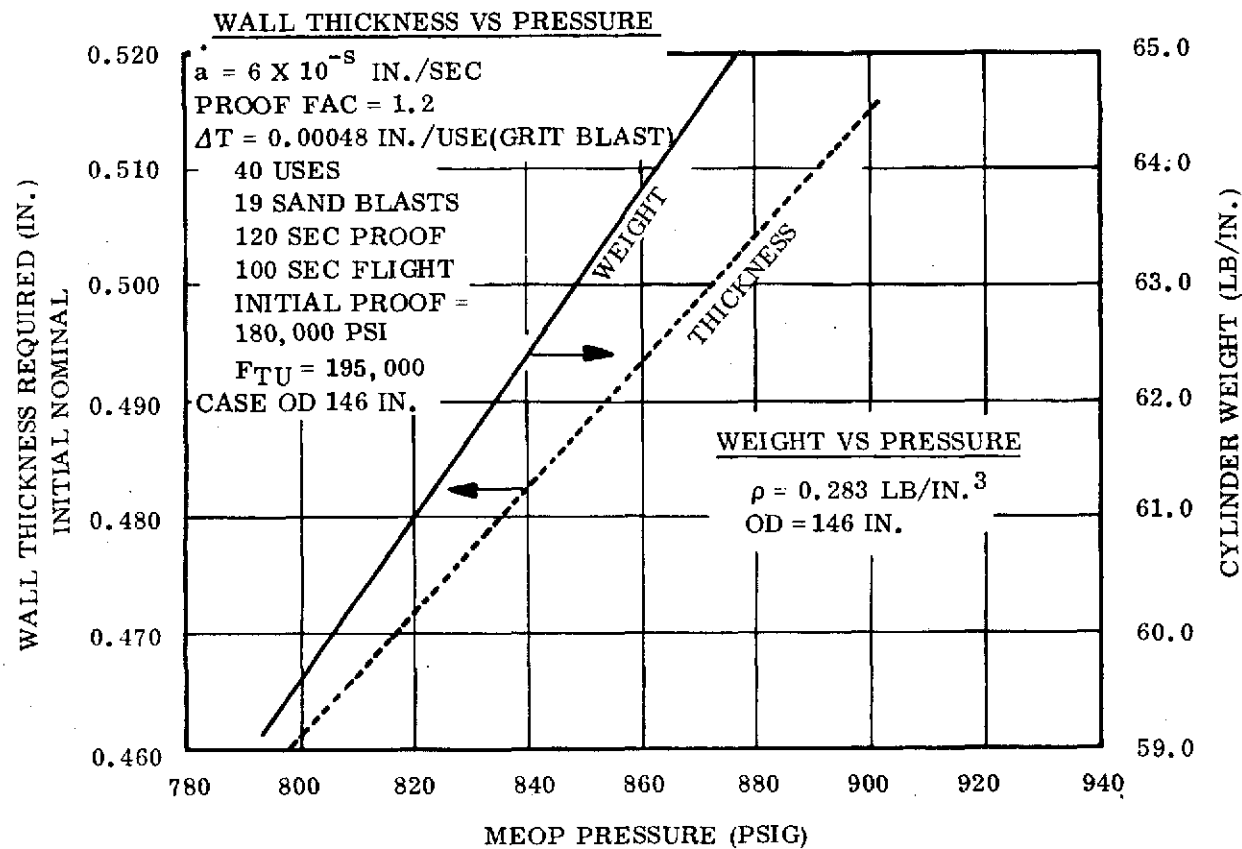


Figure 3-9. Weight Versus Pressure

INPUT DATA (Cont)

Given:

- F_{TU} = Ultimate Strength (195,000 psi)
 σ_{ip} = Initial Proof Stress = 180,000 psi
 ξ = Number of Cycles Where Δt is Removed (19)

ANALYTICAL PROCEDURE

FRACTURE MECHANICS APPROACH TO CALCULATING WALL THICKNESS INCLUDING GRIT BLAST REMOVAL EFFECTS

CALCULATE

(Pressure) + (Grit Blast) (Going to Grit Blast)

$$t_o = \frac{PR}{F_{TU}} (F.S.) + \xi \Delta t \quad \xi \text{ times}$$

$$a_o = \frac{K_{IC}^2}{1.2 \pi \sigma_{ip}^2} \leq \begin{cases} \text{Max Flaw Depth to Survive Initial Proof} \\ \text{Constant in Problem, No Matter What} \\ \text{the Wall Thickness Requirements We Can} \\ \text{Proof Test to } \sigma_{ip} - \text{The Initial Will Drop} \\ \text{Out Later} \end{cases}$$

INTEGRATE CRACK GROWTH

Return All Calculated Values
to Zero Except New t_o and a_o

$$a_n = \sum_{i=1}^N \Delta a_i = \sum_{i=1}^M \left\{ \begin{array}{l} \frac{da}{dn} \Big|_{K_i} + aT_1 \quad i \text{ odd} \\ \frac{da}{dn} \Big|_{\phi K_i} + aT_2 \quad i \text{ even} \end{array} \right\}$$

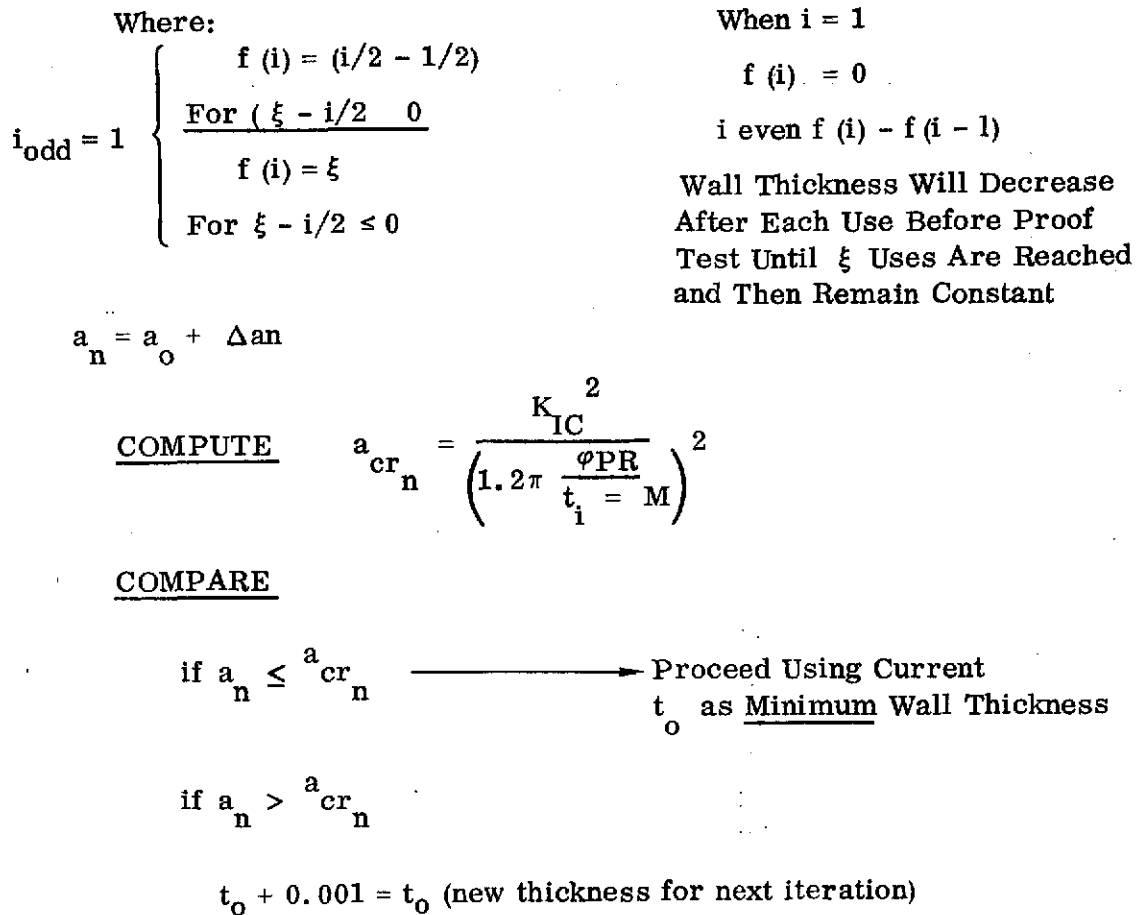
$M = 2N$ (Each Use is a Two Event Sequence)

Where:

$$K_i = 1.1 \frac{PR}{t_i} \sqrt{\pi(a_o + \Delta a_i)_{\text{previous}}} \leq \begin{cases} \text{Stress Intensity} \\ \text{a Function of} \\ \text{the Instantaneous} \\ \text{Crack Depth and} \\ \text{the Existing} \\ \text{Wall Thickness} \end{cases}$$

Where:

$$t_i = t_o - f(i) \Delta t$$



3.2.1.4 Skirt Attachment Joints

Figures 3-10 and 3-11 (Sketches SK50183 and SK50184) are conceptual drawings of clevis type attachment mechanisms for the forward and aft SRM skirts, respectively.

The sketches have been "rough sized" to accept the peaking loads as presented in S & E-ASTN-AS (74-15). See figure 2-1. Enough analysis has been completed to insure the utility of the basic concept; however, far more detailed analysis will be required as final designs evolve.

The forward joint concept (figure 3-10) incorporates a provision for a single O-ring seal. The joint could also be protected externally in the same manner that the case joints will be protected. Very minimal clearance is required between the female clevis and the dome due to the displacement characteristics of a 2:1 dome.

Figure 3-10. Clevis Type Attachment Mechanism for Forward Skirt (SK50183)

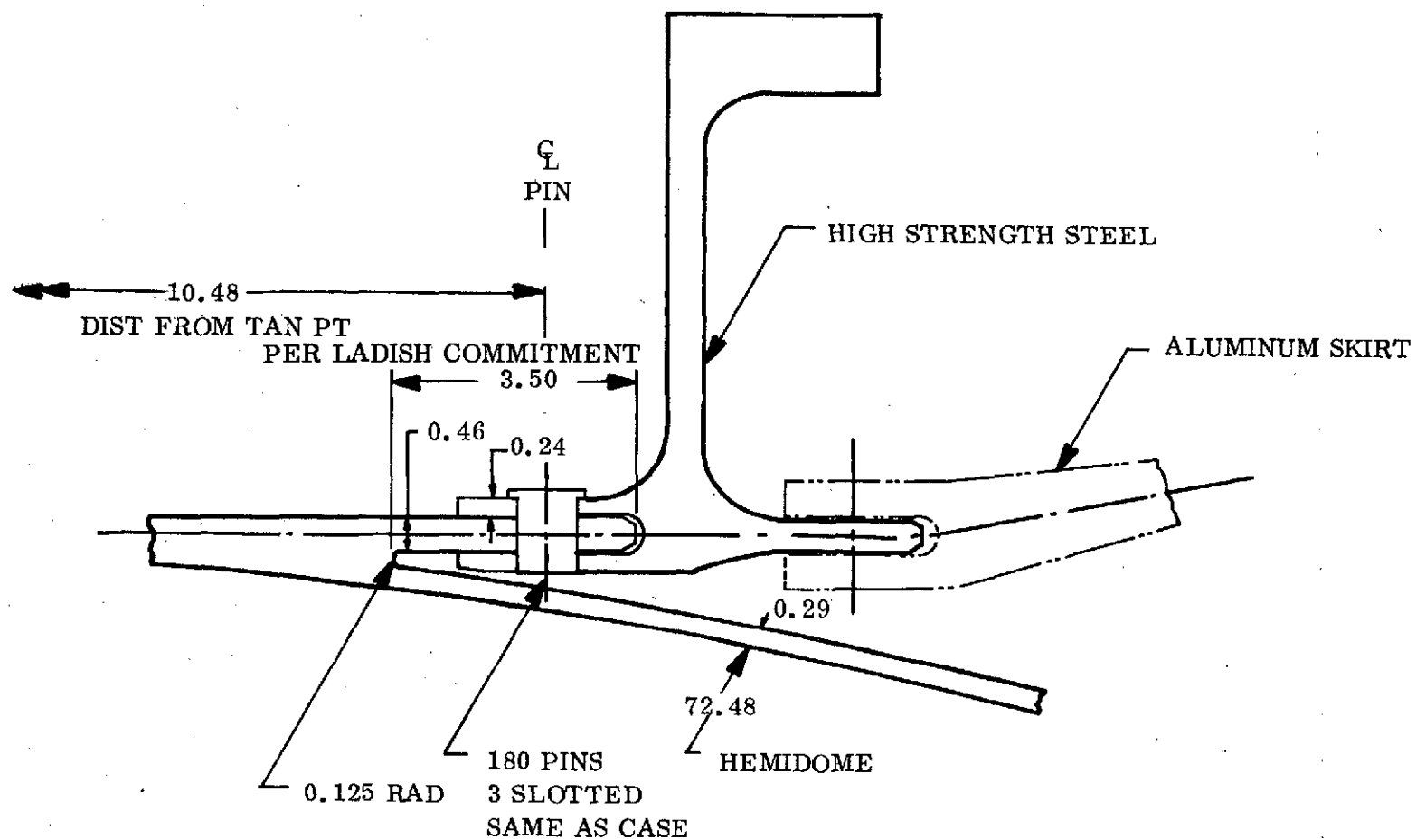


Figure 3-11. Clevis Type Attachment Mechanism for Aft Skirt (SK50184)

The aft joint concept (figure 3-11) does not incorporate a seal as none is required. Adequate clearance is provided between the joint and the dome to accommodate dome growth at limit pressure. It can be noted on figure 2-1 that the applied compressive loads are much higher than the applied tensile loads, and, therefore, the shear out and between hole tensile requirements of the joint are quite minimal.

The same pin size and hole pattern is maintained as in the primary segment joints. This will greatly facilitate case manufacturing processes and will also help in assembly through the use of three slotted holes.

The kick ring and skirt outline shown on the aft concept are merely schematic and can be altered to accommodate alternate skirt-actuator requirements.

Both forward and aft skirt lengths are shown as 3.5 inches. This is the maximum skirt length which can be provided based upon fore and aft dome forged preform constraints. This study indicates that this length is adequate to effect a workable, clevis type connection on both skirts.

3.2.1.5 Aft ET Attach Ring

On the basis of the RFP ET attach requirements TC developed an attach ring design with a "T" cross section. Subsequent changes in the strut support pattern and load magnitudes tended to make the "T" ring concept less attractive. A free ring analysis performed with the new loads indicated excessive tensile stress on the inside surface. A two flange design was also evaluated.

Two conditions were initially identified as the most severe: Liftoff and hi "Q" boost.

A free ring analysis was conducted on the design in order to determine the point of maximum stress. A shell supported ring analysis was conducted at this point.

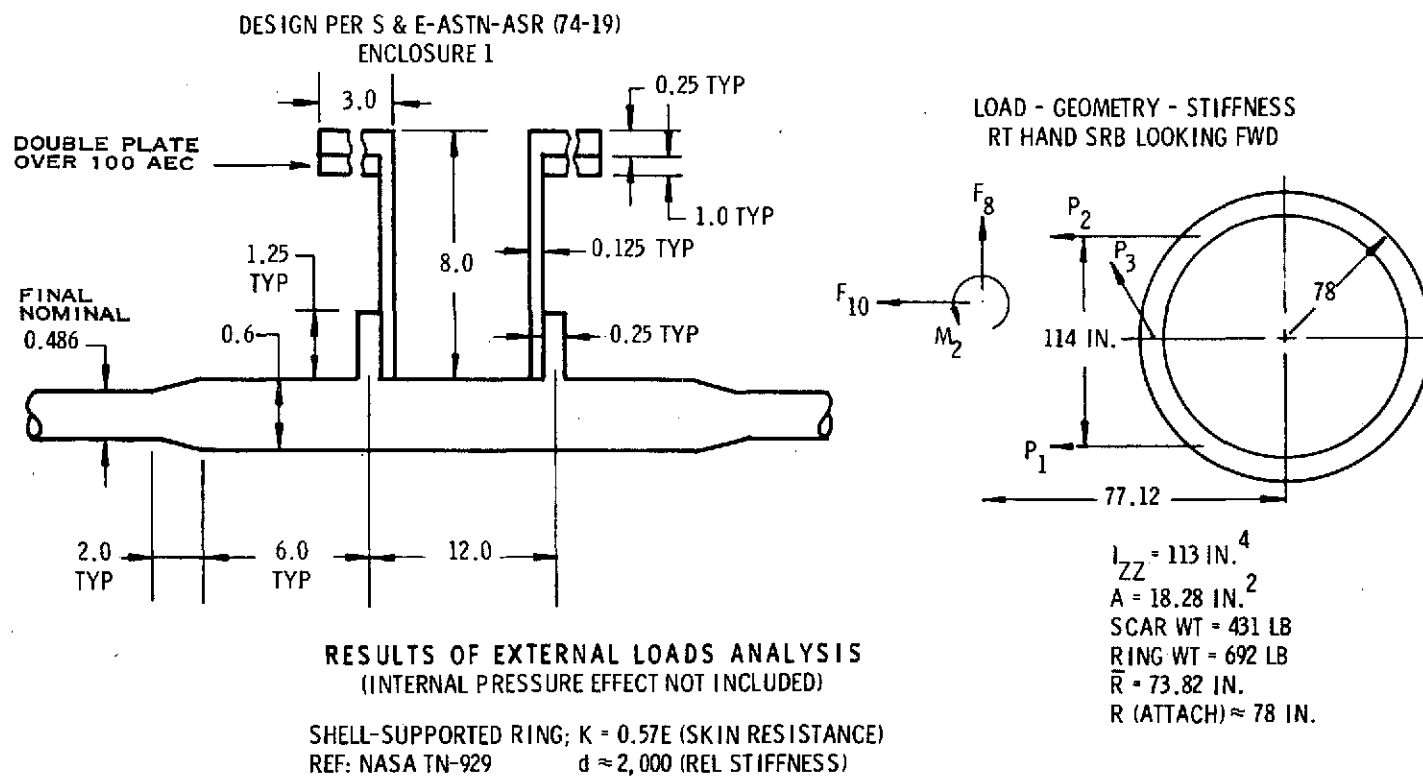
Figure 3-8 is a summary of the shell supported ring analysis as well as a description of the basic geometry involved. The table summarizes all applied loads involved in the analysis as well as the resulting strut loads.

The maximum strut load (P_2) was calculated to be 237,000 pounds occurring during the liftoff event. The maximum stress in the ring (σ_2) was determined to be -91,200 psi on the OD surface of the ring.

No compliance requirements have been defined, so various approximate stiffness parameters were calculated and are listed on figure 3-12. Included are the radial displacement R_2 (2 denotes under load P_2), the radial spring constant (K_R) and an approximate natural frequency f_n range for the loaded motor supported at the aft attach ring.

An internal pressure discontinuity stress analysis (figure 3-13) was conducted to determine the state of combined stress. The maximum inside surface stress at the center of the ring is 90,500 psi. This must be combined with a 17,200 psi inside surface stress due to ring bending for a total stress of 107,200 psi.

To verify these preliminary results a BOSOR analysis was conducted. The analysis considered the combined effects of internal pressure and externally applied loads. The design used in the analysis was Configuration 1-1 which has an internal MEOP of 861 psig.



	LIFTOFF	HIGH "Q" BOOST		LIFTOFF	HIGH "Q" BOOST
F_8	20,000 LB	206,000 LB	P_3	-20,865 LB	-214,900 LB
F_{10}	-72,500 LB	-88,000 LB	σ_2	91,200 PSI	<LIFTOFF
M_2	$23.4 \times 10^6 \text{ IN. -LB}$	$11.2 \times 10^6 \text{ IN. -LB}$	ΔR_2	+0.068 IN.	<LIFTOFF
P_1	171,040 LB	75,160 LB	K_R	$0.37 \times 10^6 \text{ LB/IN.}$	
P_2	-237,600 LB	-102,000 LB	f_N	6-12 HZ (LOADED)	

Figure 3-12. Aft Attach Ring Frame Analysis (Configuration 1-1)

REF: S & E - ASTN - ASR (74-19)
ENCLOSURE 1

(NO EXTERNAL LOADS)

$P = 849 \text{ PSIG}$

$T = 3.161 \times 10^6 \text{ LB}$

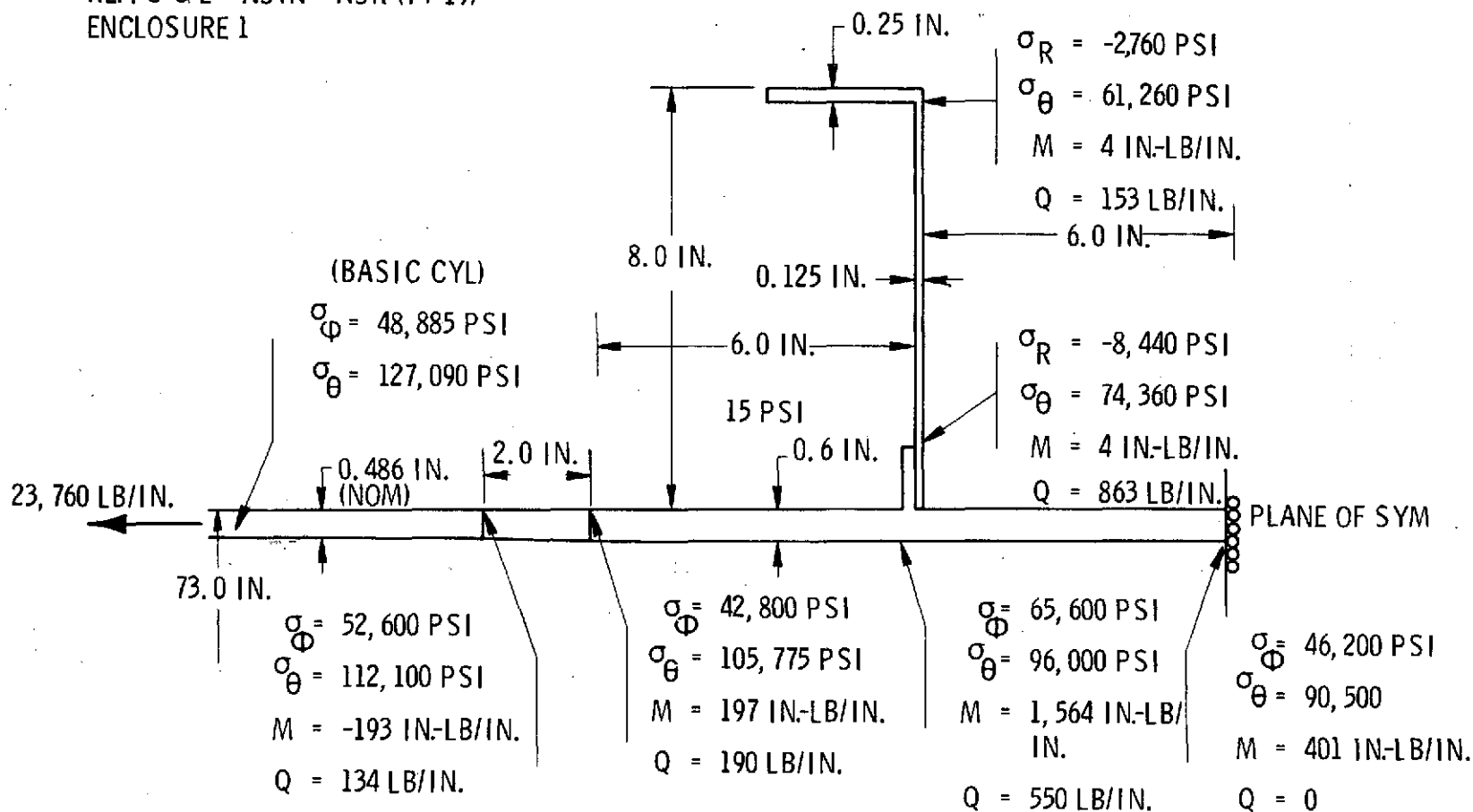


Figure 3-13. Aft Attach Ring Results of Discontinuity Analysis (Configuration 1-1)

The liftoff strut loads shown in figure 3-12 were applied to the ring. The resulting case wall inside and outside combined hoop stresses are shown in figure 3-14; the maximum values being 87,200 psi and 89,000 psi, respectively. The resulting margin of safety is 2.19 (case wall).

Figure 3-15 is a plot of the stress distribution along a meridian which intersects the strut load point P_2 (See figure 3-12). It is on this meridian that the maximum stress levels were observed. The stresses shown are for a combined condition of liftoff strut loads and 861 psig (MEOP) internal pressure. The maximum stress level shown is 132,000 psi which gives the required 1.4 factor of safety.

This indicates that the wall thickness taper as described in figure 3-12 is adequate to dampen out discontinuity stresses in the case wall.

An additional loading requirement was introduced during the interim contract period. The condition existed during partial fueling of the ET tank where thermal shrinkage loads are combined with one day wind loads. The maximum strut load during liftoff (237,000 lb) is sufficiently greater than the partial fueling condition; therefore, the partial fueling condition is not a factor in the design.

In summary, the ET ring design as shown in figure 3-12 appears adequate to react the specified design loads as shown in figure 2-1.

3.2.1.6 Water Impact

The SRM case and nozzle have been analyzed and designed for various configurations and loads during the contract period. Trends have also been established for various design parameters such as wall thickness, stiffener sizes, stiffener spacing, etc. The results are shown under each individual load condition.

A summary of the final analysis results for these water impact events is shown in Table XII.

The two main configurations investigated were Configuration 0 and Configuration 1-1. Configuration 0 is not adequate for the latest cavity collapse loads nor the

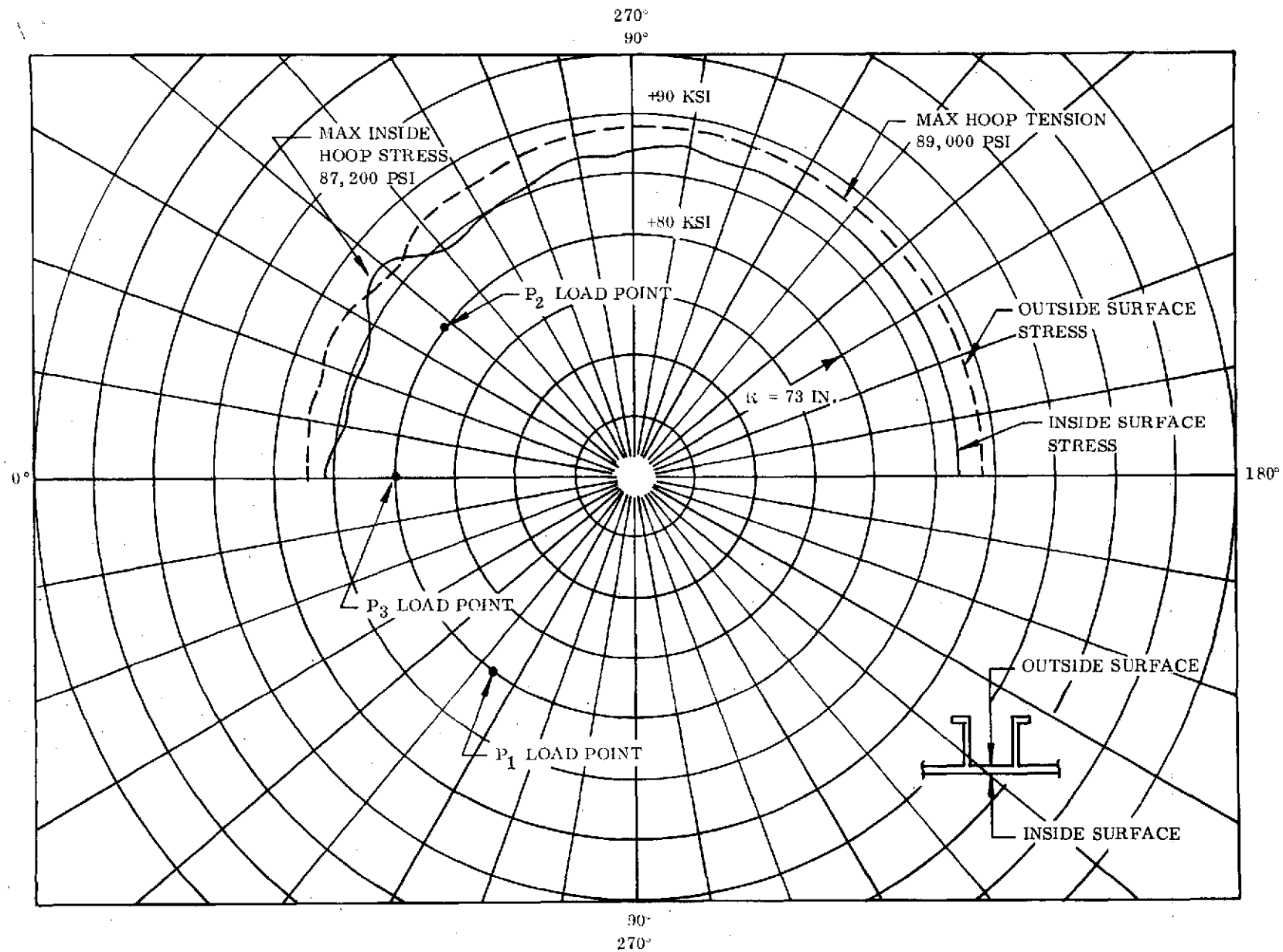


Figure 3-14. ET Attach Ring - Liftoff Condition Plus 861 psi Internal Pressure (Configuration 1-1)

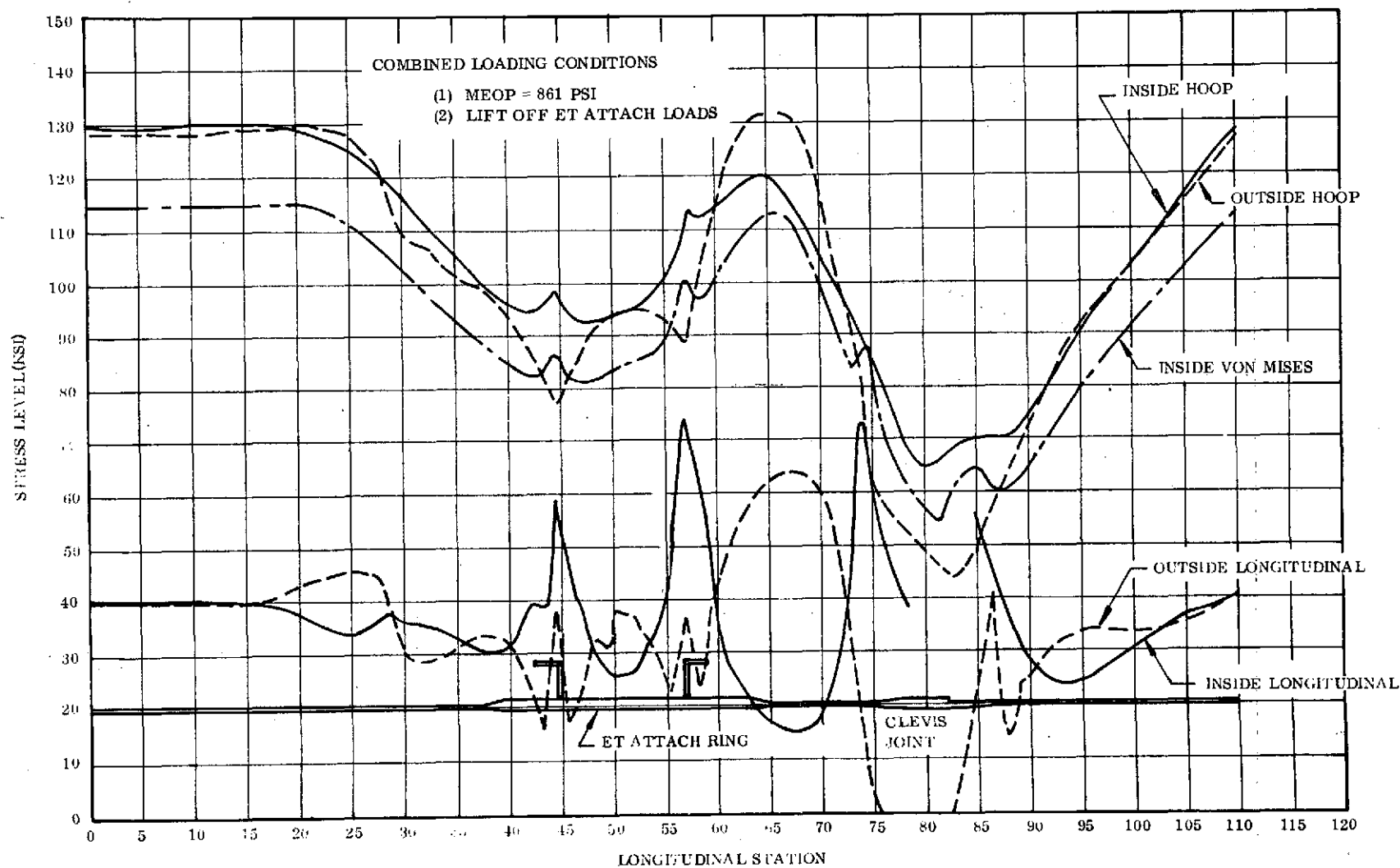
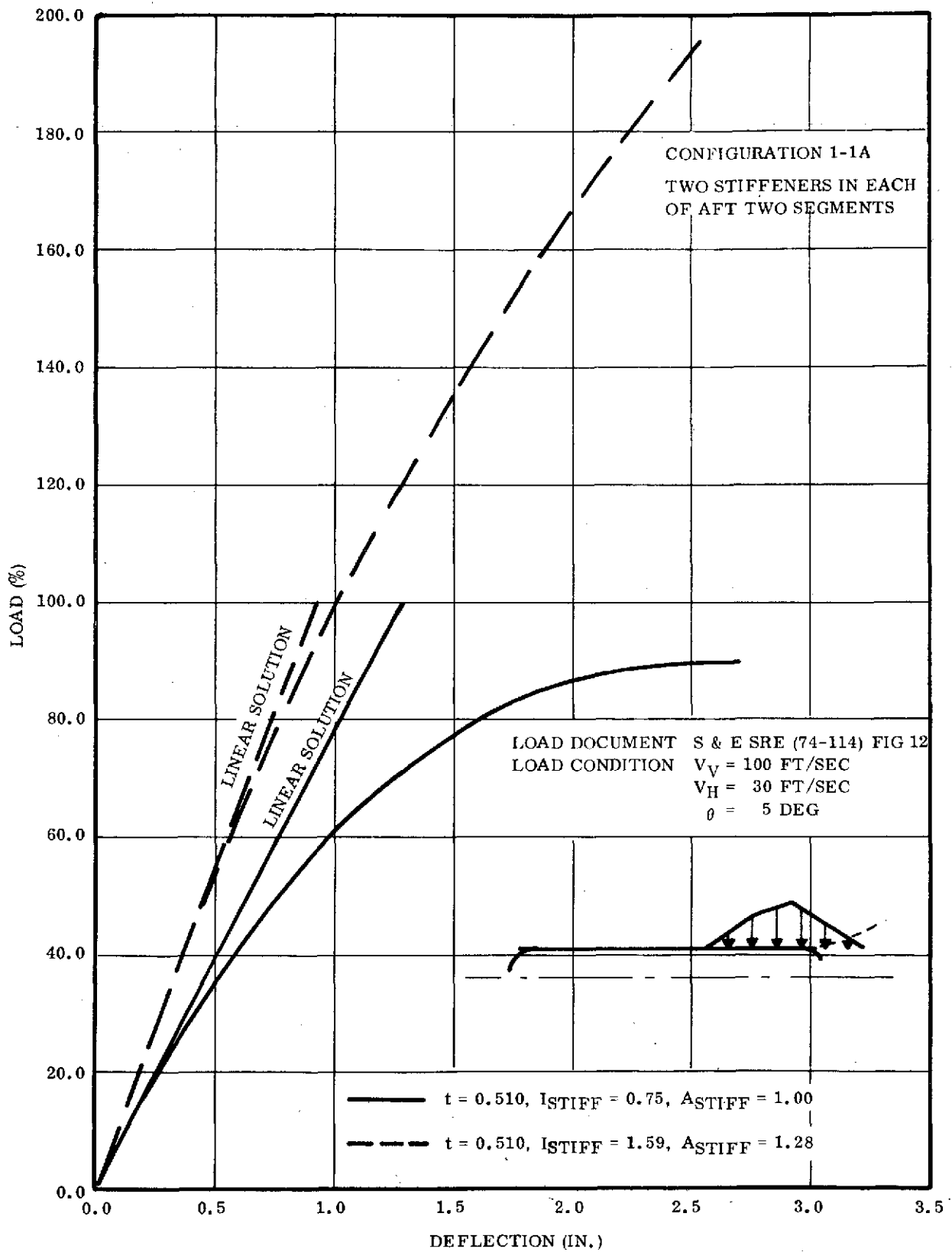


Figure 3-15. Combined Stress Distribution in SRM Case on the Meridian Containing Strut Load "P₂" (Configuration 1-1)

TABLE XII
SRM BUCKLING SUMMARY - WATER IMPACT LOADS

<u>Component</u>	<u>Configuration</u>	<u>Load</u>	<u>Analysis</u>	<u>Eigenvalue</u>	<u>KDF</u>	<u>FS</u>
Case Cylinder	Conf. 0	Slapdown- $V_V = 100$, $V_H = 45$, $\theta = 5^\circ$	STAGS-Nonlinear	--	--	1.31
			BOSOR-Indic 4	1.83	0.717	1.31
	Conf. 1-1	-same-	STAGS-Nonlinear (extrapolated)	--	--	1.50
	Conf. 1-1	Cavity Collapse- $V_V = 100$, $V_H = 30$, $\theta = 5^\circ$	BOSOR-Indic 1	1.38	0.75	1.03
	Conf. 1-1A ($I_{ST} = 1.59$, $t = 0.51$)	Cavity Collapse- $V_V = 100$, $V_H = 30$, $\theta = 5^\circ$	STAGS-Nonlinear	--	--	1.94*
	Conf. 0	Cavity Collapse-Old Loads- $P_{max} = 135$	BOSOR-Indic 1	0.52	0.75	0.39
	Conf. 0	Penetration- $V_V = 100$, $V_H = 0$ $\theta = 0^\circ$	BOSOR-Indic 1	4.19	0.75	3.14
Case Aft Dome	Conf. 0 ($t = 0.274$)	Max. Axial Acc. - $P = 253$ psi	BOSOR-Indic 1	1.60	0.75	1.20
	Conf. 1-1 ($t = 0.279$)	-same-	BOSOR-Indic 1	1.67	0.75	1.25
Nozzle	Conf. 0	Max. Axial Acc. - $V_V = 100$ $V_H = 0$, $\theta = 10^\circ$	BOSOR-Indic 1	7.55	0.75	5.66
	Conf. 0 (with abla- tives)	Max. Pitch Acc. - $V_V = 100$, $V_H = 45$, $\theta = 0^\circ$	BOSOR-Indic 4	5.92	0.50	2.96

*This nonlinear analysis has not been completed to date. A value higher than this will be attained as shown on figure 3-16.



maximum pitch acceleration loads on the nozzle. STAGS calculations were used to assess effects of cavity collapse loads on the aft two segments of Configuration 1-1A. Indications are that the wall thickness (0.51 in.) is adequate.

At the point in the program where consideration of Configuration 1-1A was initiated, it was mutually agreed by Thiokol and MSFC that performance studies would be based upon the basic design shown in TUL 13936. In order to withstand current cavity collapse loads and pad loads it was anticipated that the aft cylindrical segment would require a wall thickness of 0.56 in. and two ring stiffeners of $I = 7.7 \text{ in.}^4$ and $A = 3.50 \text{ in.}^2$. (See Table X, Run No. 42.) The next to last cylindrical segment would require a wall thickness required for motor operating pressure only and would have provisions for external ring attachment but would use no actual rings. From a weight-performance standpoint this initial assumption proved to be conservative, however, subsequent structural analysis indicated that some modification would be necessary in order to make Configuration 1-1A adequate for cavity collapse loads.

The latest assessment for a design which will endure cavity collapse consists of two aft segments with a final nominal wall thickness of 0.51 in. with two stiffening rings in each segment located at the third points. The new rings have an I of 1.59 in.^4 and an area of 1.26 in.^2 . The new configuration actually results in an overall weight savings over the initial assumption.

During a 20 February meeting between MSFC and Thiokol, several water impact conditions were identified by MSFC as being critical for the SRM design. These conditions are listed in the 14 February column of figure 2-1. It was further agreed that Thiokol would evaluate these conditions using the BOSOR computer program, applying a knockdown factor "KDF" of 0.5 to all nonaxisymmetric loading results and a KDF of 0.75 to symmetric loads such as occur during penetration.

The analysis was conducted and a summary presentation of the design trends was given to NASA. The main thrust of the presentation was that an estimated weight of 23,670 pounds would have to be added to the Configuration 0 structure in

order to provide a structurally acceptable design. In addition, an estimated 1,900 pounds would be required to accommodate grit blasting. It was apparent that the primary reason for the large added weight requirement was the conservative nature of the BOSOR program with the agreed on KDF. The most expeditious solution to the problem appeared to be to analyze the SRM with a nonlinear analysis technique such as STAGS.

A second reason for the weight increase was a rather significant change in water impact loads from the time of the RFP. These loads were reviewed by NASA and some changes were made; principally in the area of the entry angle of the slapdown condition which was changed from -10° to -5° .

The results of the STAGS analysis did substantiate the conservative nature of the BOSOR-KDF approach. The minimum KDF for the slapdown condition was determined to be 0.717 instead of 0.5 as assumed. The net effect of this analysis was to determine the minimum wall thickness required for slapdown to be at least 0.461. Additional STAGS work by NASA indicates that it may be as low as 0.41. Since 0.461 is under the wall required for internal pressure no additional weight was required for slapdown.

Cavity collapse loads for Configuration 0 could be accommodated by the addition of a stiffener ring at the midjoint of the aft segment. The addition of this stiffener ring also made the case adequate for penetration.

When new cavity collapse loads were developed, the design was no longer suitable. Additional performance requirements along with the new cavity collapse loads and fabrication limitations created a need for two aft segments with two stiffening rings in each segment at the 1/3 points. It was estimated a 0.51 inch (final nominal) thickness would be required in the aft segments to accommodate cavity collapse and aft peaking loads. Further analysis indicated that 0.51 inch was adequate for the aft peaking loads and the cavity collapse condition.

The BOSOR results for the slapdown loads were confirmed by two STAGS runs. The STAGS results gave a KDF of 0.717 for a thickness of 0.496 inch . The KDF increases for lower thicknesses (higher R/t ratios). For a thickness of 0.466 inch the KDF is 0.767. However, all final designs will require verification with a STAGS nonlinear analysis.

The revised cavity collapse loads are much more severe than the old loads. The slapdown loads at $\theta = 10^\circ$ were more severe than the old slapdown loads, and the $\theta = 5^\circ$ loads are very close to the old loads. The penetration loads are slightly more critical than the old loads.

All nozzle loads are much higher than the RFP loads (by a factor of about 10) and, in general, the water impact design loads for the nozzle are more severe than the internal pressure and actuator loads.

3.2.1.7 Slapdown

Slapdown conditions were originally modeled on BOSOR 4. This analysis of Configuration 0 at $\theta = -10^\circ$ revealed an unsatisfactory safety factor (0.95 for KDF = 0.717). Subsequent stiffening of the segments of the SRM indicated that an adequate factor of safety could be attained with a small sacrifice in weight.

To obtain a factor of safety of 1.25 with a KDF of 0.717 either the wall thickness must increase or the spacing between stiffeners must decrease. The minimum wall thickness required for a spacing of 156 inches is 0.501 inch. (See figure 3-17.) This is a weight increase of 709 pounds per segment. The moment of inertia of the joint required for a wall thickness of 0.466 inch and a spacing of 156 inches is approximately 3.8 in.⁴ as shown in figure 3-18. This increases the weight per joint 273 pounds.

Additional analysis was carried out on the model for a θ of -5° as updated by NASA. This condition reduced the severity of the slapdown loads considerably and, as may be noted in figure 3-19, Configuration 0 had a conservative factor of safety of 1.31. Configuration 1-1 has a factor of safety of 1.50 by extrapolating the STAGS analysis in relation to the BOSOR analysis. Figure 3-20 displays the complete STAGS analysis results. Table XIII is a summary of the BOSOR results for various configurations investigated.

3.2.1.8 Cavity Collapse

A summary of the case configurations with the factors of safety for the cavity collapse loads is shown in figure 3-21. Figure 3-22 shows the effect of varying the moment of inertia of the stiffeners in the aft segment with the original cavity collapse loads. This curve shows an optimum stiffener inertia of 0.58 to 0.60 in.⁴. The eigenvalue drops off very rapidly for a smaller inertia and remains constant for a larger inertia. The optimum stiffener inertia must be sufficient to force the buckling mode in the shell between stiffeners. Once this is accomplished, increasing the stiffener size has no effect.

The revised cavity collapse loads have a higher peak pressure, are higher on the case, and are generally spread over a longer length of the case. Either double stiffeners, a thicker wall, or a combination of the two is required to withstand the

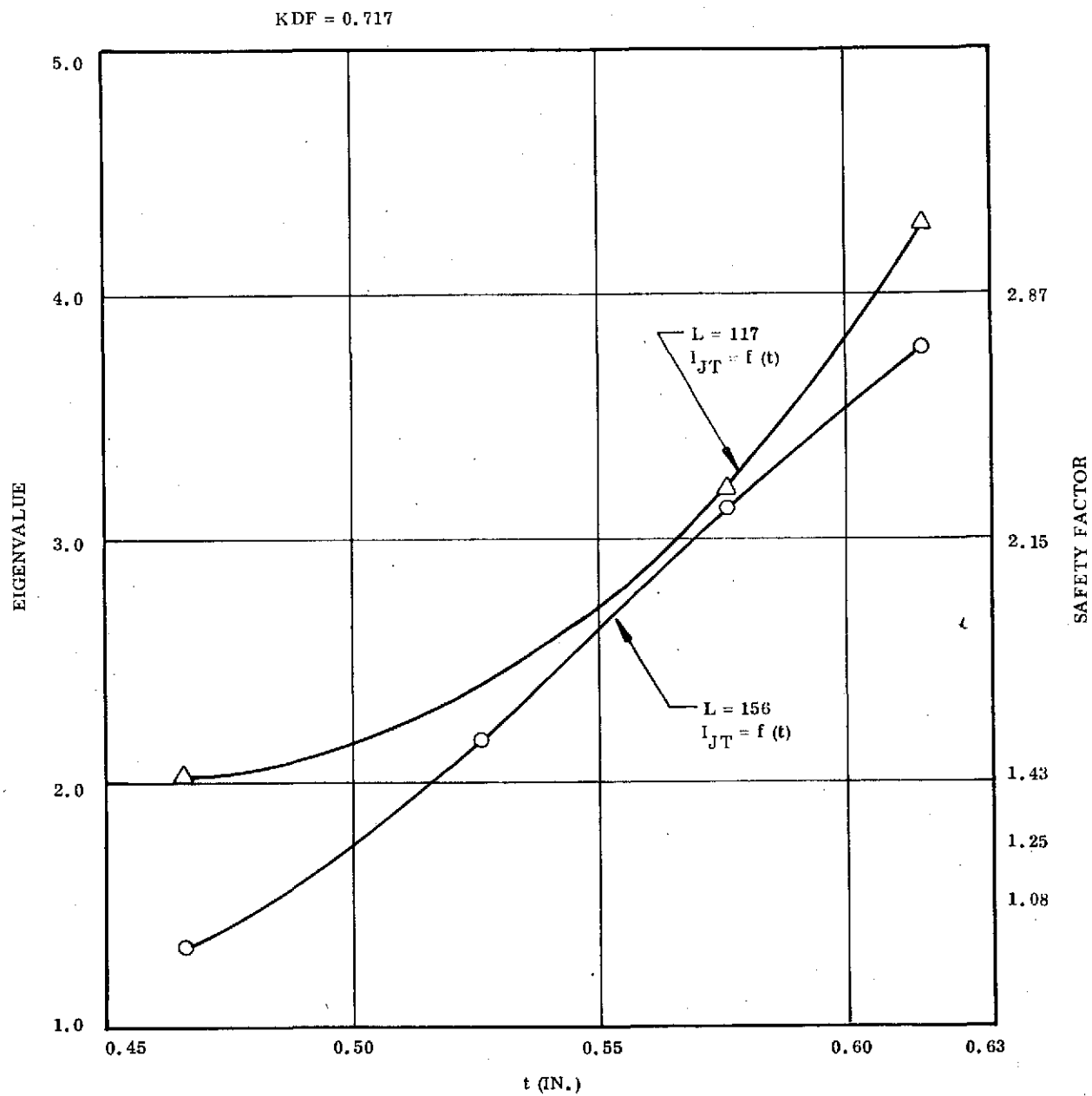


Figure 3-17. Slapdown Results, $t = 0.486$

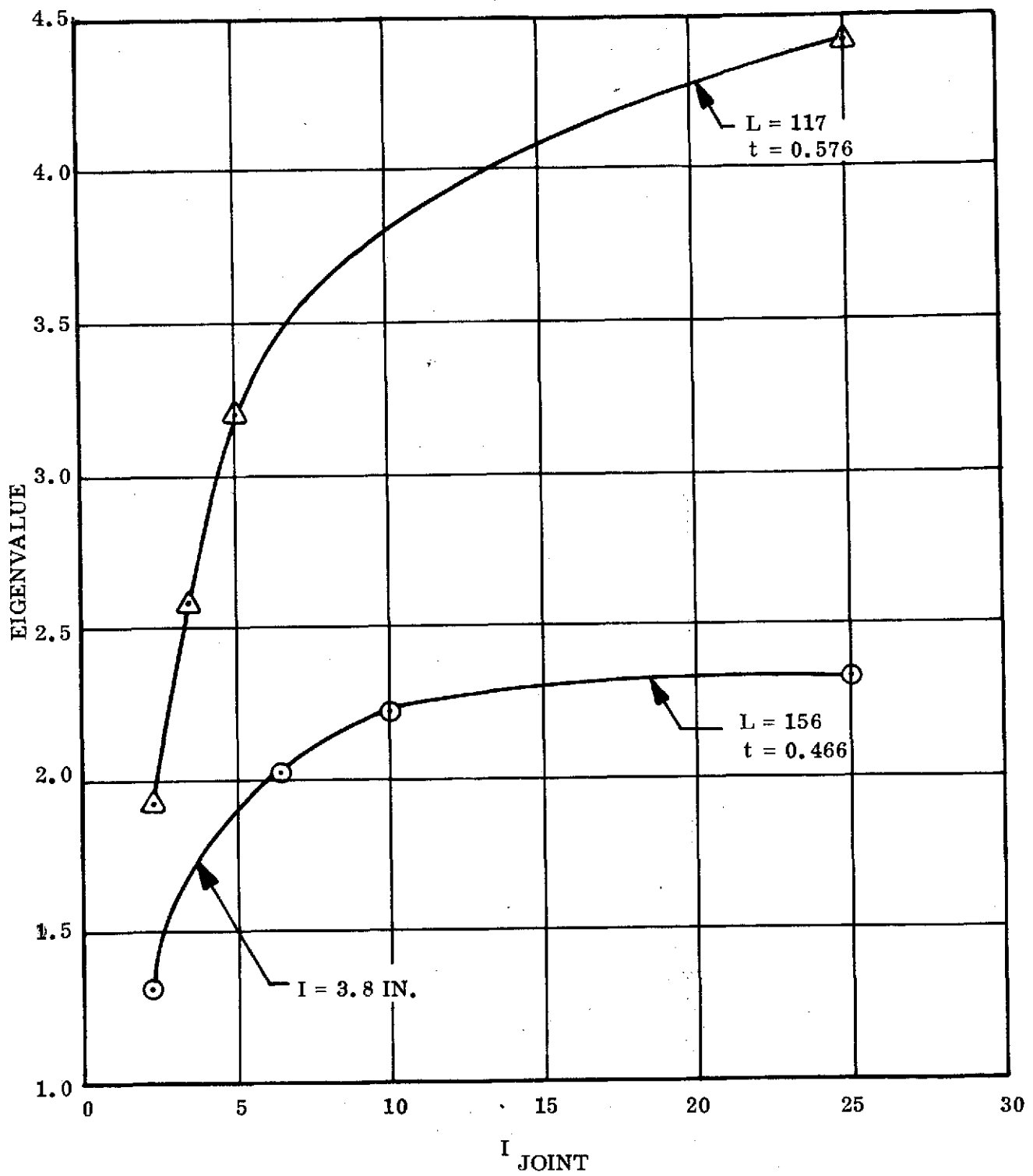


Figure 3-18. SRM Case Buckling Parameters (Slapdown $\theta = -10^\circ$)

3-2

$\theta = -5^\circ$; $T = 1.5$ AND 2.5
 $V_V = 100$ FT/SEC $V_H = 45$ FT/SEC

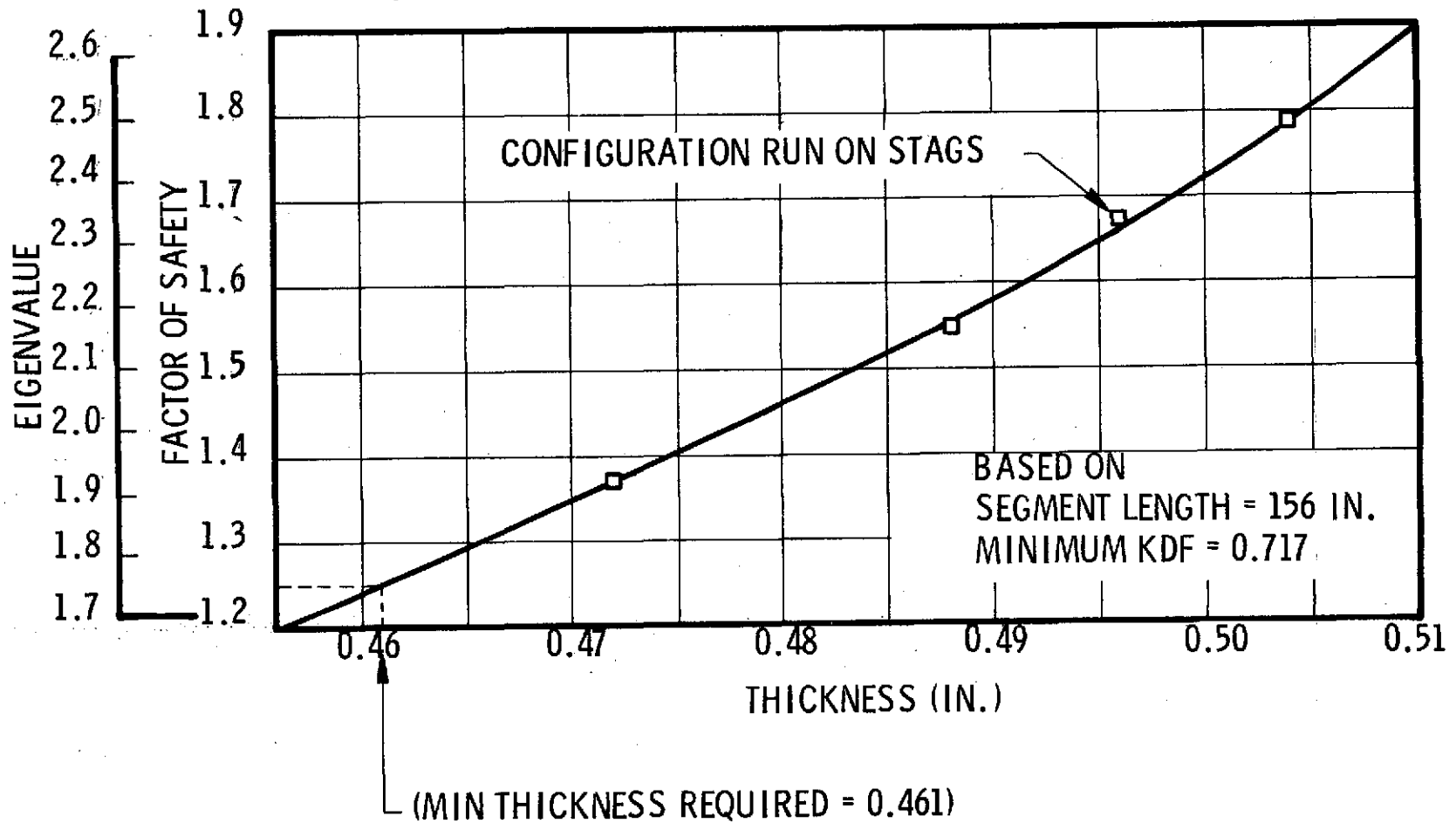


Figure 3-19. BOSOR Slapdown Results

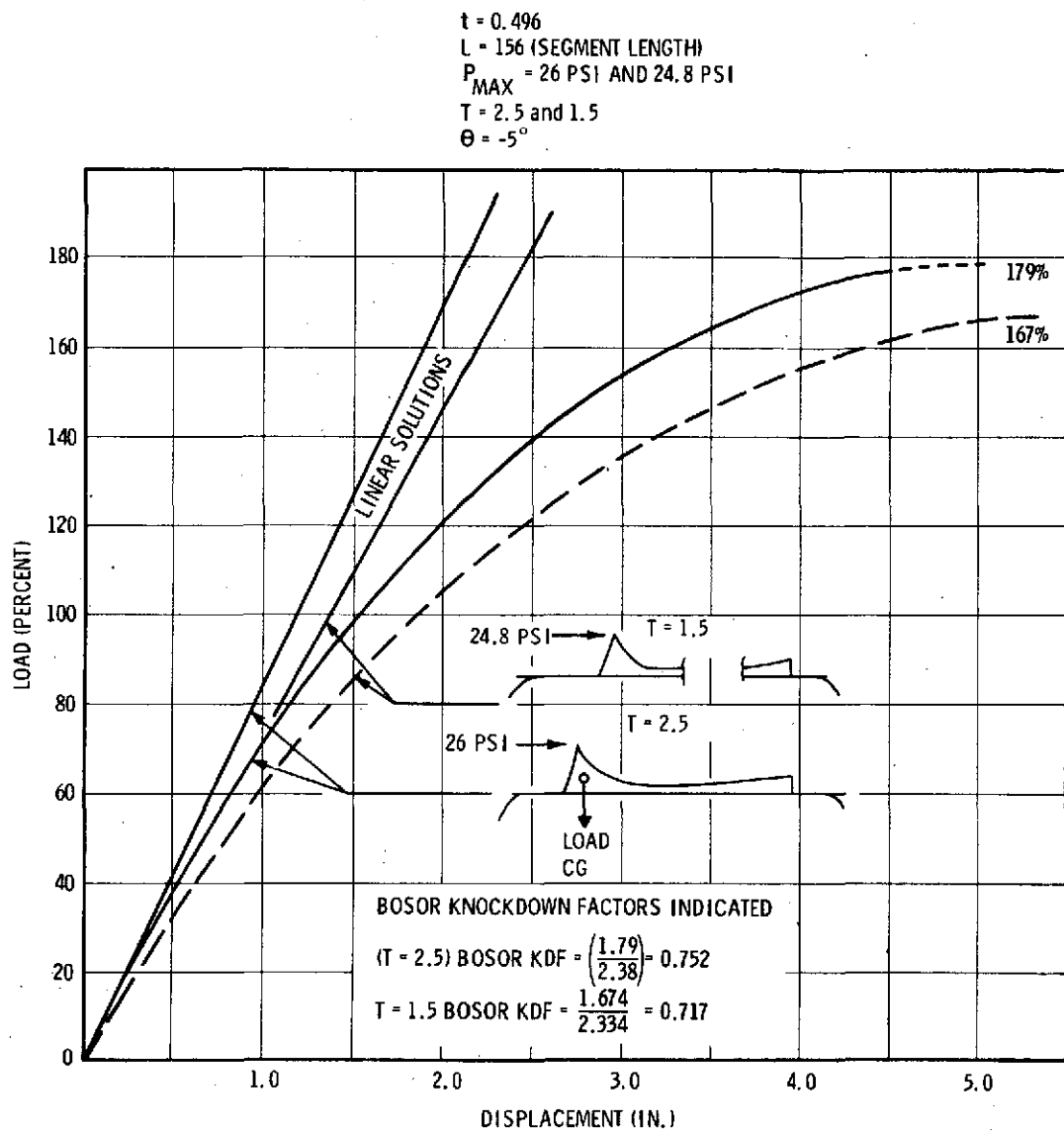


Figure 3-20. SRB Slapdown - STAG Analysis Results

TABLE XIII
SLAPDOWN BOSOR SUMMARY SHEET

Run	t	L	I_{jt}^{\dagger}	$I_{st}^{\dagger\dagger}$	N	E	FS*	Load***	Type** Problem	Comments
1	0.466	156	2.155	--	3	1.321	0.95	1	4	
2	0.466	156	4.310	--	3	2.034	1.46	1	4	Did Not Reach Minimum Eigenvalue
3	0.466	156	6.470	--	7	2.016	1.45	1	4	
4	0.466	156	10.0	--	7	2.225	1.60	1	4	
5	0.466	156	2.155	2.155	3	1.473	1.06	1	4	Maximum Load Over Stiffener
6	0.466	156	2.155	2.155	3	1.473	1.06	1	4	Maximum Load Between Stiffener and Joint
7	0.466	156	2.155	23.5	3	5.3	3.80	1	4	Maximum Load Over Stiffener
8	0.576	156	2.155	--	3	1.918	1.38	1	4	
9	0.530	117	2.155	--	3	1.450	1.04	1	4	
11	0.576	156	3.50	--	3	2.402	1.72	1	4	
12	0.466	156	25.0	--	7	2.325	1.67	1	4	
13	0.616	117	6.6	--	3	4.293	3.08	1	4	
14	0.576	117	5.0	--	3	3.200	2.29	1	4	
15	0.466	50	2.155	--	3	1.764	1.26	1	4	
16	0.576	90	5.00	--	3	3.812	2.73	1	4	
17	0.576	156	5.00	--	7	3.126	2.24	1	4	
18	0.616	156	6.6	--	6	3.781	2.71	1	4	
19	0.616	200	6.6	--	6	2.934	2.10	1	4	
20	0.576	117	2.155	--	3	1.937	1.39	1	4	
21	0.576	117	25.0	--	7	4.43	3.18	1	4	
22	0.526	156	3.50	--	3	2.170	1.55	1	4	
23	0.466	117	2.155	--	7	2.037	1.46	1	4	
24	0.496	156	2.762	--	3	2.334	1.67	2	4	$\theta = -5^\circ$
25	0.472	156	2.267	--	3	1.912	1.37	2	4	$\theta = -5^\circ$
26	0.488	156	2.566	--	3	2.161	1.55	2	4	$\theta = -5^\circ$
27	0.504	156	2.948	--	3	2.491	1.79	2	4	$\theta = -5^\circ$
28	0.576	117	3.50	--	3	2.588	1.86	1	4	
29	0.576	156	3.50	--	3	2.396	1.72	1	4	The Load is 20 In. Forward of Run 11
30	0.466	156	2.155	--	3	1.972	1.41	2	4	

*A knockdown factor of 0.717 is used for all points.

**Type 4 = asymmetric loading, Type 1 or -1 = axisymmetric loading.

***Load 1 is for $V_V = 100$ ft/sec, $V_H = 45$ ft/sec, and $\theta = -10^\circ$, Load 2 is the same except $\theta = -5^\circ$.

\dagger Joint moment of inertia.

$\dagger\dagger$ Moment of inertia of the stiffening rings.

N = number of buckling nodes

E = eigenvalue

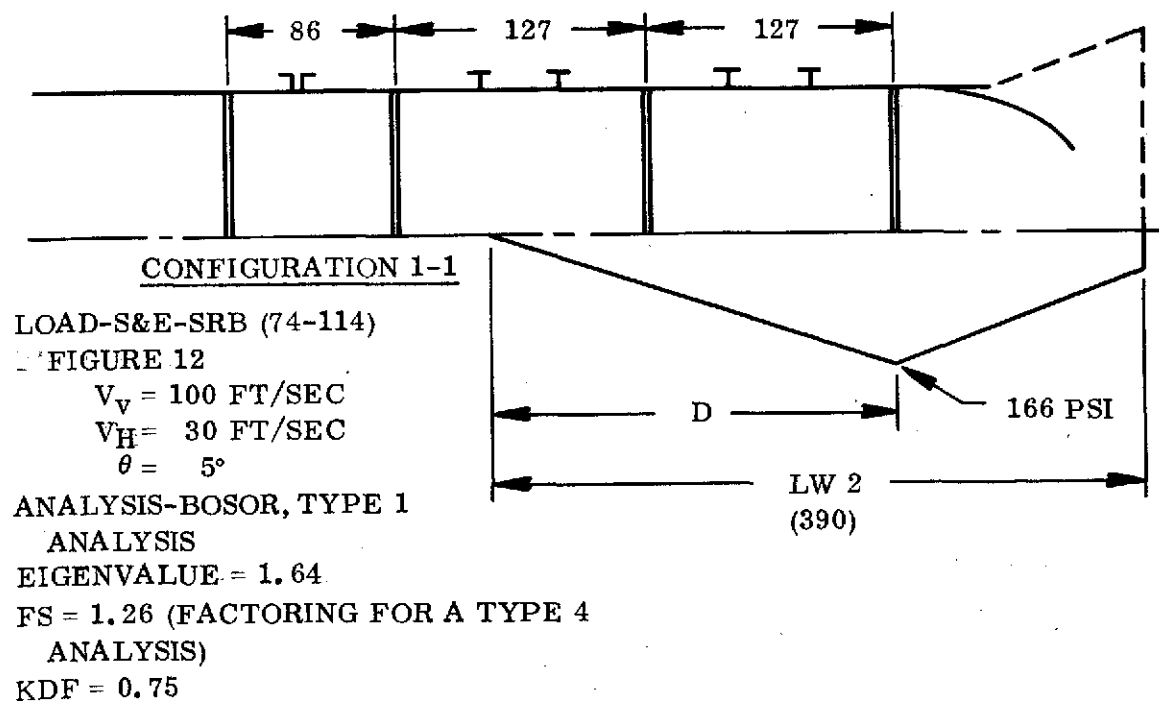
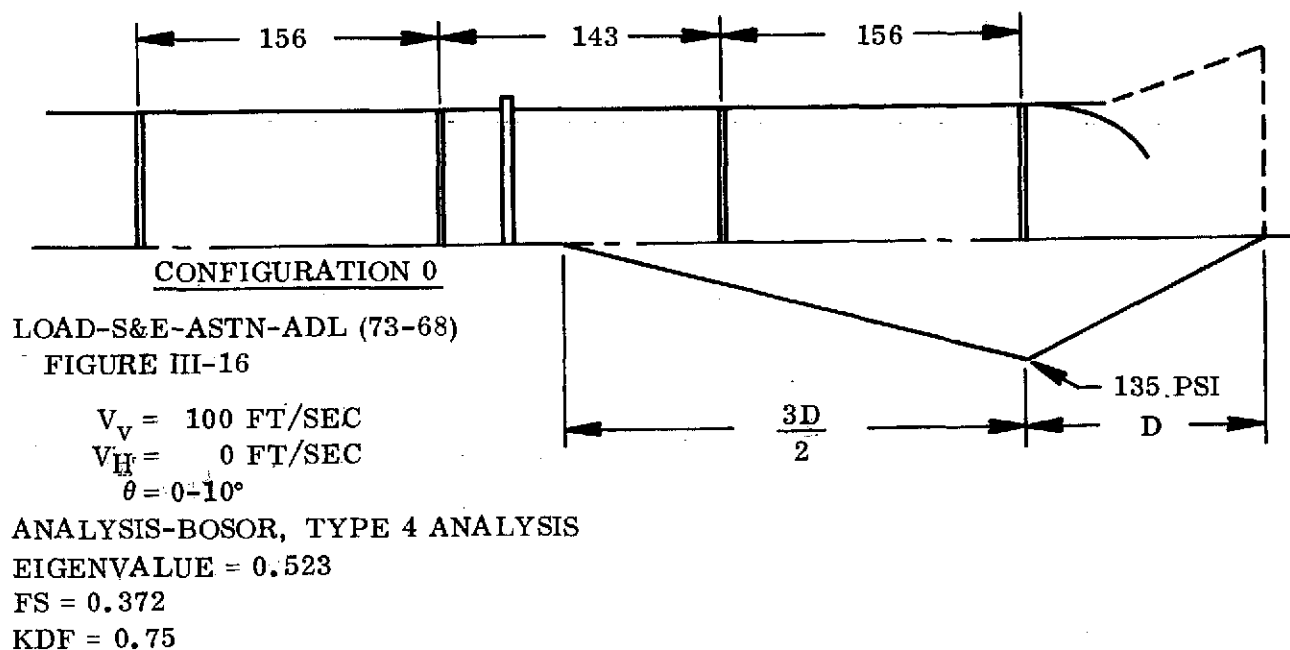


Figure 3-21. Cavity Collapse Summary

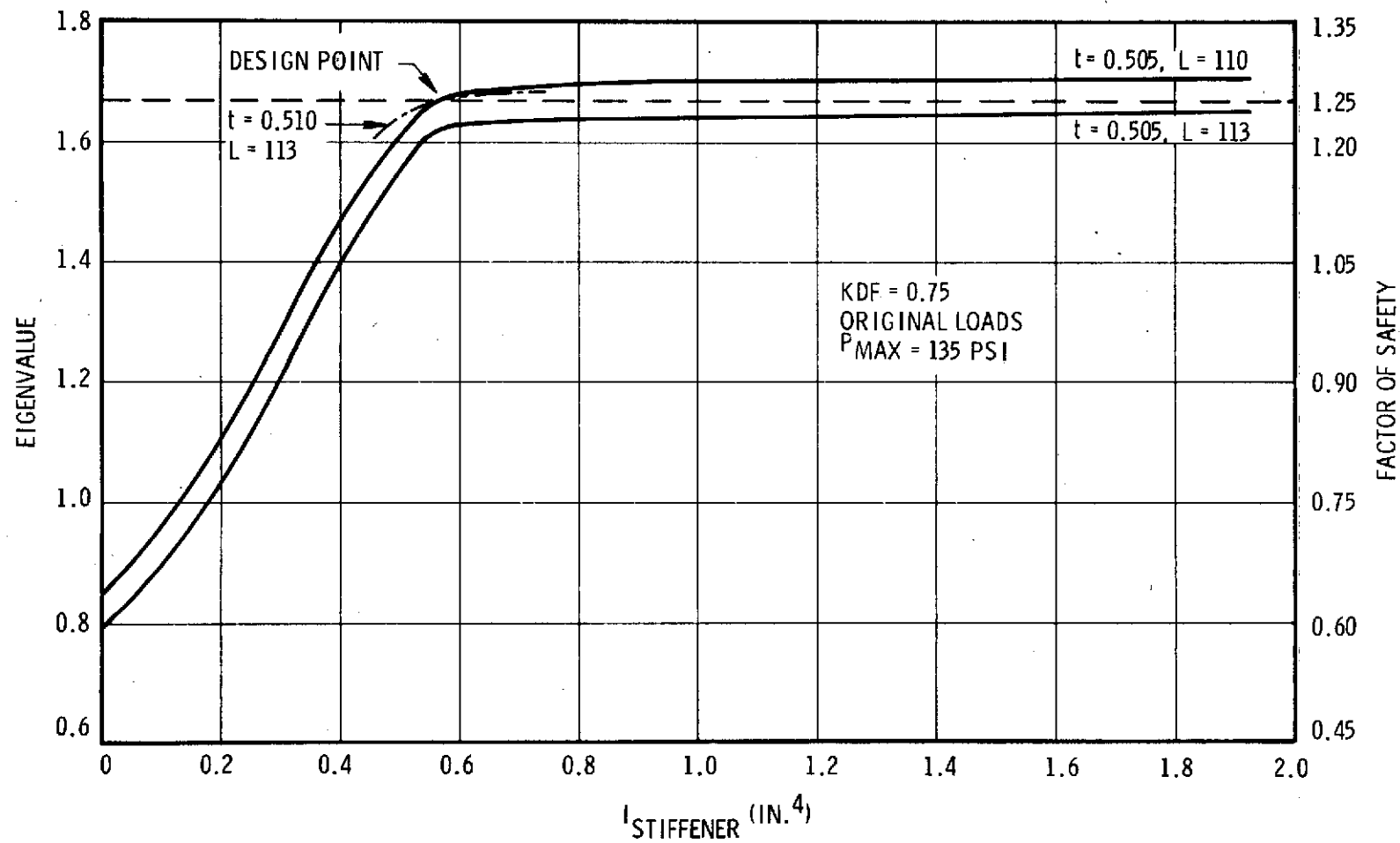


Figure 3-22. Cavity Collapse BOSOR 4 Results

new loads. An aft segment thickness of 0.510 inch was estimated to prevent buckling due to the aft launch pad peaking loads, and, therefore, it was assumed this thickness with two stiffeners in each segment would prevent cavity collapse buckling. The BOSOR results (Indic = 1) show a FS of 1.03 for this assumption (Configuration 1-1, $V_V = 100$, $V_H = 30$, $\theta = 5^\circ$). The buckling pressure for a type 1 problem (axisymmetric load) is lower than for a type 4 problem (asymmetric load) (See runs No. 23 and 34 on table X). Therefore, the results are conservative for this type of loading. An increase of 22 percent was shown on run 23 (type 4 problem) over run 34 (type 1 problem). Applying the 22 percent for this run would give a factor of safety of $1.03 (1.22) = 1.26$. This was verified with a STAGS analysis as shown in figure 3-16. Increasing the stiffener moment of inertia to 1.59 increased the buckling pressure above 194 percent of design load as shown on the STAGS nonlinear run.

A summary sheet showing the BOSOR runs made during the contract for the cavity collapse load is shown in Table XIV.

3.2.1.9 Penetration

The penetration analysis was also performed on BOSOR. The loads during penetration are much lower than the cavity collapse loads, and, therefore, do not design the aft segments.

Configuration 0 with no stiffener in the aft segment gave an eigenvalue of 1.38 for a factor of safety of 1.03. The addition of one small stiffener in the center of the aft segment increases the eigenvalue to 1.90 for a factor of safety of 1.43.

BOSOR gave an eigenvalue of 4.19 on Configuration 1-1 for a factor of safety of 3.14. A summary of all the BOSOR runs on penetration models is shown in Table XV.

3.2.1.10 Aft Dome

The aft dome was analyzed on the basis of several references to determine the effects of each on the delta case weight. A summary of the results is shown

TABLE XIV

CAVITY COLLAPSE BOSOR SUMMARY SHEET

Run	t	L	I_{jt}^1	I_{st}^2	N	E	FS ³	Load ⁴	Type ⁵ Run	Comments
1	0.466	156	2.155	--	7	0.523	0.40	1	4	Configuration 0
2	0.466	156	2.155	0.900	10	0.955	0.72	1	4	
3	0.466	156	2.155	5.000	10	0.963	0.72	1	4	
4	0.466	156	2.155	19.000	10	0.965	0.72	1	4	
5	0.466	100	2.155	--	8	0.748	0.56	1	4	
7	0.656	100	2.155	--	5	1.453	1.09	1	4	
8	0.466	100	2.155	11.400	12	1.624	1.22	1	4	Did Not Reach Minimum Eigenvalue
9	0.576	100	2.155	5.030	11	2.644	1.98	1	4	
10	0.576	100	2.155	2.900	7	1.203	0.90	1	4	
11	0.496	100	2.760	11.400	2	2.071	1.55	1	4	
12	0.496	100	2.760	19.000	6	2.097	1.57	1	4	
13	0.466	100	2.155	19.000	10	1.799	1.35	1	4	
14	0.472	100	2.267	11.400	9	2.260	1.70	1	4	
15	0.472	100	2.267	7.200	9	2.255	1.69	1	4	
16	0.466	100	2.155	8.000	10	1.975	1.48	1	4	
17	0.486	110	2.155	--	8	0.756	0.57	1	4	
17A	0.486	110	2.155	0.580	11	1.523	1.14	1	4	
17B	0.486	110	2.155	1.270	11	1.540	1.16	1	4	
18	0.476	110	2.155	1.270	11	1.471	1.10	1	4	
19	0.496	110	2.155	0.580	11	1.593	1.19	1	4	
20	0.506	110	2.155	0.580	11	1.675	1.26	1	4	
20A	0.506	110	2.155	0.580	11	1.675	1.26	1	4	Stiffener in Last Segment Only
20B	0.506	110	2.155	0.580	8	1.616	1.21	1	4	All Segments Except Last 0.466 Th
22	0.506	113	2.155	0.580	11	1.627	1.22	1	4	
23	0.506	110	2.155	0.580	11	1.820	1.37	1	4	Short Model
25	0.506	110	2.155	0.294	5	1.253	0.94	1	4	
26	0.506	113	2.155	0.940	11	1.639	1.23	1	4	
27	0.510	113	2.155	0.580	11	1.660	1.25	1	4	
28	0.506	110	2.155	0.350	5	1.361	1.02	1	4	
29	0.506	110	2.155	--	8	0.831	0.62	1	4	
30	0.500	107	2.155	0.580	11	1.087	1.27	1	4	
31	0.490	103	2.155	0.580	11	1.663	1.25	1	4	
32	0.500	107	2.854	0.580	11	1.696	1.27	1	4	
33	0.516	118	2.155	0.580	10	1.619	1.21	1	4	
34	0.506	110	2.155	0.580	11	1.486	1.11	1	1	Short Model
35	0.510	127	2.508	0.750	4	1.375	1.03	2	1	Short Model 2 Stiffeners in Each of Aft 2 Segments.
36	0.510	127	2.508	0.750	4	1.375	1.03	2	-1	Same as Run 35
37	0.560	127	2.508	0.750	4	1.479	1.11	2	1	Short Model
38	0.600	127	2.508	0.750	4	1.564	1.17	2	1	Short Model
39	0.620	127	6.280	0.750	4	1.839	1.38	2	1	Short Model
40	0.510	127	2.508	0.580	4	1.348	1.01	3	-1	Short Model
41	0.510	127	2.508	0.750	4	1.417	1.06	2	-1	Same as Run 36 Except Different Boundary Condition
42	0.560	127	3.750	7.700	7	1.439	1.08	3	-1	Second Seg = 0.535, No Stiffeners in 2nd Segment 4 Stiffeners
43	0.560	127	3.750	7.700	4	4.261	3.20	2	-1	
44	0.560	127	3.750	5.460	4	4.435	3.33	2	-1	
45	0.560	127	3.750	4.150	4	3.591	2.69	2	-1	
46	0.560	127	3.750	1.590	4	2.285	1.71	2	-1	
47	0.560	127	3.750	2.900	4	3.114	2.34	2	-1	
48	0.560	127	3.750	7.700	11	3.190	2.39	3	-1	2nd Segment t = 0.535, 4 Stiffeners
49	0.560	108	3.750	7.700	3	4.239	3.18	3	-1	100 Inch Attach Segment
50	0.560	127	3.750	0.580	4	1.531	1.15	2	-1	
51	0.560	127	3.750	0.0	7	0.658	0.49	2	-1	
52	0.535	127	3.750	0.580	4	1.481	1.11	2	-1	
53	0.535	127	3.750	2.900	4	2.995	2.25	2	-1	
54	0.560	127	3.750	7.900	4	4.334	3.25	2	-1	
55	0.535	127	3.750	1.590	4	2.210	1.66	2	-1	
56	0.535	127	3.750	7.900	4	4.135	3.10	2	-1	
57	0.510	127	3.150	1.590	4	2.090	1.57	2	-1	
58	0.535	127	3.750	4.150	4	3.454	2.59	2	-1	
59	0.510	127	3.150	1.590	4	2.776	2.08	2	-1	New Stiffener Configuration
60	0.510	127	3.150	0.750	5	0.771	0.58	2	-1	d for Joint and Stiffener = 0
61	0.510	127	2.259	1.590	3	2.732	2.05	3	-1	Corrected Joint Properties
62	0.510	127	2.259	1.590	4	2.674	2.01	2	-1	

Notes:

- 1 Moment of inertia of the joint.
- 2 Moment of inertia of the stiffeners.
- 3 Factor of safety assuming a knockdown factor of 0.75.
- 4 Load 1 = S & E-ASTN-ADL (73-68) Figure III-16, $V_V = 100$, $V_H = 0$, $\theta = 0$ to 10° .
Load 2 = S & E-SRE (74-114) Figure 12, $V_V = 100$, $V_H = 30$, $\theta = 5^\circ$.
Load 3 = S & E-SRE (74-114) Figure 12, $V_V = 100$, $V_H = 15$, $\theta = 5^\circ$.
- 5 Type 4 or -1 is asymmetric loading.
Type 1 or -1 run is axisymmetric loading.

TABLE XV

PENETRATION BOSOR SUMMARY SHEET

<u>Run</u>	<u>t</u>	<u>1</u>	<u>Ijt</u>	<u>Ist</u>	<u>N</u>	<u>E</u>	<u>FS</u>	<u>Comments</u>
1C	0.466	156	2.155	--	7	1.379	1.03	
1C-1	0.466	156	4.310	--	7	1.474	1.11	
1C-2	0.466	156	6.465	--	7	1.508	1.13	
2	0.466	156	2.155	2.155	4	2.570	1.93	
2A	0.466	156	2.155	1.078	4	2.394	1.80	
2A-1	0.466	156	2.155	0.30	5	1.899	1.42	
3	0.466	100	2.155	--	8	2.778	2.08	
10	0.506	100	2.155	--	5	1.716	1.29	
11	0.510	113	2.155	0.58	4	4.186	3.14	First 2 Segments 0.510, 0.486 On Others

Notes:

All analysis was performed for a Type 1 (axisymmetric) loading. The loads are taken from S & E-ASTN-ADL (73-68) Figures III-19 and III-201. The factor of safety is calculated assuming a knockdown factor of 0.75.

in figure 3-23. The NASA SP-8032 equation is based on all data available with no consideration as far as boundary conditions, R/t, ratios, flaws, etc., and is considered much too conservative. The David Taylor Model Basin results from reference NASA TND-1510 are based on thick walled shells with R/t ratios similar to those of the SRM aft closure. It is felt that the NASA TND-1510 results are more correct for our application being based on correct R/t test results.

A composite model of the nozzle, closure, and into the cylindrical shell was also run with the maximum axial acceleration loads for $\theta = 5^\circ$. The eigenvalue for BOSOR for a thickness of 0.279 inch is 1.67 and for a KDF of 0.75 the FS = 1.25. The KDF of 0.75 correlates with the results of the David Taylor Model Basin work.

3.2.1.11 Nozzle

The nozzle analysis was also performed on BOSOR. It should be pointed out that the actuators were not used to transfer any loads because BOSOR is not capable of handling a problem containing loads applied at one point in these two directions. All analyses were performed without the nozzle extension.

The static analysis results are shown in figures 3-24 and 3-25. The maximum stress is 185,000 for the maximum pitch condition giving a minimum FS of 1.05. This is primarily a bending stress at the juncture in the nozzle throat area. No ablatives were included in this analysis, and, therefore, the results are conservative. A slight increase in the local thickness (0.544 inch thick in the throat area) will increase this FS to 1.25.

The maximum pitch acceleration buckling analysis included the ablative materials as well as the structural materials of the nozzle. The char line for the ablative material included is shown in figure 3-26. The maximum axial acceleration buckling analysis showed the aft dome to be much more critical than the nozzle with the ablatives included. The results are shown in Table XVI.

3.2.1.12 Aft Peaking Loads

The aft peaking load analysis was performed on NASTRAN. The loading condition is for on-pad mode with orbiter engines ignited and a 34.4 knot wind, as

REFERENCE	EQUATION	RESULTS	Δ WT (NORMALIZED)
TIMOSHENKO, THEORY OF ELASTIC STABILITY (THEORETICAL)	$P_{cr} = P_{cl} = \frac{1.154 E}{\sqrt{1-\nu^2}} \left(\frac{t}{R}\right)^2$	$t_{REQ'D} = 0.216$ F.S. = 1.25 (MUST USE 0.274)	0
NASA TND-1510 (DAVID TAYLOR MODEL BASIN RESULTS)	$P_{cr} = \frac{0.80 E}{\sqrt{1-\nu^2}} \left(\frac{t}{R}\right)^2$	$t_{REQ'D} = 0.259$ F.S. = 1.25 (MUST USE 0.274)	0
NACA TN-3783 (SPHERICAL SEGMENT)	$P_{cr} = \frac{K\pi^2 E}{B(1-\nu^2)} \frac{t^3}{D(d)^2}$ $\left\{ \begin{array}{l} K = f(Z_d) \\ Z_d = \frac{d^2 \sqrt{1-\nu^2}}{Rt} \end{array} \right\}$	$t_{REQ'D} = 0.334$ F.S. = 1.25	+393
BOSOR-COMPUTER PROGRAM	(BOSOR) KDF = 0.75 KDF = 0.5	$t = 0.274$ (BASELINE) F.S. = 1.39 F.S. = 0.93 (0.274 IS MIN REQ'D FOR PRESSURE)	0
NASA SP-8032	$P_{cr} = P_{cl} \left[0.14 + \frac{3.2}{\lambda^2} \right]$ $\lambda = \left[12(1-\nu^2) \right]^{1/4} \left(\frac{R}{t}\right)^{1/2} 2 \sin \frac{\Phi}{2}$	$t = 0.56$ F.S. = 1.25	+1,875
CONCLUSION: NASA-TC AGREEMENT 22 MAR 1974 TO USE A CONSERVATIVE THICKNESS VALUE OF 0.41 (0.40 PLUS CONDITION: 0.010 FOR GRIT BLAST ALLOWANCE)			+885
$\ddot{Z} = \text{MAX}$ $\theta = 5^\circ$ $P = 253 \text{ PSI}$			

Figure 3-23. Aft Dome Buckling Calculations Summary

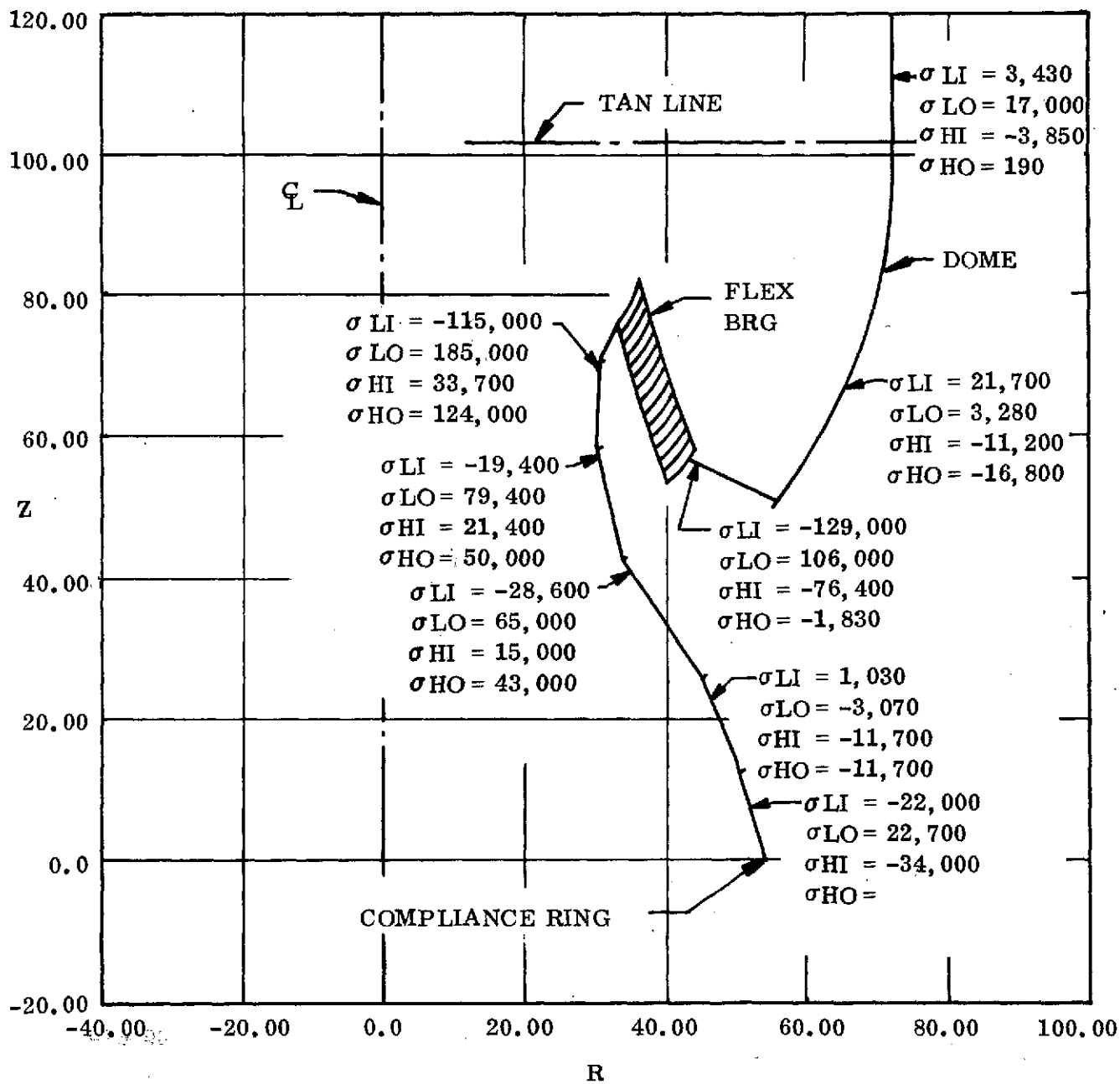


Figure 3-24. Nozzle Analysis (Max. Pitch, $\theta = 0$ Deg)

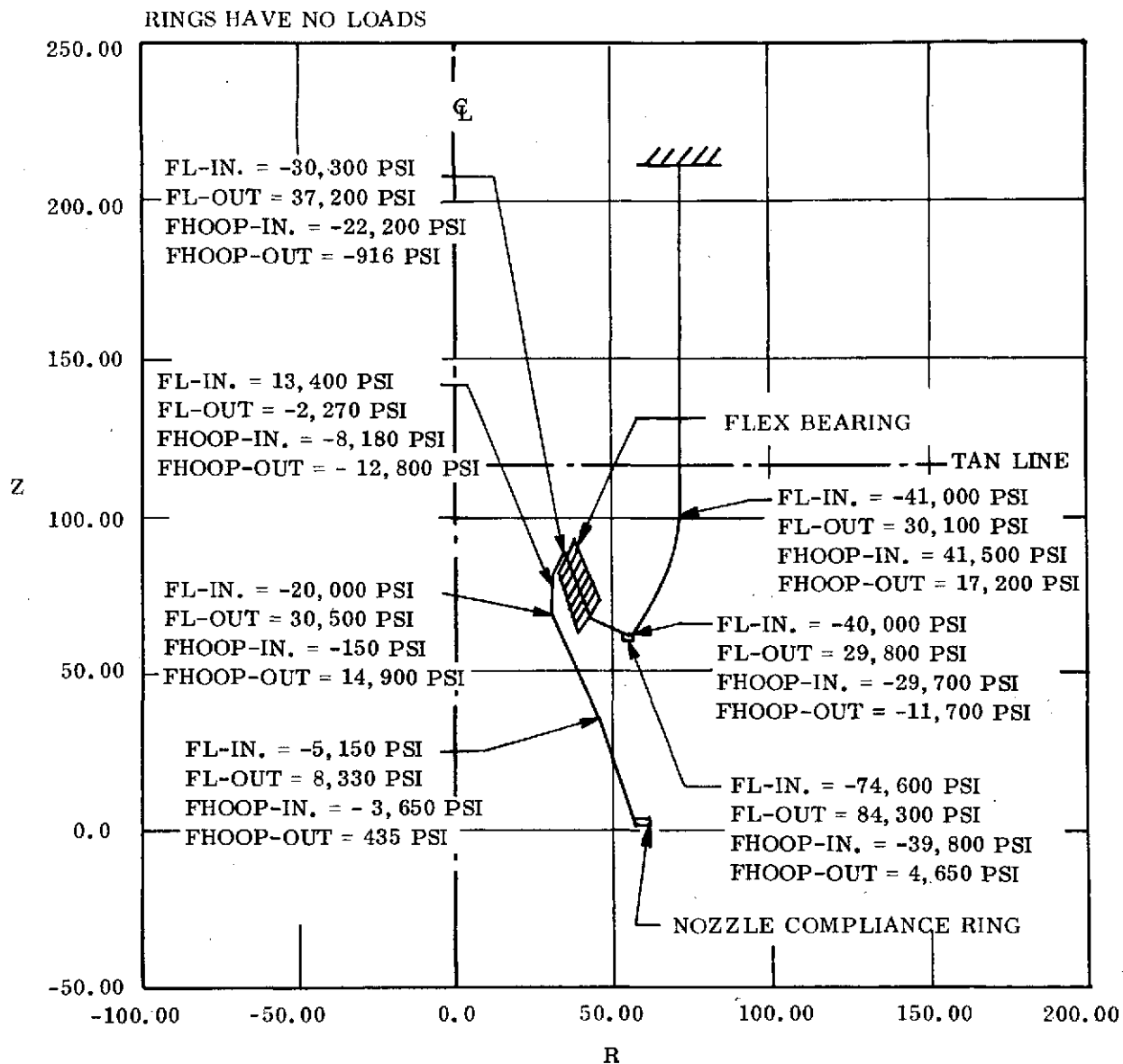


Figure 3-25. SRM Nozzle Buckling Analysis - Configuration 0
(Max. Axial Acc, $\theta = -10$ Deg - Initial Undeformed Structure)

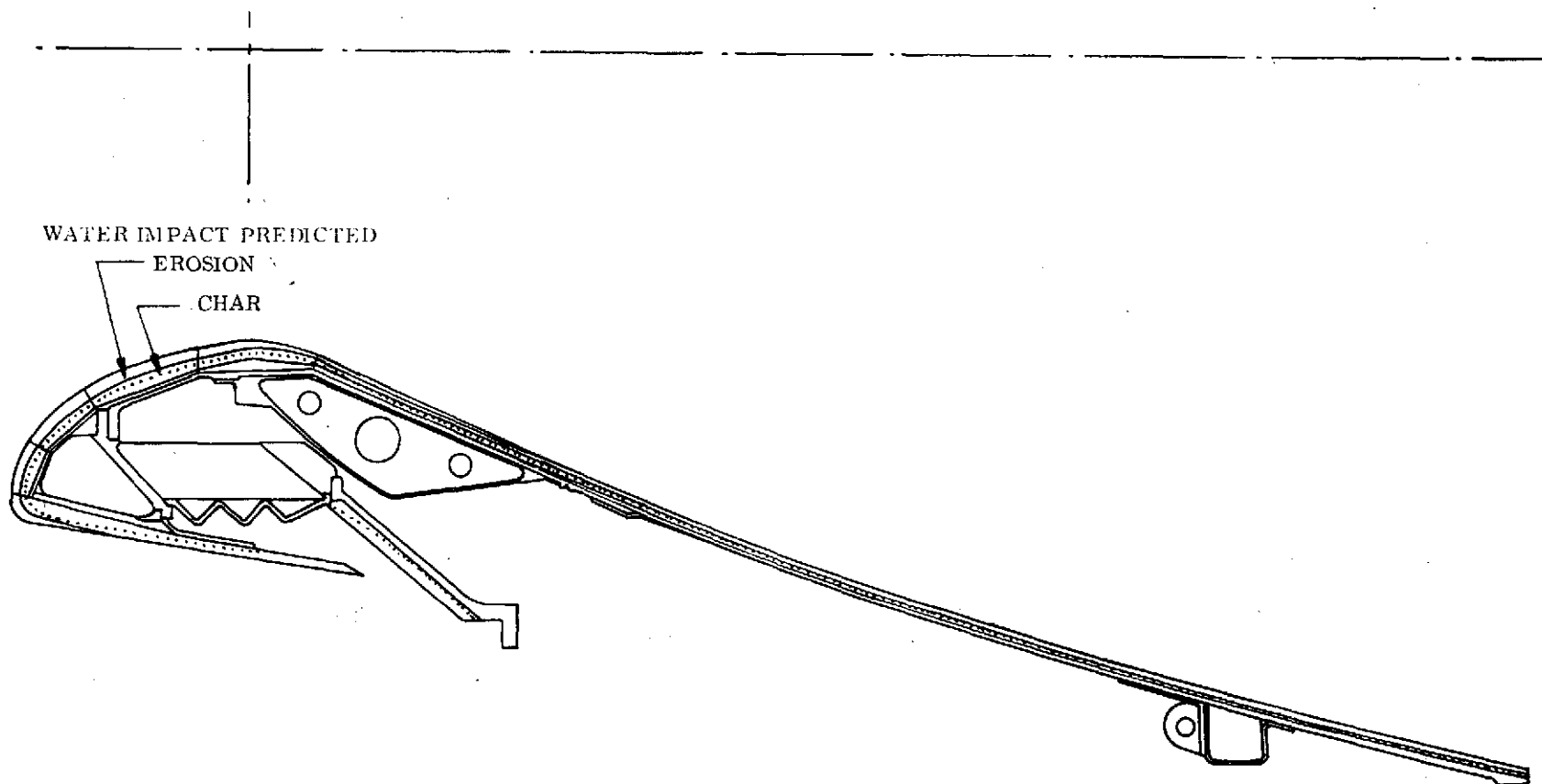


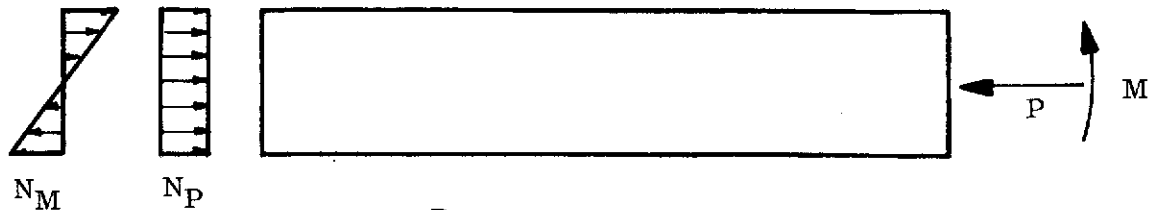
Figure 3-26. Nozzle Showing Char Line

TABLE XVI

NOZZLE BUCKLING ANALYSIS

Load Condition	<u>V_V(FPS)</u>	<u>V_H(FPS)</u>	<u>θ (0°)</u>	<u>E</u>	<u>KDF</u>	<u>FS</u>	<u>N</u>	<u>Comments</u>
<u>Max. Axial Accel</u>								
Configuration 0	100	45	5	7.86	0.75	5.90	4	No Ablatives
<u>Max. Pitch Accel</u>								
Configuration 0	100	45	-10	2.49	0.5	1.244	14	No Ablatives
Configuration 1-1	100	45	-5	6.47	0.5	3.23	12	Ablatives Included
Configuration 1-1	100	45	0	5.92	0.5	2.96	12	Ablatives Included

outlined in memo S & E-ASTN-AS (74-15), dated 7 Mar 1974. The loads were integrated to determine the axial load and bending after the load becomes completely distributed. The results are shown below.



$$P = \sum dp d\alpha \frac{\pi D}{360} = -1,976,000 \text{ lb}$$

$$M = \sum dp R \cos \alpha d\alpha \frac{\pi D}{360} = 307,854,000 \text{ in. -lb}$$

$$N = N_P \pm N_M = \frac{P}{2\pi R} \pm \frac{M}{\pi R^2}$$

$$N = \frac{-1,976,000}{2\pi(73.0)} \pm \frac{307,854,000}{\pi(73.0)^2} = -4,308 \pm 18,389$$

$$N = -22,697 \text{ lb/in.}$$

The stress and critical stress in the basic shell (the attach segment and above) for Configuration 1-1 is:

$$\sigma_{cr} = 0.6 \gamma E \frac{t}{R} \text{ (NASA SP-8007)}$$

$$\gamma = 1 - 0.73 (1 - e^{-\phi}) \text{ (for bending)}$$

$$\phi = \frac{1}{16} \sqrt{R/t}$$

$$\gamma = 1 - 0.901 (1 - e^{-\phi}) \text{ (for axial load)}$$

$$\sigma_{cr} = 61,990 \text{ psi (axial)}$$

$$\sigma_{cr} = 72,886 \text{ psi (bending)}$$

$$\sigma = \frac{N}{t}$$

$$t = 0.484 \text{ in.}$$

$$\sigma_A = 8,901 \text{ psi (axial)}$$

$$\sigma_B = 37,994 \text{ psi (bending)}$$

$$FS = \frac{1}{\frac{890}{61,990} + \frac{37,994}{72,886}} = 1.503$$

This is very conservative since the weight of the aft segments will be subtracted from these loads at the point where the thickness decreases to 0.484 inch.

The ratio of the axial load to bending is:

$$R_B = \frac{18,389}{22,697} = 0.81 \text{ (bending)}$$

$$R_A = 1 - 0.81 = 0.19$$

The load distribution in the aft 2 segments were determined from a NASTRAN analysis. The model with the load distribution is shown in figure 3-27. Figure 3-28 shows the stress pattern with the peak stress forward of the aft joint shown as 53,266 psi. The factor of safety at this location is shown below for Configuration 1-1.

$$t = 0.510 \text{ in.}$$

$$R = 72,759 \text{ in.}$$

$$\sigma_{cr} = 77,658 \text{ (bending)}$$

$$\sigma_{cr} = 66,353 \text{ (axial)}$$

$$\sigma_A = 0.19 (53,266) = 10,120 \text{ psi (axial)}$$

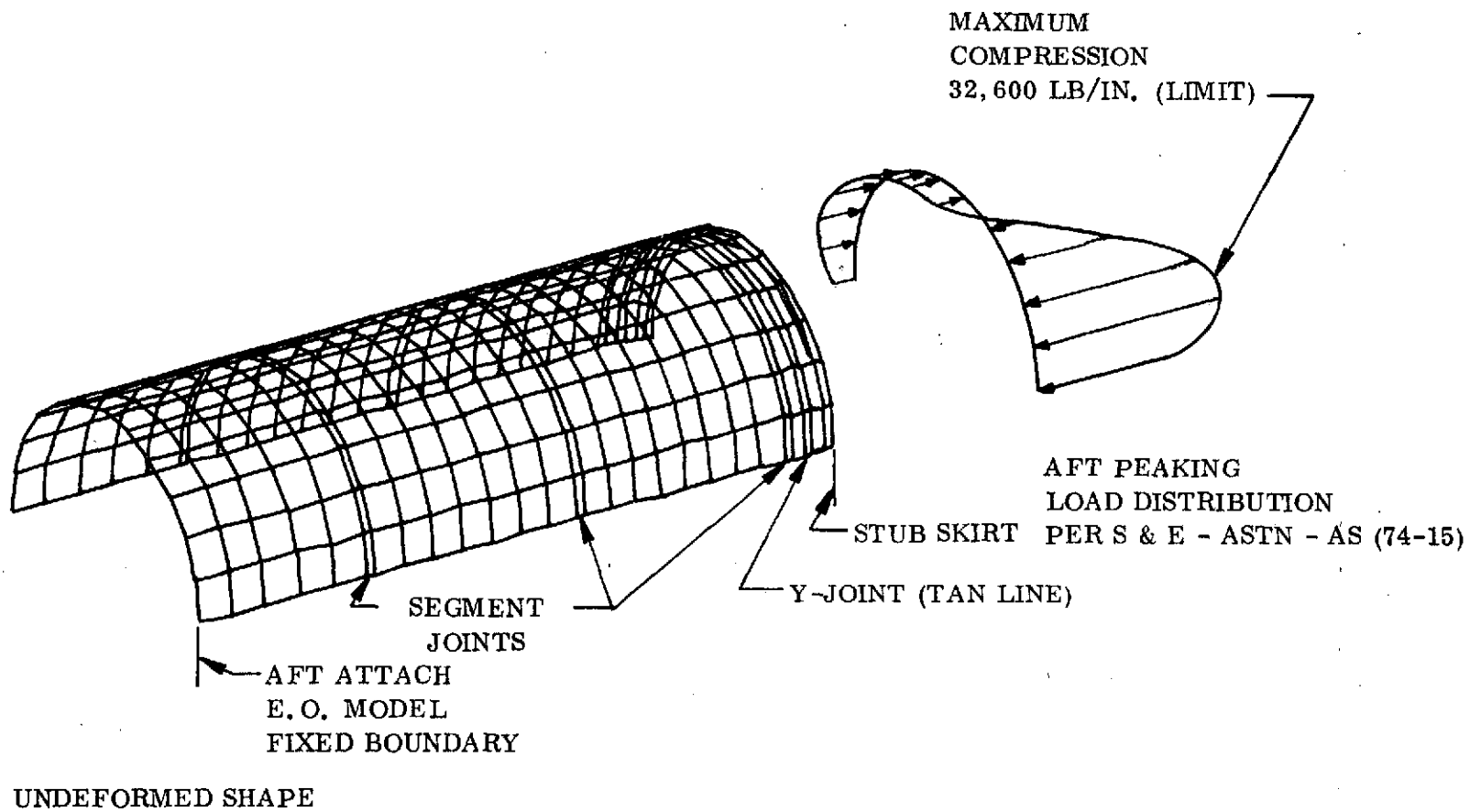


Figure 3-27. SRM Case Aft Peaking Loads Analysis NASTRAN Model

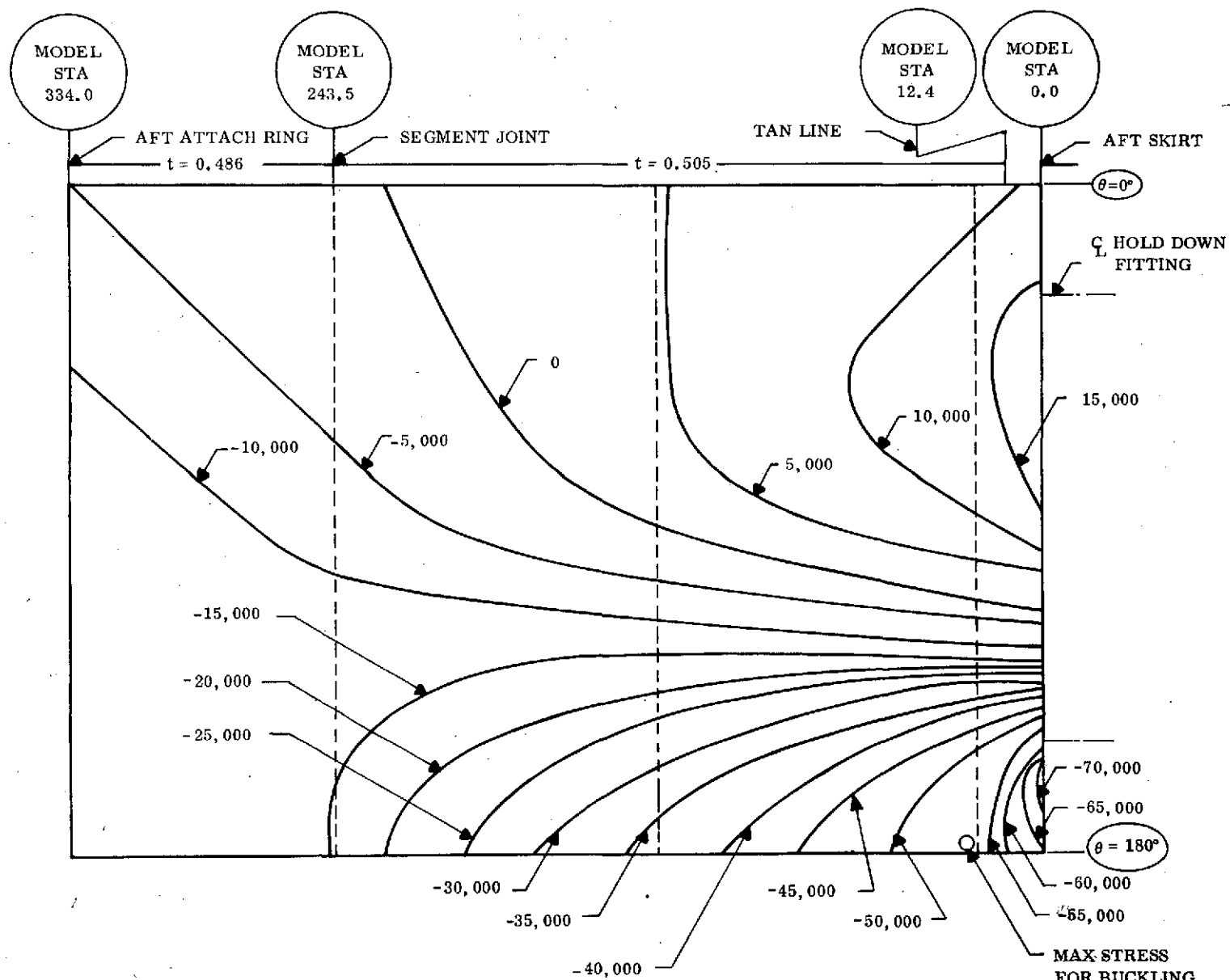


Figure 3-28. Stress Distribution (psi) - Aft Peaking Loads
(Ref: S & E-ASTN-AS (74-15))

$$\sigma_B = 0.81 (53,266) = 43,145 \text{ (bending)}$$

$$FS = \frac{1}{\frac{10,120}{66,353} + \frac{43,145}{77,658}} = 1.41$$

3.2.1.13 Forward Peaking Loads

The SRM was analyzed for the forward peaking loads shown in S & E-ASTN-AS (74-15). A summary of the results is shown in figure 3-29. The minimum factor of safety for buckling is 1.71 and the stress factor of safety in the pin joint is 2.74.

Additional analysis is required around the "Y" joint to determine the discontinuity stresses for the worst loading condition which has not been defined. This will probably be at liftoff when the internal pressure is maximum. The peaking loads at this time need to be defined, and the interface configuration between the case and barrel section must be defined to conduct an adequate analysis in this area. The internal pressure at the time of maximum acceleration (approximately 116 seconds) is only 433 psi which is a far less critical condition than when the pressure is maximum.

$$N'_{MAX, ULT} = 27,100 \text{ LB/IN. (19,357 LB/IN. LIMIT)}$$

• STABILITY (ASSUMING NO REDISTRIBUTION OF LOAD)

	<u>SKIRT</u>	<u>CYLINDER</u>
APPLIED STRESS	-57,600 PSI	-39,835 PSI
CRITICAL STRESS	1,360,000 PSI	68,000 PSI
F. S.	23.6	1.71
THICKNESS	0.336 IN.	0.486 IN.
LENGTH	3.0 IN.	156 IN.

∴ NO STABILITY PROBLEM ANTICIPATED WITH FWD PEAKING LOAD

• STRESS (LOAD COMPLETELY DISTRIBUTED $\frac{MC}{T}; \frac{P}{A}$)

CLEVIS JOINT - TENSION DUE TO COMBINED EFFECT

PIN LOAD FROM PEAKING LOAD EFFECT = 6,255 LB

$$M = 84.7 \times 10^6 \text{ IN-LB}$$

$$N = -1.2 \times 10^6 \text{ LB}$$

PIN LOAD FROM PRESSURE = 50,590 LB

$$t = 116 \text{ SEC}$$

$$P = 540 \text{ PSI}$$

$$T_N = 2.61 \times 10^6 \text{ LB}$$

TOTAL PIN LOAD (MAX AXIAL COND) = 56,845 LB

PROOF TEST PIN LOAD (1.2 X 849) = 94,795 LB

MEOP = 850 PSIG

MINIMUM PIN FAILURE LOAD = 155,970 LB

F. S. = 2.74

∴ NO STRESS PROBLEMS WITH FWD PEAKING LOAD

Figure 3-29. Effect of Forward Peaking Loads (Configuration 1-1)

3.3 NOZZLE

As various motor configurations have evolved due to requirement changes, the SRM nozzle has also changed. Table XVII delineates some of the pertinent nozzle information for nozzle Configurations 0, 1, and 1-1A. Figures 3-30, 3-31, 3-32, and 3-33 show these nozzles. Table XVIII is a summary of the actuation torque predicted for Configurations 0, 1-1, and 1-1A. The paragraphs below discuss the various changes and the applicable tradeoff studies that have been conducted in conjunction with them.

3.3.1 Nozzle Material Selection

The Thiokol baseline design, Configuration 0, used low-cost materials for the nozzle but was designed so that conventional (high-cost) materials could be substituted directly to assure performance and schedule integrity should difficulty arise with the low-cost materials. During the interim contract, this approach has been modified slightly, and it is now planned to use high-cost materials in the first demonstration motor (DM-1) and to develop the low-cost materials in time for demonstration in DM-2. This concept will assure high reliability and initial test success in DM-1 and will permit an additional five months for development of the low-cost nozzle materials. Discussions have been held with NASA on the low-cost materials proposed, the testing that Thiokol has done to date on these materials, and on the plan and schedule for development and demonstration of the materials.

Thiokol has also been participant in discussions between NASA and Aerotherm concerning the contract under which Aerotherm will be developing thermodynamic properties of the low-cost materials. This interface will help to assure that the latest data will be used in the Thiokol design.

Configurations 1, 1-1, and 1-1A use the high-cost nozzle materials and consequently represent the configuration of DM-1. It is expected that the low-cost materials development program will reduce both the weight and the cost of the nozzle on DM-2 as compared to DM-1.

Data on the low-cost materials and their use in the nozzle are presented below.

TABLE XVII

NOZZLE SUMMARY DATA

	Configuration			
	0	1	1-1	1-1A
Throat Diameter (in.)	56.4	56.6	57.3	54.4
Expansion Ratio (initial)	6:1	6:1	6:1	7.16:1
Submergence Depth of Throat (in.)	25.3	25.1	25.1	28.7
Submergence Ratio (%)	20.0	19.9	17.5	20.0
Exit Plane Diameter (in.)	138.2	138.6	140.34	145.6
Lengths (in.)				
Throat to Exit	126.2	141.5	143.24	143.70
Flange to Exit	100.9	116.4	118.14	118.0
Nose to Exit	149.2	164.8	166.60	167.0
Initial Contour Angle (deg)	23.6	23.6	23.6	24.6
Turnback Angle (deg)	11.2	13.8	13.8	13.25
Length/Throat Radius	4.5	5.0	5.0	5.28
Cold Pivot Point Location (in.)*	39.3	35.36	35.78	17.60
Hot Pivot Point Location (in.)*	56.9	52.20	52.3	29.5
Nozzle Weight (lb)	16,401	20,578	21,192	20,892
Materials	Low Cost	High Cost	High Cost	High Cost
Safety Factor Interpretation	Thiokol	NASA	NASA	NASA

*Inches aft of throat

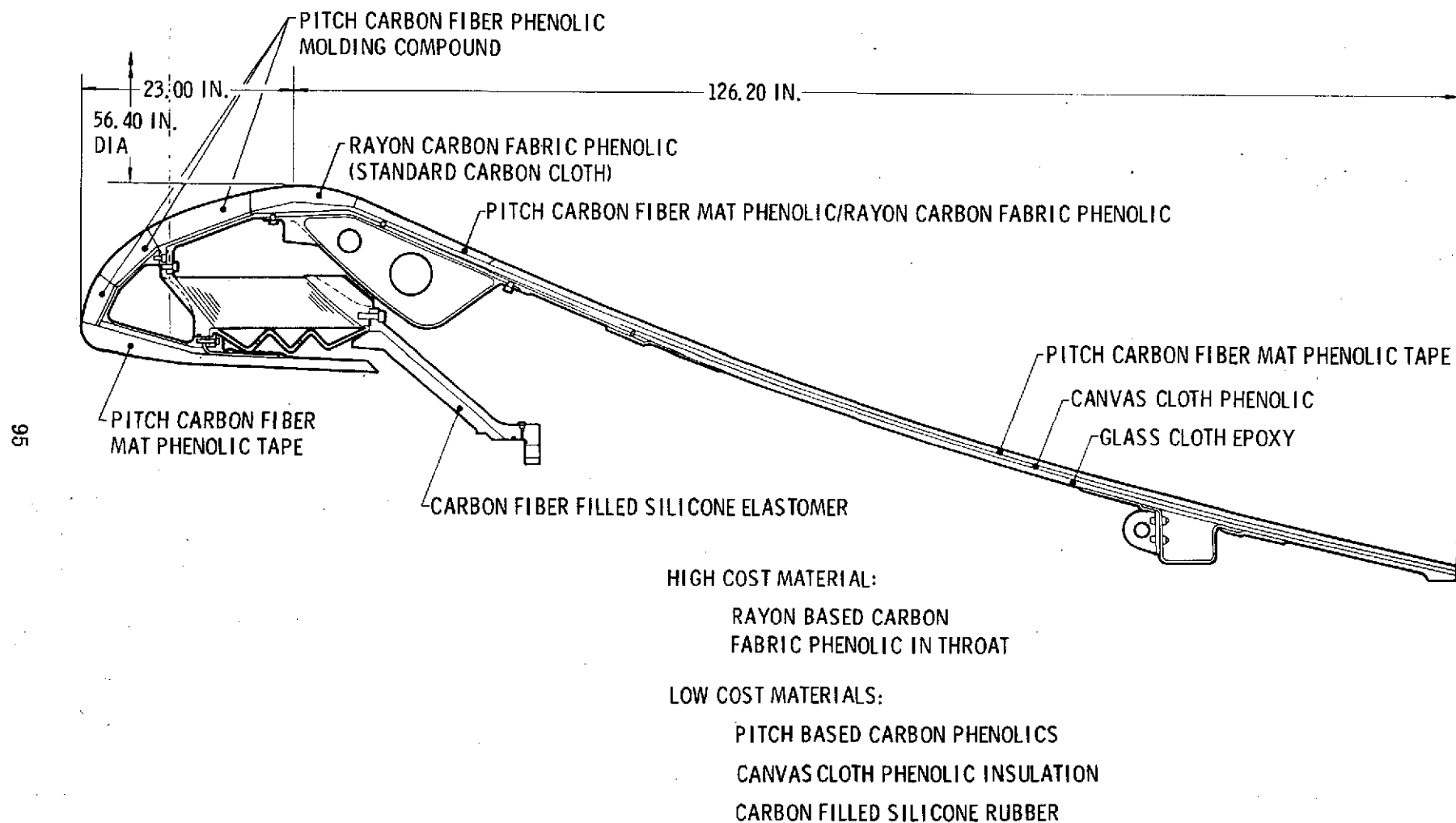


Figure 3-30. Baseline Low Cost Nozzle - Configuration 0

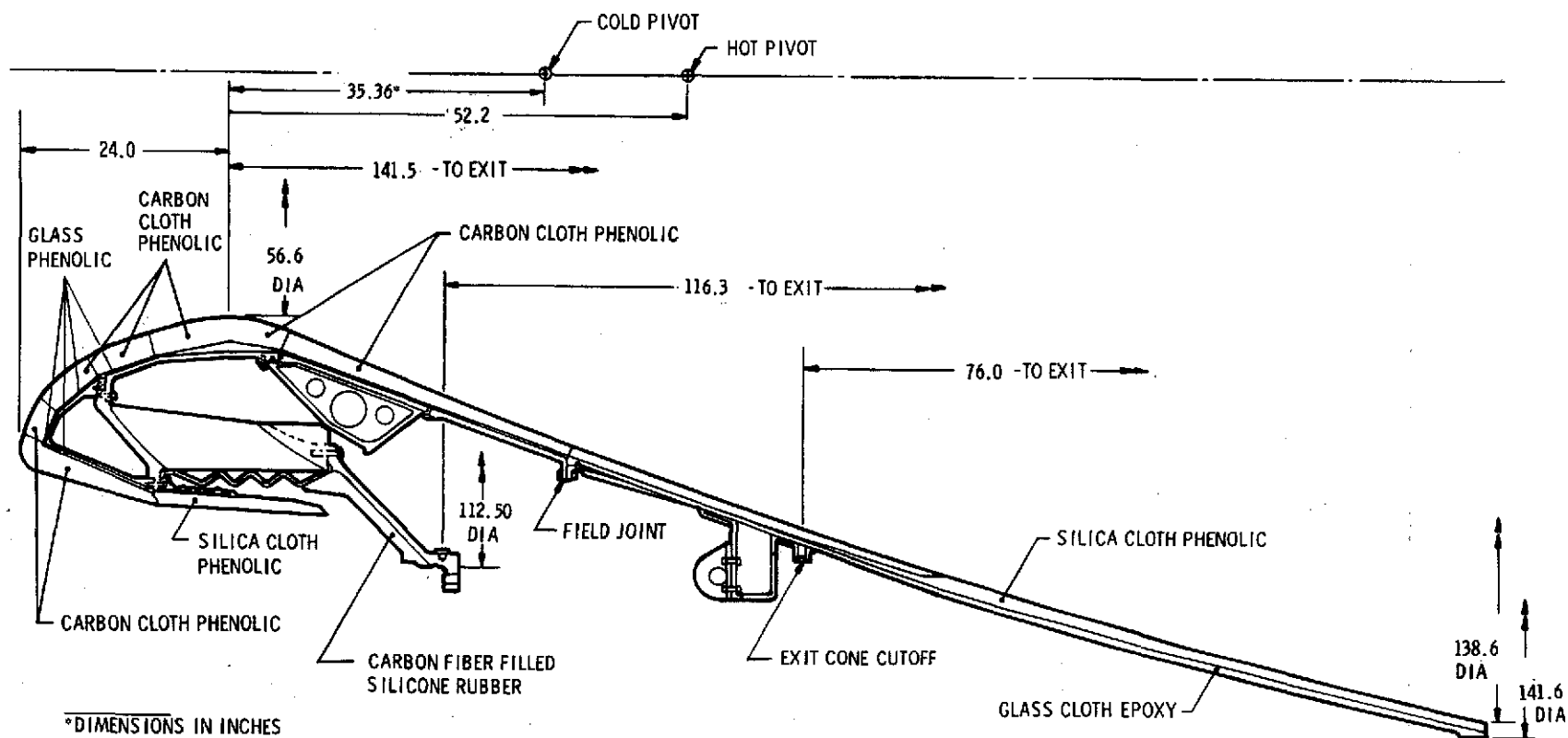


Figure 3-31. SRM Nozzle - Configuration 1

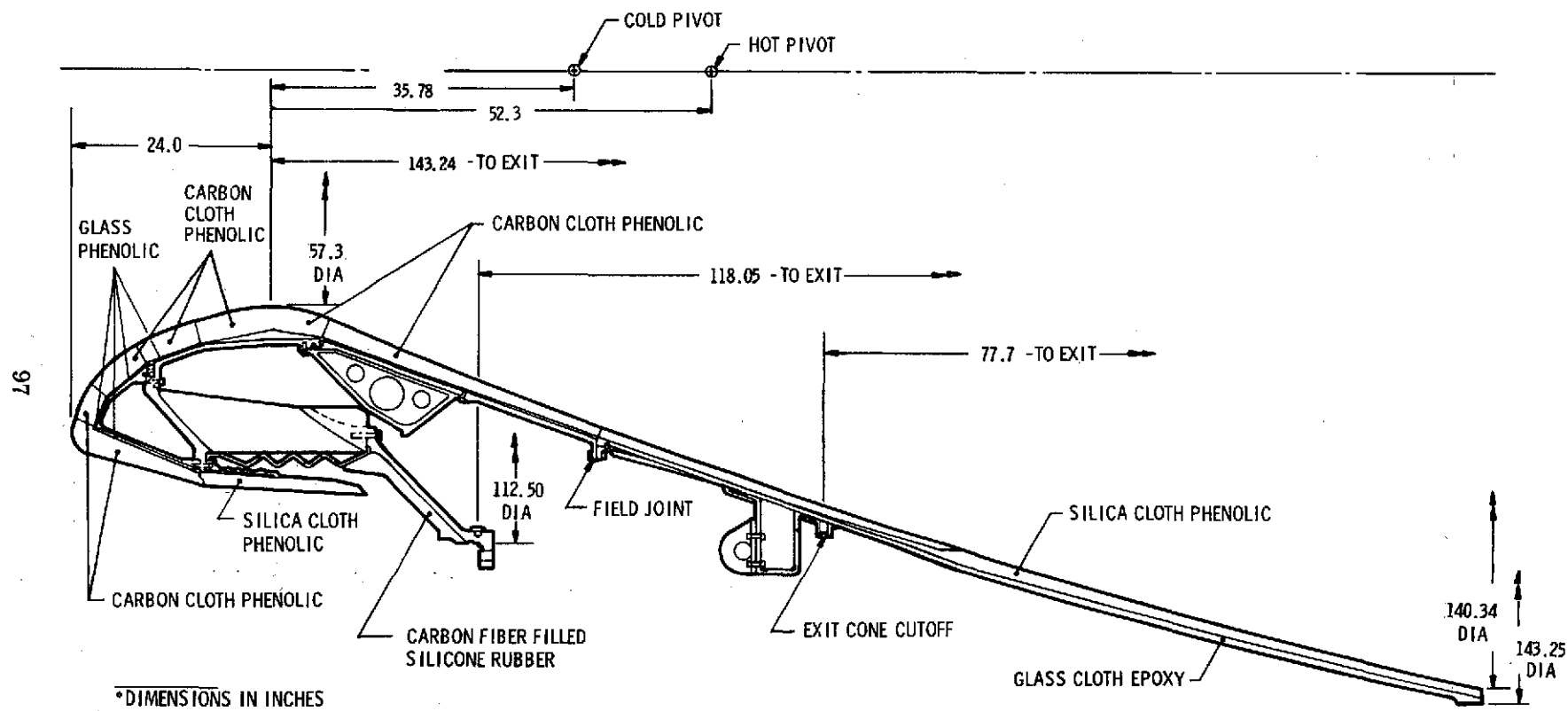


Figure 3-32. SRM Nozzle - Configuration 1-1

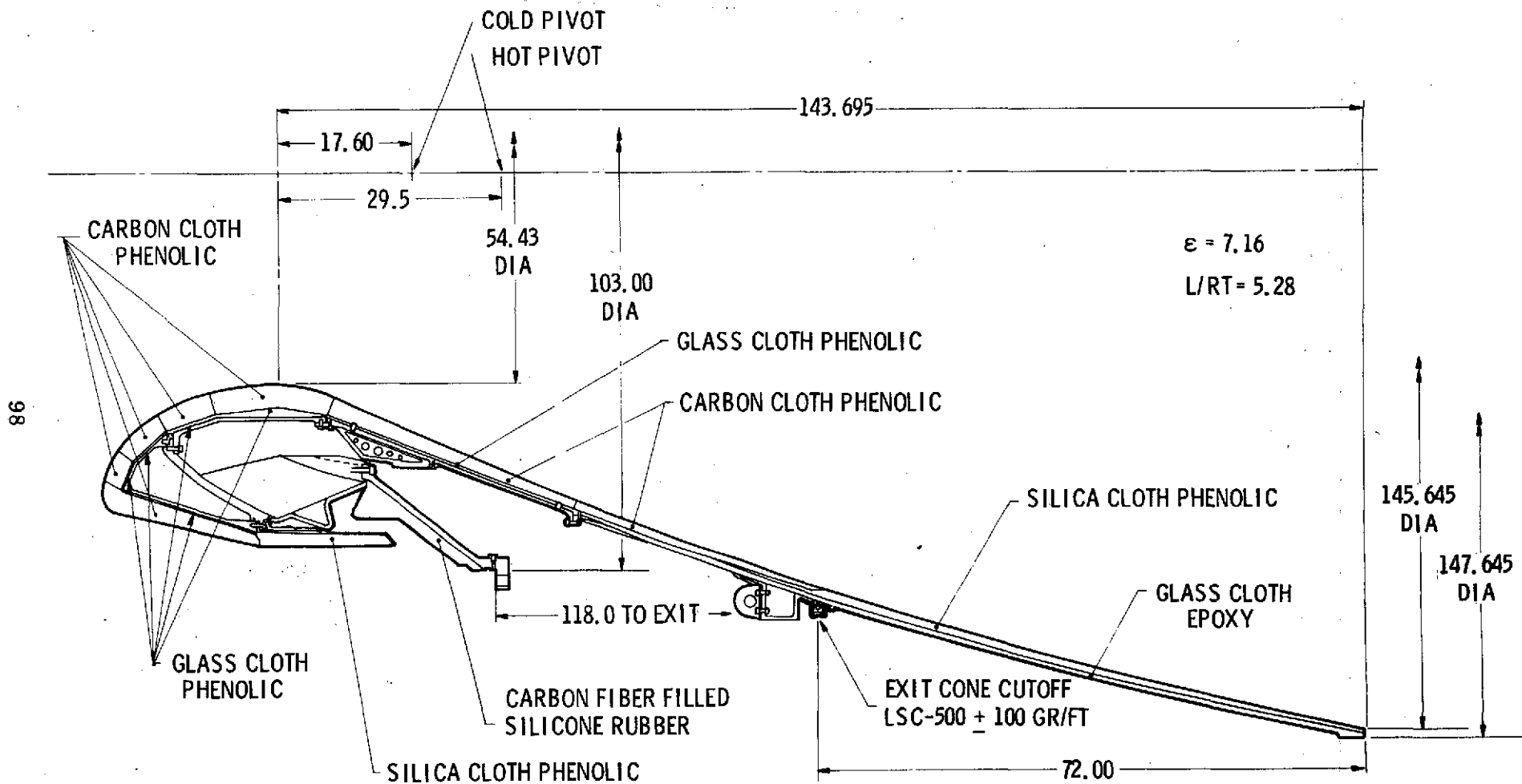


Figure 3-33. SRM Nozzle - Configuration 1-1A

TABLE XVIII

ACTUATOR TORQUE SUMMARY
(Million Inch Pounds)

	Configuration 0 In Plane of Actuator (5° Vector)		Configuration 1-1 In Plane of Actuator (5° Vector)		Configuration 1-1A In Plane of Actuator (5° Vector)	
1. Nominal Bearing Torque		2.35		3.007		2.404
2. SRM Misalignment Torque for 0.25°	0.129		0.165		0.132	
3. Torque Due to Bearing Aging (20%)*		0.470		0.601		0.481
4. Prediction Uncertainty in Bearing		0.235		0.301		0.240
5. 3 σ Variation in Bearing Reproducibility	0.362		0.464		0.370	
6. Null Bias Torque		0.060		0.060		0.060
7. Nominal Boot Torque		0.235		0.301		0.240
8. Prediction Uncertainty in Boot		0.024		0.030		0.024
9. 3 σ Variation in Boot Reproducibility	0.035		0.046		0.037	
10. Internal Aerodynamic		0		0		0
11. Offset Torque	0.533		0.533		0.321	
12. Torque Due to 3-g Axial Acceleration	0.070		0.069		0.035	
13. Torque Due to 1-g Lateral Acceleration	0.260		0.257		0.132	
14. Inertial Torque		0.258		0.290		0.250
15. External Aerodynamic	?	?	?	?	?	?
16. Base Pressure Effects	?	?	?	?	?	?
Direct Sum	1.389	3.632	1.534	4.590	1.027	3.699
RSS	0.711		0.774		0.527	
Worst Case	1.389 + 3.632 = 5.021		1.534 + 4.590 = 6.124		1.027 + 3.699 = 4.726	
Statistical Combination	0.711 + 3.632 = 4.343		0.774 + 4.590 = 5.364		0.527 + 3.699 = 4.226	

*20% used by agreement with NASA

The low-cost, baseline design of Configuration 0 uses low-cost material throughout the nozzle with the exception of the critical throat area where a standard carbon cloth phenolic is used. A development plan to fully qualify the low-cost materials prior to the fabrication of the second demonstration motor (DM-2) is presented in the data that follows. The use of low-cost materials in DM-2 and standard (high-cost materials) in DM-1 provides the advantages that the first motor can be fired using materials that are presently fully qualified, and a longer time can be allocated to the development of the low-cost materials. The material properties of the high- and low-cost carbon materials are sufficiently similar that designing metal structures for either low- or high-cost materials is feasible. The metal structure of all the configurations is designed so that either low- or high-cost ablative materials can be incorporated into the same nozzle structure.

Figure 3-30 shows the Configuration 0 nozzle. A standard rayon precursor carbon fabric phenolic is used in the throat. A carbon fiber filled silicone elastomer is used as insulation for the fixed housing. The remaining ablative materials are various forms of pitch carbon fiber phenolic. The nose and lower exit cone are fabricated of pitch carbon mat tape. The inlet rings are fabricated from pitch carbon fiber molding compound, and the upper exit cone is fabricated from a hybrid consisting of alternate layers of pitch carbon fiber mat phenolic and standard rayon carbon fabric phenolic. The insulation material in the nozzle is canvas cloth phenolic. Each of these materials is discussed in more detail in subsequent paragraphs.

The pitch base materials used in Configuration 0 are manufactured by the Union Carbide Company; the Kureha Company in Japan also manufactures like products. The pitch used by the Union Carbide Company is a by-product of their polyethylene plant and is available in large quantities. The low cost of the pitch carbon material is due to the fact that it is manufactured from essentially a waste material, and in the manufacturing process it is not necessary to use an intermediate precursor. The pitch is converted directly to carbon filament with a yield of 90-95 percent.

The erosion resistance of a carbon material is directly related to the specific gravity of the material. The pitch carbon has a specific gravity of approximately 2.0

as compared to 1.6 for rayon carbon, thus this material has potentially better erosive characteristics than does the standard rayon material.

The pitch based carbon is being developed by the Union Carbide Company for commercial applications. There is wide use for the material irrespective of whether it is used on the Space Shuttle nozzle or not. This large commercial application will assure that the material is available at a low cost.

Pitch carbon fiber in a mat form is currently available from Union Carbide. There has been approximately 10,000 pounds of the mat manufactured. The mat manufacturing line has been shut down to permit some equipment used in the mat line to be used in the development of a continuous pitch fiber filament and to permit the mat line to be moved from the laboratory environment to a manufacturing environment. The mat line was restarted in May 1974.

The resin impregnated mat material is presently available from several prepreg suppliers in at least three forms: 1) A mat tape either with or without a thin cotton scrim (the cotton scrim neither enhances nor detracts from the use of the mat tape in nozzle manufacturing); 2) A mat tape or mat broadgoods with a standard rayon carbon cloth as a scrim; and 3) A molding compound made from either a macerated mat or from 1/2 inch X 1/2 inch chopped mat.

Pitch based carbon materials in these three forms have been used to manufacture a large nozzle at Thiokol which was successfully test fired. They are presently viable materials for nozzle manufacturing. Discussions on these materials are presented below.

3.3.1.1 Mat Tape

Thiokol has used mat tape on a cotton scrim from the Fiberite Corporation to make small test nozzles (for 5-pound propellant motors) and to manufacture a nose ring for a Poseidon C3 size nozzle. Thiokol has also wrapped small test rings from mat tape without a cotton scrim which was supplied by U. S. Polymeric and Hexcel. Any of the above materials are satisfactory for use in the SRM nozzle, and these tapes will be used in the nose ring and for the lower exit cone.

Thiokol fabrication experience in using this material is that the material wraps well, and no fabrication difficulty was experienced. The material wrapped particularly well on angle wraps and in areas where a bias cut would have been necessary had woven material been used. The material does need further development to determine the optimum resin content.

3.3.1.2 Hybrid Tape

At the time the first hybrid tape was supplied to Thiokol by Fiberite, it was necessary that a scrim be used by the prepreg manufacturers to handle the mat tape. The carbon scrim was used on this material to support the tape and to supply an additional erosion resistant fabric. The Fiberite hybrid tape was used to manufacture small evaluation nozzles and was used on a C3 size subscale nozzle for the throat entry ring and in the upper exit cone, U. S. Polymeric has also manufactured and supplied this material to Thiokol.

This material performed well in the upper exit cone. The performance in the inlet area was satisfactory but somewhat questionable. This material is used in the upper exit cone of the Configuration 0 nozzle.

TC experience in the fabrication of parts using the hybrid tape is that this material is more difficult to wrap than the all mat tape and somewhat more difficult than standard carbon cloth. The main difficulties are that the material is fairly thick, and it is difficult to uniformly heat the material before it goes under the wrapping roll and to cool it afterwards. Because of the carbon scrim cloth, the hybrid material must be bias cut if the part requires angle wraps. This material needs further development to determine the optimum resin content and the relative thicknesses between the scrim and the mat material.

3.3.1.3 Molding Compound

Pitch carbon mat molding compound has been supplied to Thiokol by Fiberite Corporation and U. S. Polymeric. The Fiberite material is manufactured from a macerated mat; U. S. Polymeric chops the mat in 1/2 inch X 1/2 inch squares. The Fiberite material has been evaluated in small test nozzles, has been used in an entrance ring in a C3 size subscale nozzle, and has also just been fired in the

entrance ring in a C4 nozzle. Performance in both of these nozzles was very good. This molding compound was used in the three nozzle entrance rings on the Configuration 0 nozzle.

It has been Thiokol's experience that this material molds well and is easily machined in the approximately 21 inch diameter ring used on the C3 size subscale as well as on the smaller C4 entrance ring.

Development work is required to insure that there are no problems in scaling up to rings of the size required for the SRM nozzle.

A disadvantage of the material has been the large bulk factor of this material. Some work has been done by U. S. Polymeric to provide the material in preformed disks about 3 inches in diameter and 1/2 inch thick. Using the preformed material, the bulk factor is significantly reduced.

Union Carbide has been working to develop a continuous filament from the pitch base material. They have succeeded in developing these techniques and small quantities have been supplied to the industry. Present plans are to manufacture several thousand pounds of continuous filament in 1974.

With the development of the continuous pitch filament, it is planned to weave a broadgoods cloth from the pitch fiber. There has been some concern as to whether the continuous filament with its high modulus could be woven into cloth without breaking. To demonstrate this technique, continuous PAN carbon filaments with about the same diameters and modulus were satisfactorily woven into broadgoods material. Small amounts of the continuous pitch have also been woven into cloth, impregnated with resin, and manufactured into flat laminates.

If the continuous filament and resulting broadgoods are developed as expected and costs are as projected, this material could be used for all tape wrapped parts of the nozzle. It is also possible that it could be used for the inlet rings to replace the molded parts. However, studies have indicated that molding parts would be less expensive than using tape wrapped manufacturing techniques.

The continuous pitch filament cloth is expected to be available in quantities suitable for development work in 1974. By 1980 it is expected that the woven fabric

will sell at \$2-\$4 per pound. If this pitch carbon cloth is as completely successful and inexpensive as projected, it will undoubtedly be the standard material by 1978, and possibly the only carbon cloth available.

Canvas cloth phenolic is a standard well characterized material that has been used as insulator and ablator in several Thiokol nozzles. It is used in the Configuration 0 nozzle as the insulator under the carbon ablative materials. This material has a low cost and a low density which makes it very attractive. Thiokol's experience has been that this material is easy to handle and parts are readily fabricated from it. The material is compatible with the carbon materials proposed. As a result, canvas cloth can be overwrapped over the staged and machined carbon materials and cured simultaneously with the carbon materials.

Early in the development of canvas cloth material some difficulty was experienced with parts that had been wrapped of canvas cloth, machined and exposed to a high humidity atmosphere. Apparently, the cotton fibers on the machined edge absorbed moisture and caused warpage. This can be easily prevented by sealing the machined surfaces as would be normally done during the fabrication of the nozzle. There has also been some concern that inflation in the cotton market will raise the price of this material so that it is no longer cost effective. If this is true, other materials such as glass can be substituted for the canvas cloth. Substitutions of glass, however, would result in a higher weight part.

Carbon filled silicone rubber is used as the fixed housing insulator on both the low-cost and standard materials nozzle. This material has been demonstrated on several Thiokol nozzles and performs very well. The material is vacuum mixed and vacuum cast directly onto the primed metal housing. The material cures at room temperature.

This material is the only plastic material on the nozzle that can be refurbished. This will be done by placing the fixed housing in a vertical boring mill and machining away the heat affected material. The carbon filler in the material gives it enough rigidity that machining is a practical operation. After the heat affected material

has been machined away, the fixed housing is placed in the same mold that was used for the original casting and new material is vacuum cast to replace that which had been machined away. The new material will self-vulcanize to the machined surface on the old material.

There are three other candidate materials for use as low-cost nozzle ablative materials. These are KYNOL carbon, filled carbon cloth, and silica cloth phenolic.

The KYNOL material has been developed for flame resistant materials. The basic fiber is manufactured from a phenolic. This phenolic fiber is woven into cloth and then carbonized and impregnated with the same phenolic from which the basic fiber was made. This material has been demonstrated in small motors and is now being tested on the Trident C4 program. There are two disadvantages in the material at the present time. One of them is that the C4 program has had difficulty in obtaining the carbonized KYNOL material to conduct their tests. The other is that the cost of the KYNOL material is significantly higher than the pitch based material.

The price of standard carbon cloth phenolic can be reduced about one-half by the addition of a higher than normal amount of resins and fillers such as chopped carbon and/or ceramic. Thiokol tested this material in the throat of the C3 size subscale nozzle which was tested in July 1973. The material did not perform well in the severe throat environment. It may be that in the nose or the exit cone that performance would be adequate. Again, this material is significantly more costly than the proposed pitch based material.

Silica cloth phenolic has been used for years in areas of the nozzle where the environment will permit, particularly on the back side of submerged nozzles and in the outer exit cone. This material is very satisfactory for these areas, however, it has about a 20 percent higher density than carbon cloth and subsequently adds weight to the nozzle.

There are three other candidate materials that could be used as insulators in the low-cost nozzle. They are silica cloth phenolic, paper phenolic, and glass cloth phenolic.

The silica cloth phenolic is an excellent material but is higher in cost and has a higher density than the canvas cloth used on the Configuration 0 nozzle.

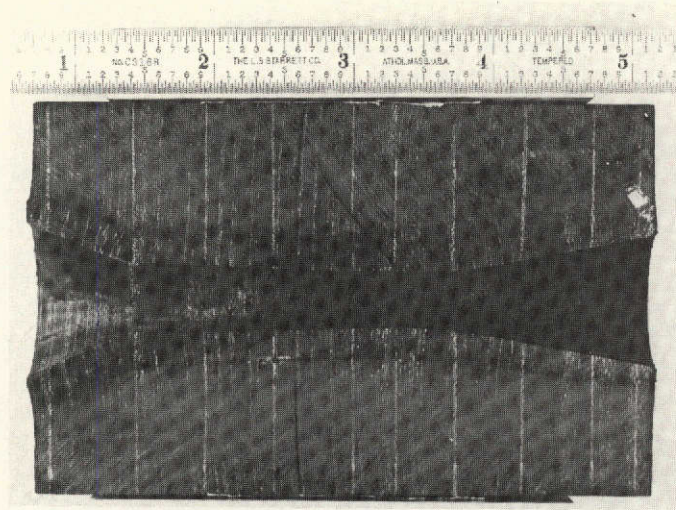
Paper phenolic materials show potential but have not been well characterized at the present time and would require more development work than the other two alternatives.

Prior to selecting the low-cost materials which Thiokol used for the Configuration 0, SRM nozzle, a three-part testing program was conducted. Twenty-three different low-cost materials were evaluated in this testing program. The three parts of the program were:

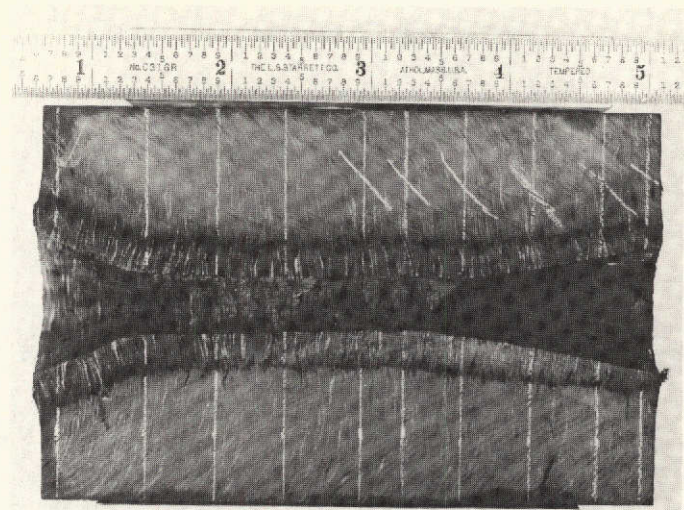
1. Nozzles for small subscale test motors were made from each of the candidate materials. These TU-379 motors each contained 5 pounds of SRM propellant and burned for approximately 10 seconds at a chamber pressure similar to that of the SRM.

Figure 3-34 is a series of photographs which show cross sections of four nozzle billets fired on Thiokol TU-379 motors during the material selection process. The photographs show a standard carbon cloth nozzle, a nozzle made from pitch carbon molding compound, a nozzle made from pitch mat tape, and a nozzle from a filled carbon cloth material. As measured from these nozzles, the erosion rate of the pitch carbon molding compound and pitch mat tape was very similar to that seen on the standard carbon cloth nozzle. As is evident in the photograph of the filled carbon cloth nozzle, this material had an erratic erosion pattern. The material was not deemed suitable for further evaluation.

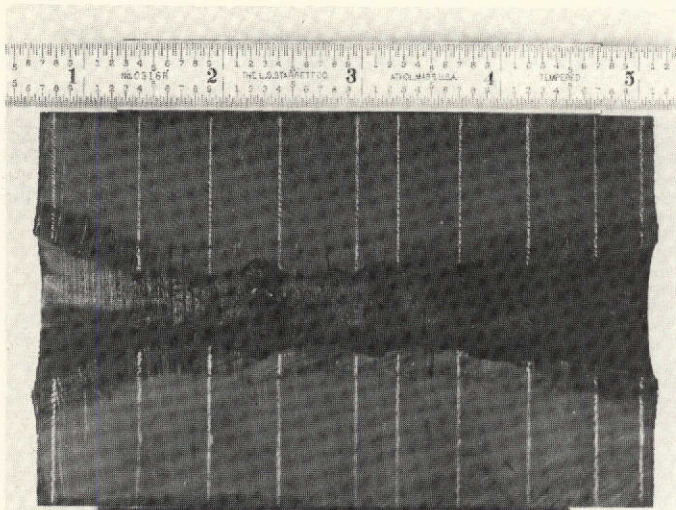
TYPICAL TU-379 BILLETS



STANDARD CARBON CLOTH

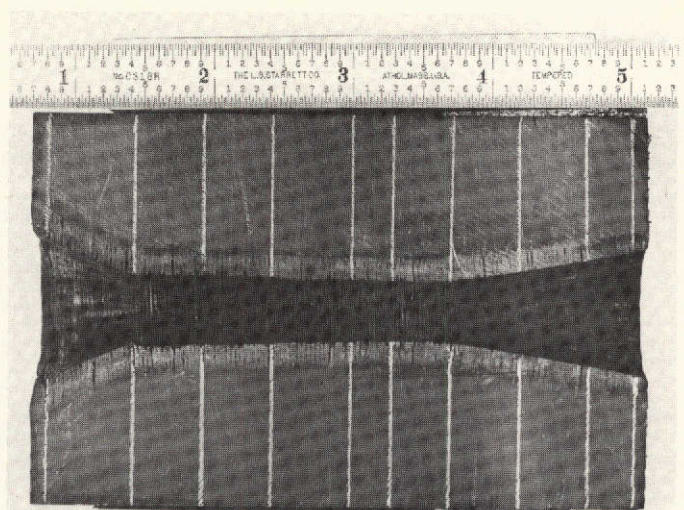


PITCH CARBON MOLDING COMPOUND



FILLED CARBON CLOTH*

*THIS MATERIAL REJECTED BASED ON THIS FIRING



PITCH MAT TAPE

2. Laboratory tests were conducted on the candidate materials to determine structural and therodynamic properties. The laboratory tests were conducted on samples of the cured material to obtain the structural and thermal properties shown on Table XIX

One of the interesting data points on this table is the specific gravity of the pitch fiber mat of 1.27. This was lower than the usually desired value of approximately 1.4. Subsequent data at Thiokol indicate that by increasing the wrapping and curing pressure this density can be increased to 1.4 or greater. The value of 1.27 shown here confirms data that U. S. Polymeric has developed which shows that the density of the pitch fiber mat is sensitive to the wrapping and curing pressure. Thus, it may be possible to obtain a low density carbon for use in the outer exit cone by varying the wrapping pressure.

3. A subscale nozzle was manufactured from selected low-cost materials and fired on a Poseidon Stage I motor. This was a significant test in that (a) the Poseidon propellant is near identical to that proposed for the SRM, (b) the chamber pressure of the Poseidon is approximately the same as the SRM, and (c) the subscale Poseidon nozzle and motor are large enough to give meaningful results. The subscale nozzle throat diameter was 11.596 inches. The expansion ratio was 8.2. The motor contained 38,000 pounds of propellant and had a 64 second burntime. The motor is 74 inches in diameter. Figure 3-35 is a sketch of the subscale nozzle manufactured and test fired by Thiokol

TABLE XIX

MATERIAL PROPERTIES FROM THIOKOL LABORATORY TESTS

SUPPLIER	MATERIAL	FLAT LAMINATES SPECIFIC GRAVITY	VOLATILE CONTENT (%)	RESIN CONTENT (%)	DOWEL PIN DOUBLE SHEAR INTERLAMINAR SHEAR (PSI)	ULTIMATE EDGEWISE COMPRESSION (PSI)	ULTIMATE TENSILE STRENGTH (PSI)	YOUNG'S TENSILE MODULUS $E_T \times 10^6$ (PSI)	WITH PLY (100°-300°F) COEFFICIENT OF LINER THERMAL EXPANSION (IN/IN/°F)
FIBERITE	MX4926 - STANDARD CARBON CLOTH PHENOLIC - RAYON CLOTH BASE	1.45	0.46/0.34	36.67/35.55	4,095	30,150	23,475	1.373	5.0
FIBERITE	MX4927 - FILLED STANDARD CARBON CLOTH PHENOLIC - RAYON CLOTH BASE	1.43	0.35	NA	2,755	27,166	17,220	2.64	NA
FIBERITE	MX4928 - CARBONACEOUS PITCH FIBER MAT/CARBON FABRIC (RAYON) CARRIER/ PHENOLIC	1.37	0.40	NA	1,805	23,366	5,861	4.12	6.1
FIBERITE	MXC-313P - CARBON PITCH FIBER PHENOLIC MOLDING COMPOUND	1.40	1.11	NA	1,665	10,875	4,400	1.078	8.7
FIBERITE	MX4929 - CARBONACEOUS PITCH FIBER MAT/COTTON SCRIM CARRIER	1.27	1.26	NA	4,163	27,490	10,025	1.465	NA
FIBERITE	MX2600 - STANDARD SILICA CLOTH PHENOLIC - GLASS CLOTH BASE	1.69	0.13	31.72	6,127	42,633	10,142	2.94	6.7
FERRO	ACFX-R96 SILICA CLOTH PHENOLIC - GLASS CLOTH BASE DOUBLE THICK	1.71	0.77	34.91	1,855	14,383	6,619	2.28	NA

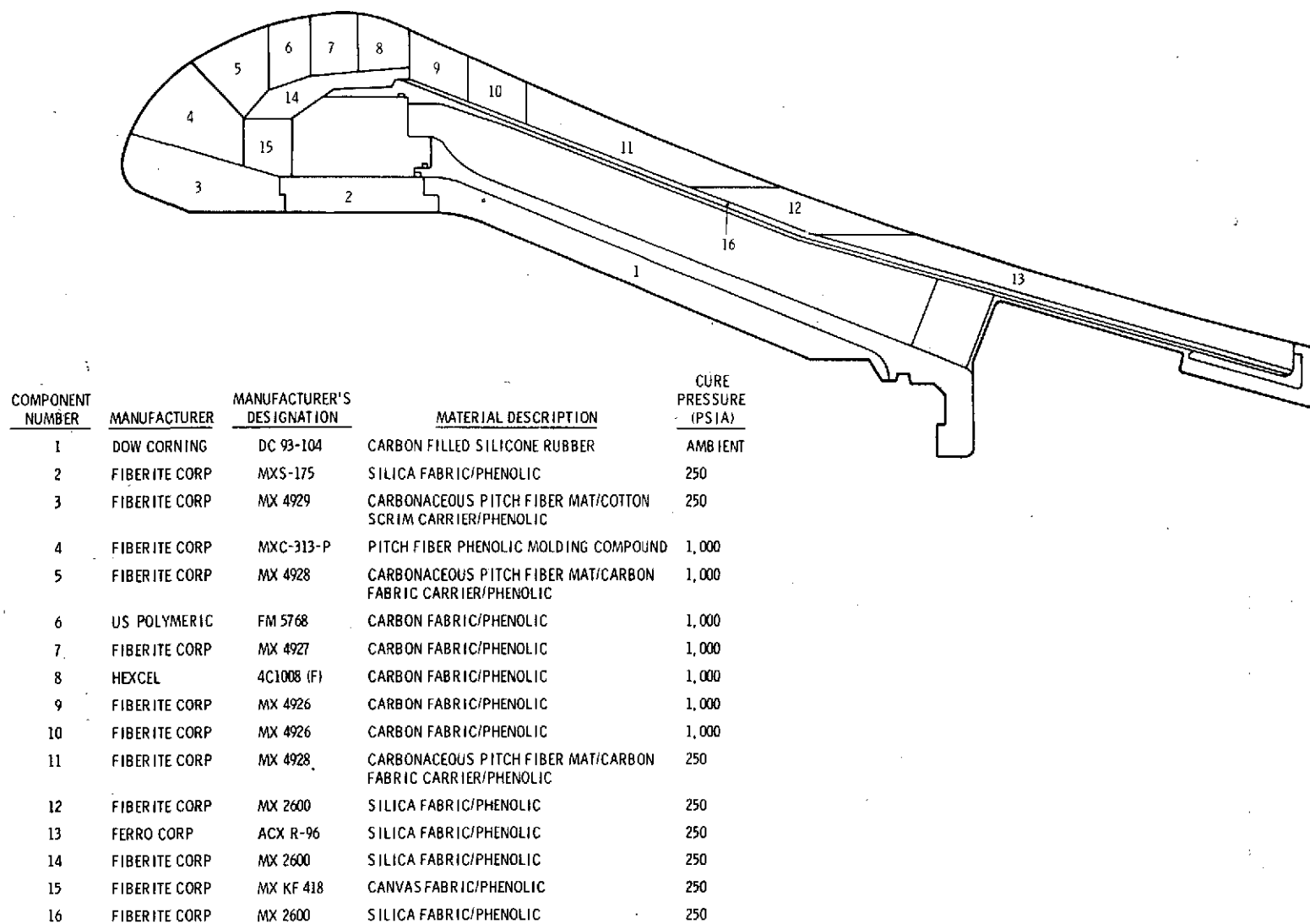


Figure 3-35. Poseidon C3 First Stage Low-Cost Nozzle (Tested 5 July 1973)

to demonstrate the low-cost materials. This test firing was completely successful and served the desired purpose of identifying those low-cost materials which are suitable for use in the SRM nozzle.

Figure 3-36 shows a comparison between the erosion rate of the low-cost materials and standard materials in the same environment.

In the nose, the erosion rate of the pitch carbon fiber mat compares quite well with graphite cloth phenolic. Previous data showed that density of the pitch carbon fiber was quite low in this part (specific gravity = 1.27). By increasing the pressure during wrapping, the performance of this pitch mat in the entrance section could be improved.

The pitch carbon fiber molding compound in the entrance ring performed better than standard graphite cloth phenolic. In the throat region, the low-cost nozzle did not perform well. The erosion rate of filled carbon cloth phenolic in the throat was erratic and so high that it affected the other materials in the throat region. Thiokol did not use any of these filled materials in the SRM nozzle. Standard carbon cloth phenolic is used for the throat of all SRM configurations.

In the upper exit cone the pitch carbon fiber phenolic with a carbon scrim material did not perform quite as well as carbon cloth phenolic but is certainly very satisfactory.

Thiokol is encouraged by the performance of the pitch carbon mat materials in this first demonstration motor and is confident that with some development work these materials will be completely satisfactory for use in the SRM nozzle.

A Development Program has been delineated which is a logical extension of the work done to date. It consists of:

1. Additional material screening, using the small 5-inch TU-379 motors

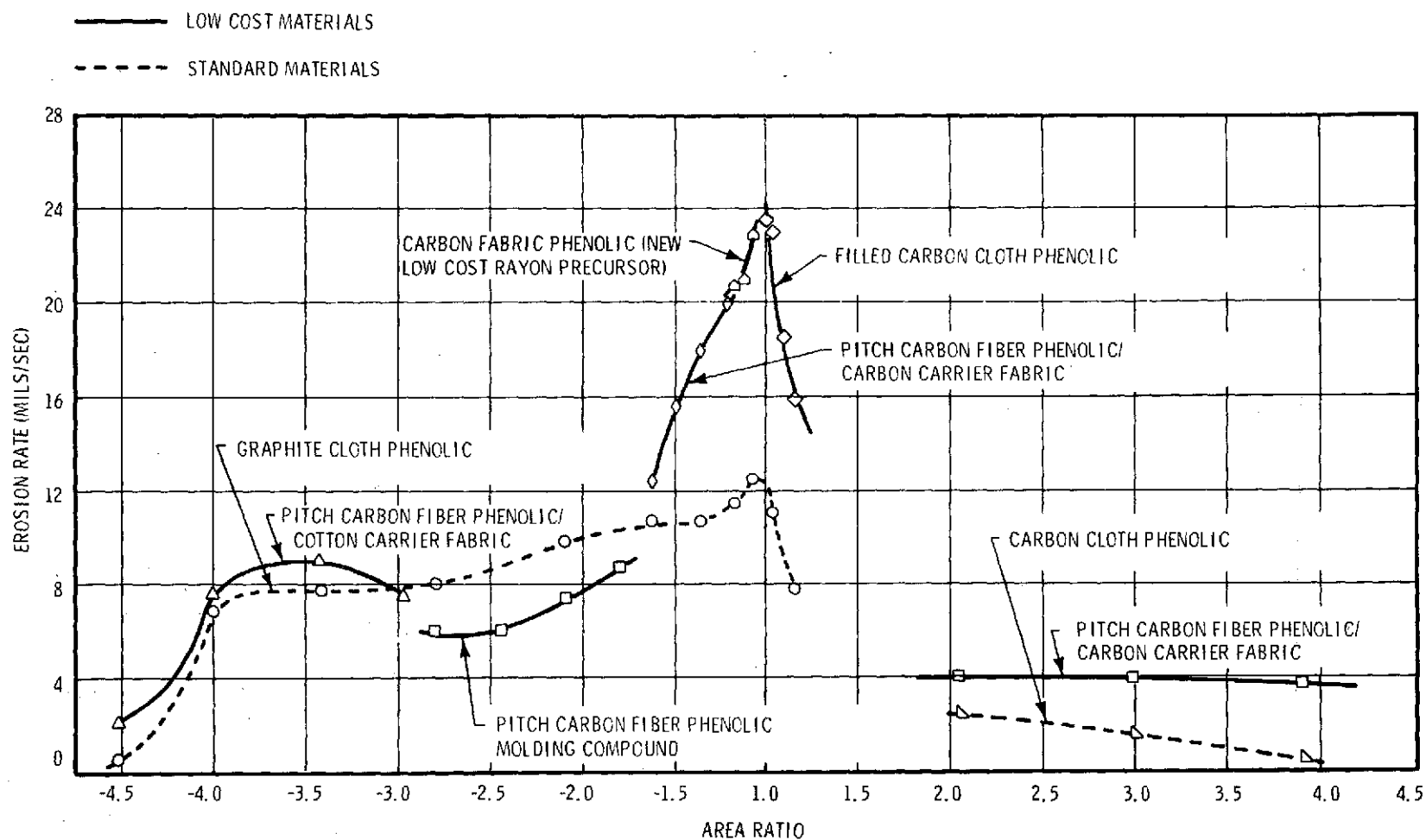


Figure 3-36. Low-Cost Materials Test Performance Comparison

2. Laboratory tests to obtain additional material properties over a range of material temperatures
3. Fabrication development to optimize the prepreg material characteristics such as the percent solvent, percent resin, wrapping pressure and the cure cycles
4. The demonstration of the pitch fiber molding compound in molded rings of the size required for the full scale nozzle and definition of the fabrication procedures
5. Additional subscale motor tests (Poseidon size) to further demonstrate and confirm the performance of the selected material

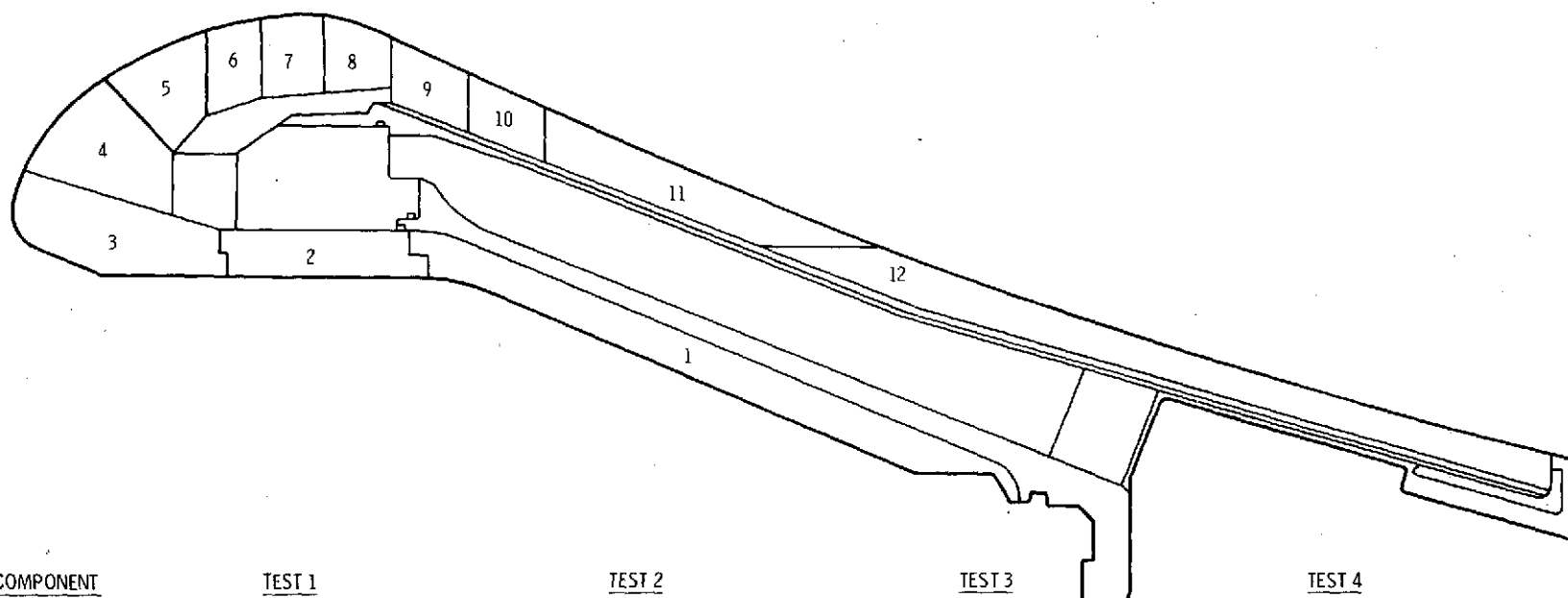
Figure 3-37 shows a material matrix which is a logical follow-on to the C3 motor fired at Thiokol in July 1973. The selection of materials for tests 2, 3, and 4 are based on the assumption that the materials would perform as expected in the previous tests. If any material performs exceptionally well, or not as well as expected, the test matrix for succeeding nozzles would be modified to account for these anomalies.

There have been discussions with NASA on the desirability of including additional subscale motor tests for a total of six. If this is done, it is Thiokol's recommendation that the last two tests would be material confirmation tests and would use the same matrix of materials as fired in test 4. This would permit data to be obtained on reproducibility of the materials.

A schedule showing the above development program is shown in figure 3-38. The schedule assumes a Thiokol ATP at 1 July 1974 and the static firing of DM-1 and DM-2 in December 1976 and March 1977, respectively.

The schedule further assumes that the first demonstration motor would use standard (high-cost) materials throughout the nozzle and that the nozzle for DM-2 would contain the first low-cost materials fired in a full scale nozzle.

The development program is amenable to either four subscale motors or six subscale motors as shown in the figure.



COMPONENT	TEST 1	TEST 2	TEST 3	TEST 4
1	CARBON FILLED SILICONE RUBBER	CARBON FILLED SILICONE RUBBER	CARBON FILLED SILICONE RUBBER	CARBON FILLED SILICONE RUBBER
2	PITCH MAT TAPE (V1)*	PITCH MAT TAPE (V3)	PITCH FABRIC	PITCH FABRIC
3	PITCH MAT TAPE (V2)	PITCH MAT TAPE (V1)	PITCH FABRIC	PITCH FABRIC
4	PITCH MOLDING COMPOUND (V1)	PITCH MOLDING COMPOUND (V3)	PITCH MOLDING COMPOUND	PITCH MOLDING COMPOUND
5	PITCH MOLDING COMPOUND (V2)	PITCH MOLDING COMPOUND (V1)	PITCH MOLDING COMPOUND	PITCH MOLDING COMPOUND
6	PITCH MOLDING COMPOUND (V3)	PITCH MOLDING COMPOUND (V2)	PITCH MOLDING COMPOUND	PITCH MOLDING COMPOUND
7	STANDARD CARBON CLOTH	STANDARD CARBON CLOTH	PITCH MOLDING COMPOUND	PITCH FABRIC
8	STANDARD CARBON CLOTH	STANDARD CARBON CLOTH	STANDARD CARBON	STANDARD CARBON
9	STANDARD CARBON CLOTH	HYBRID TAPE (V2)	PITCH FABRIC	PITCH FABRIC
10	HYBRID TAPE (V1)	PITCH FABRIC	PITCH FABRIC	PITCH FABRIC
11	HYBRID TAPE (V2)	HYBRID TAPE (V1)	PITCH FABRIC	PITCH FABRIC
12	PITCH MAT TAPE (V1, V2, AND V3)	PITCH MAT TAPE (V1, V2, AND V3)	PITCH MAT TAPE	PITCH FABRIC

*V1, V2 AND V3 INDICATE POTENTIAL VENDORS

Figure 3-37. Material Matrix Subscale (C3 Size) Motor Tests

115



Thiokol is pleased with the progress made thus far on the continuous filament pitch material, and the prospects of woven pitch carbon cloth continue to be favorable. If this development continues on the schedule and at the cost projected by Union Carbide, the woven material will certainly revolutionize the carbon cloth industry and may replace what is now the conventional materials. It would seem essential to actively pursue the development of this material.

The pitch molding compound also seems to be a very viable material for use in the entrance sections of the nozzle because of the potential cost savings of making molded parts as opposed to tape wrapped parts.

The tape mat and the hybrid pitch materials certainly show promise, but could be replaced by the continuous filament pitch cloth. The continued development of these materials should be tempered by the progress on the continuous filament cloth.

The schedule shows that there is time to develop the low-cost materials and to delay the decision on their use until these data are available from the development program. Thiokol strongly recommends that the low-cost materials be developed and used in the SRM nozzle. In summary, Thiokol feels that the parallel approach to low-cost and high-cost materials is a sound and viable way to develop a low-cost nozzle while simultaneously protecting the SRM schedule. There is a significant cost saving which can be implemented by using a low-cost material and the development work done to date indicates that the material development is relatively low risk.

3.3.2 Plastic Material Safety Factor Interpretation

The safety factor Thiokol used in the design of the nozzle plastic parts on the baseline (Configuration 0) nozzle was different than the approach that NASA used in evaluating the nozzle. The differences as Thiokol understands them are delineated on figure 3-39. If the NASA approach is applied to the Thiokol nozzle, the effect is to increase the thickness of the ablative material and decrease the thickness of the insulation material. Because the ablative material is a higher density and higher cost than the insulative material, the result is a weight and cost increase.

If normal nozzle erosion occurs (and we have every confidence that after definition in the DDT&E program that the erosion rate will be well defined), then a nozzle designed by either criterion will perform satisfactorily. This means that at motor burnout there will be no temperature rise in the nozzle structure and that at water impact the nozzle structural parts will not have increased in temperature to the point that any damage has occurred.

Using the NASA approach to the safety factor, the above statements hold even if double erosion occurs. If double erosion occurs on the Thiokol design, there is still no temperature rise in the structural parts at motor burnout. However, the insulating liner under the ablative material would be charred. Thiokol feels that these conditions do not constitute any reliability degradation for the performance of the motor and the safety of the mission.

If double erosion did occur on a nozzle designed to the Thiokol criteria, at the time of water impact the structural temperature would be too high to assure that the metal parts could be refurbished and reused.

Figure 3-40 shows the Thiokol Configuration 0 nozzle which uses the safety factors as Thiokol interpreted the requirement. The thickness of the carbon cloth material at the throat was 1.8 inches. At an expansion ratio of approximately 3:1, the thickness of the ablator was 0.5 inch with a thickness of canvas cloth phenolic insulation of 0.5 inch. The effect of changing the safety factors on this nozzle is shown on figure 3-41 where the thickness of ablative material at the throat has

	<u>THIOKOL APPROACH</u>	<u>NASA APPROACH</u>
• ABLATIVE MATERIAL DESIGN CRITERIA	2 X NOMINAL EROSION	2 X NOMINAL EROSION + 1.25 X CHAR
• INSULATIVE MATERIAL DESIGN CRITERIA	1.25 X CHAR + THERMAL PROTECTION	THERMAL PROTECTION
• PROGRAM EFFECTS ARE:		
WEIGHT INCREASE OF 812 LB		
IF NORMAL EROSION OCCURS, BOTH NOZZLES PERFORM SATISFACTORILY		
IF DOUBLE EROSION OCCURS ON TC DESIGN, STRUCTURAL PARTS EXPERIENCE NO TEMPERATURE RISE AT MOTOR BURNOUT, HOWEVER:		
THERE WOULD BE CHAR IN THE INSULATOR		
AT WATER IMPACT, STRUCTURAL TEMPERATURE WOULD BE TOO HIGH TO ASSURE REFURBISHMENT		

Figure 3-39. Plastic Material Safety Factor Interpretation

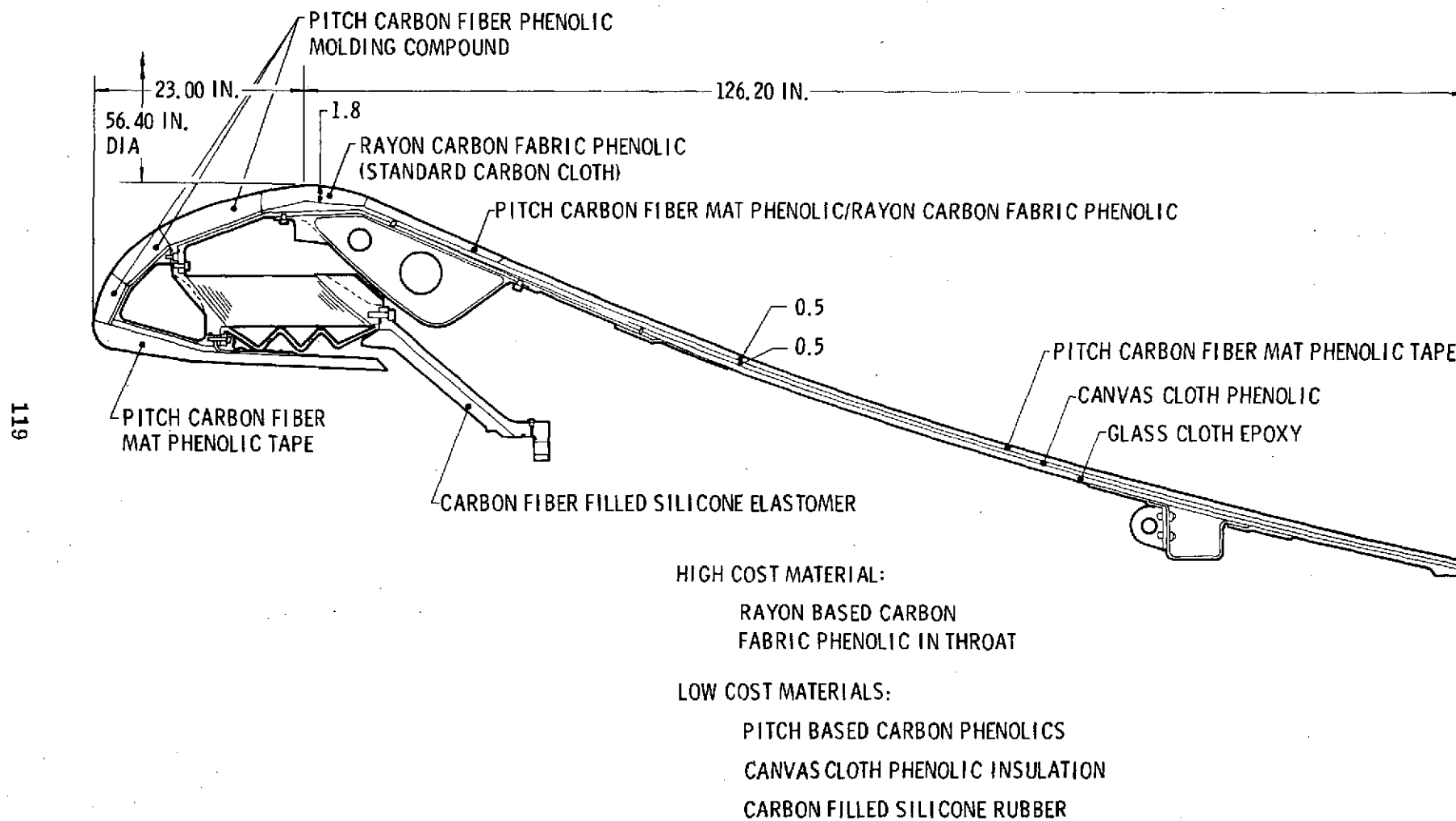
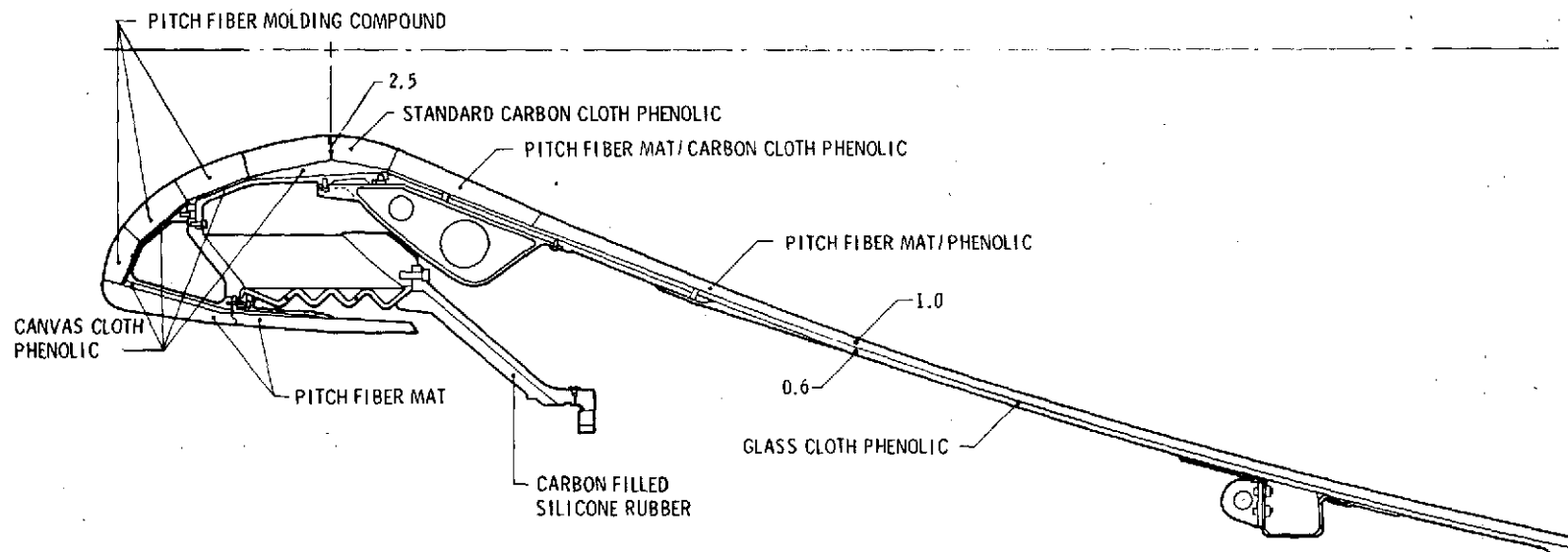


Figure 3-40. Baseline Low-Cost Nozzle



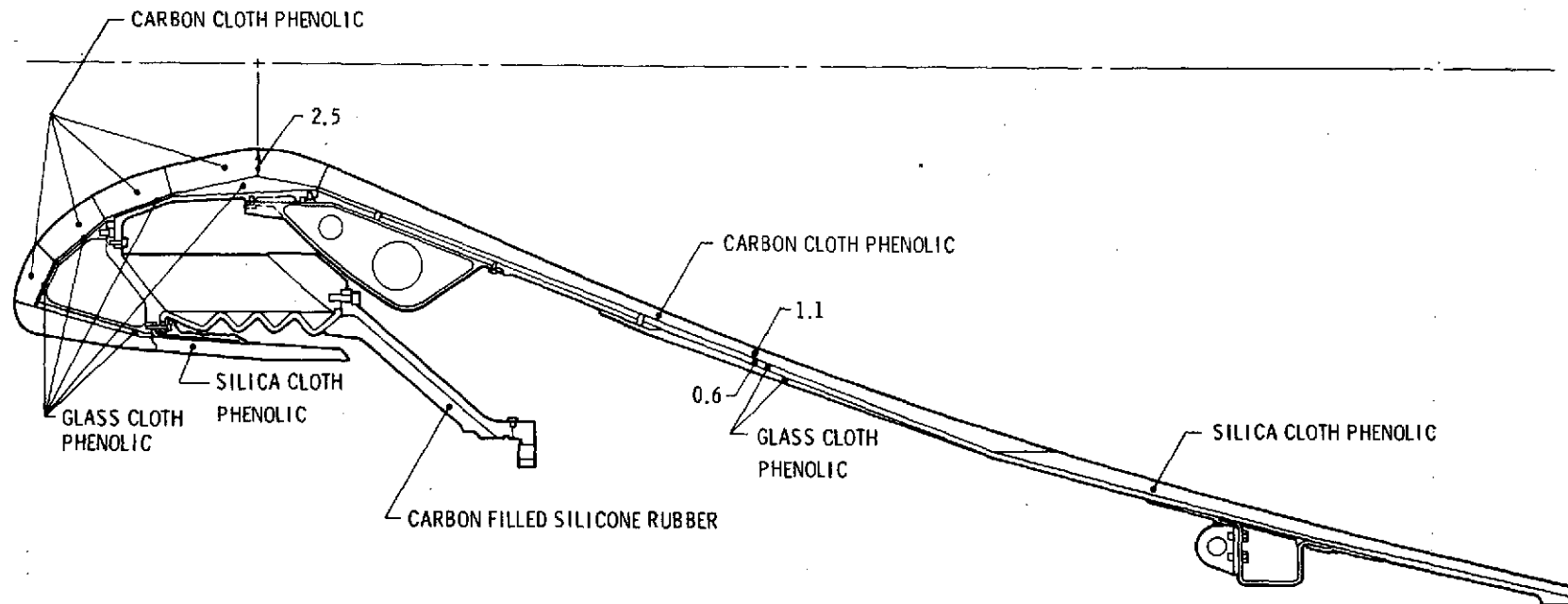
Δ WEIGHT = +812 LB

Figure 3-41. Revised Baseline Design Low-Cost Materials -
NASA Safety Factors

increased from 1.8 inches to 2.5 inches. In the exit cone the thickness of the ablative material has increased and the thickness of the insulation material has decreased to the point that it is probably impractical to use a separate insulative material. Consequently, the canvas cloth insulator has been eliminated in the exit cone and the glass cloth thickness has been increased so that it can serve both as insulator and as the structure for the exit cone. Changing to this safety factor approach has increased the weight of the nozzle by 812 pounds. The estimated cost increase is \$7,000 per nozzle.

Figure 3-42 shows the nozzle configuration using the NASA safety factor application and with high-cost materials in the nozzle. A weight increase of 1,783 pounds occurs. This weight increase includes the 812 pounds due to safety factor changes and 971 pounds due to changes in materials. The estimated cost increase is \$74,000 per nozzle. The majority of the 971-pound weight change is due to the use of silica cloth phenolic in the exit cone rather than using pitch mat phenolic as shown on the two previous configurations.

Thiokol has been asked to compare its approach to the safety factor on the SRM nozzle with the approach used on other solid rocket motor nozzle designs. The reason that Thiokol used the approach that it did was that it was philosophically the same as that used for Minuteman nozzle design and for the design of development and prototype nozzle concepts at Thiokol. The safety factors applied to the SRM, however, were higher than those traditionally used. For example, the traditional approach to ablative liner thickness at Thiokol has been to apply a 1.5 safety factor to the maximum predicted erosion depth. On the SRM design we used a 2.0 safety factor on the maximum predicted erosion depth. The traditional approach to insulator thickness is to design insulator thickness with a safety factor of 1.0 times the maximum predicted char thickness plus sufficient additional material to reduce the temperature to ambient at the structural interface. On the SRM nozzle the same approach was used except that a 1.25 factor of safety was applied to the predicted char thickness.



Δ WEIGHT = +1,783 LB

Figure 3-42. Baseline Design High-Cost Materials -
NASA Safety Factors

Because of the manrating on the Space Shuttle Solid Rocket Motors, Thiokol feels it is realistic to increase the ablative liner safety factor to 2.0 and the insulator thickness safety factor to 1.25.

Nozzles designed by the Thiokol approach or the NASA approach are not as conservative as the actual nozzles now being used on the Titan and Poseidon programs. The Titan and Poseidon nozzles were both designed several years ago and were the first nozzles designed using an ablative throat material. Both designs were done independently, i.e., the Poseidon nozzles were designed without benefit of the Titan test data and vice versa. Test data on these nozzles prove that they are both extremely conservative.

In the past few years the analytical erosion and heat transfer prediction techniques at Thiokol and throughout the industry have significantly improved, and much better predictions are now possible. To a real extent, this improvement has been because of the experience on the Titan and Poseidon nozzles. Thiokol recommends that the capability of the current analytical techniques should be evaluated using the existing Titan and Poseidon data. In this manner the accuracy of the current prediction techniques will be established and the SRM nozzles can be designed without the large allowance for design uncertainty that was necessary in the Titan and Poseidon nozzles.

Thiokol feels that these studies on the Titan and Poseidon nozzles will show that the Thiokol approach is valid and cost effective.

3.3.3 Aft Skirt and Actuation System Interface

A significant consideration in the design of the nozzle is the interface between the nozzle, the actuation system, and the aft skirt. These interfaces influence the following design factors:

1. Nozzle pivot point location
2. Nozzle torque
3. Nozzle submergence
4. Nozzle compliance ring location

5. Nozzle field joint requirement
6. Actuation system power
7. Hydraulic power supply system output power and installation envelope
8. Actuation system kinematics
9. Servoactuator stroke, force, hydraulic pressure, envelope and re-entry loads
10. Aft skirt must provide clearance and structural support for TVC actuation system components

Data has been prepared comparing two configurations, one of which had a nozzle submergence of 22 percent and the other with a submergence of 0 percent. These data are summarized in Table XX and figure 3-43.

The comparison of the two systems from a performance point of view is highly dependent upon interactions between the nozzle and the SRB actuation system and aft skirt and upon the pad interface. Extending the nozzle length will probably require a one for one increase in aft skirt length.

In an attempt to evaluate the motor performance several different assumptions were made as listed below and the performance calculated by iteration through the design requirements equations in the Request for Proposal.

1. Performance Assumption No. 1.

Assumptions

- a. There is no length constraint and unsubmerged design is 41.3 inches longer than submerged design.
- b. The skirt increased in length by 41.3 inches and in weight by 4,130 pounds (100 lb/in.).

Results

Under these assumptions, an additional 11,548 pounds of propellant can be loaded into the case of the unsubmerged design as compared to the submerged design.

TABLE XX
SUBMERGENCE COMPARISON

	<u>Baseline</u>	<u>Desubmerged</u>
Submergence (percent)	22	0
Inert SRM Weight Changes (pounds)		
Nozzle	0	-1,768
Aft Dome	0	+74
Aft Insulation	<u>0</u>	<u>+1,038</u>
Total SRM Weight Change	0	-656
Total Motor Length Change		+41.3
Propellant Weight Change		
Due to Submergence		+11,548
To Keep Same Length (41.3 x 820 lb/in.)		-33,866

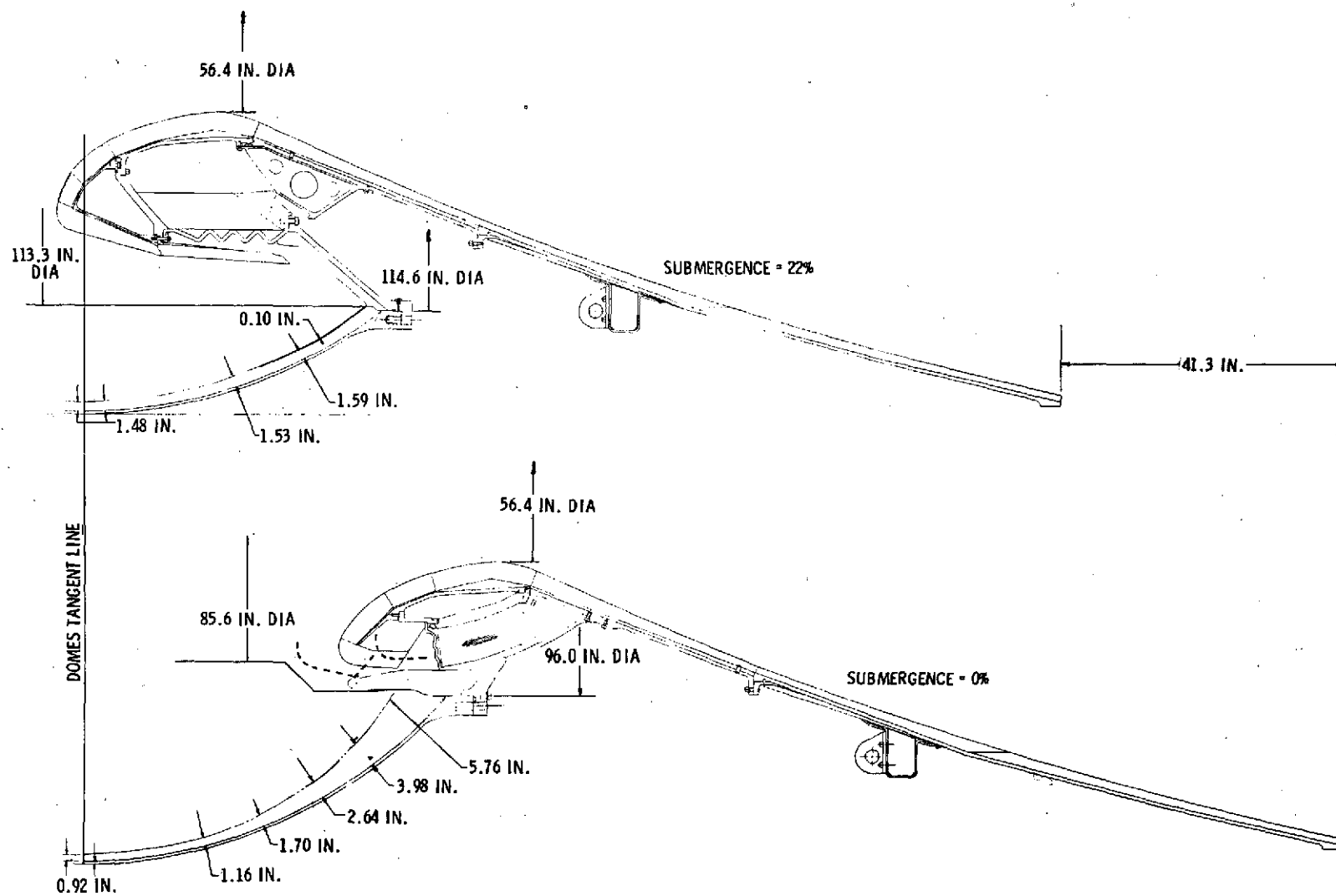


Figure 3-43. Submergence Comparison

The inert weight increase is +4,130 pounds for the skirt and -656 pounds for the SRM for a total of 3,474 pounds. Iterating the design requirement equation indicates that 6,065 pounds of propellant are required to carry the additional inert weight. This leaves 5,483 pounds of propellant that can be used for performance improvement.

2. Performance Assumption No. 2.

Assumptions

- a. There is no length constraint and unsubmerged nozzle is 41.3 inches longer than submerged design.
- b. The skirt does not change.

Results

Because of the reduced inert weight of the SRM (-656 pounds) and the additional 11,548 pounds of propellant that can be loaded in the motor, there is an excess of 12,860 pounds of propellant that can be used for performance growth.

3. Performance Assumption No. 3.

Assumptions

- a. Both systems must be the same length.
- b. The skirt weight change is neglected.

Results

The unsubmerged nozzle system must be reduced in length 41.3 inches. To do this the case must be shortened and will lose approximately 820 pounds of propellant/inch or 33,866 pounds. The aft dome of the unsubmerged nozzle will contain 11,548 pounds of propellant more than the submerged case. Thus, total propellant loss in the unsubmerged design is 22,318 pounds.

Thiokol is concerned with the concept of a zero submergence nozzle. Experience does not exist in the industry for flexible bearings having shims running near parallel to the motor centerline. Thiokol is also concerned about the flow field in the aft end of the motor if a submerged nozzle is not used.

Data were also prepared on the interface between the actuator and the SRM nozzle. This study addressed the feasibility of using the SSME actuator for the SRM. The data included three drawings which are briefly discussed and summarized below.

1. TUL 13878-SSME Actuator, MSFC Specified Attach Point and Baseline Pivot Point Nozzle Installation

TVC System geometry, kinematics, installation envelope, and water impact loads were investigated for an actuator with attach points defined by NASA. (Moment arm 62 inches, cold pivot point 39 inches aft of throat, SSME actuation pressure increase to 3,600 psi). The SSME actuator was found to be unacceptable because the nozzle torque for that specific pivot point location (4.11×10^6 in. lb) exceeded the actuator capability even at 3,600 psi operating pressure. Stroke considerations were also found to be insufficient because allowing for proper nozzle/case deformation (0.050 inch), crosstalk between actuators (0.030 inch), structural compliance requirements (0.40 inch), extend stroke (5.41 inch) and retract stroke (5.39 inches) comes to 11.28 inches total. Current SSME actuator stroke is 10.90 inches total. This basic actuator installation would increase the weight of the nozzle compliance ring by approximately 385 pounds. However, splash-down considerations are acceptable for the SSME actuator using this arrangement.

2. TUL 13874-SSME Actuator Installation Aft Pivot Point 66% of Baseline Design

This study was very similar to the above configuration except that the actuator aft attach point (on the skirt) was moved forward to relieve the stroke area problems. Again, the SSME actuator (operating at 3,600 psi system pressure) was found to be marginal. 3.61×10^6 in./lb torque would be required and the actuator capabilities are 3.73×10^6 in./lb. Similarly, the actuator stroke requirement

SSME ACTUATOR INSTALLATION STUDY

SRM CONFIGURATION

REV B

LAYOUT NUMBER 1 (BASELINE PIVOT POINT)
USE UNMODIFIED SSME ACTUATOR, MSFC SKIRT, AND TC CONFIGURATION 1 AND 2 NOZZLE

ACTUATOR AND NOZZLE DATA	REQUIRED BY DESIGN OR LAYOUT	SSME ACTUATOR CAPABILITIES BASED ON 3,600 PSI	COMMENTS
TORQUE (IN-LB)	(4.11) (10 ⁶)	ACTUATOR TORQUE = (FORCE) (MA) *SEE TYPICAL TORQUE CALCULATION RETRACT TORQUE = (3.88) (10 ⁶) EXTEND TORQUE = (3.91) (10 ⁶)	NOT ACCEPTABLE (MARGINAL)
STROKE (IN.)			
EXTEND	5.41	5.275	NOT ACCEPTABLE
RETRACT	5.39	5.623	
ΔP ALLOWANCE	0.05	--	
CROSSTALK ALLOW.	0.03	--	
COMPLIANCE	0.40	--	
TOTAL STROKE	11.28	10.90	

POTENTIAL MODIFICATIONS TO ACTUATOR

- REQUIRED ACTUATOR FORCE = $\frac{\text{MAX TORQUE}}{\text{MIN MA}} = \frac{(4.11) (10^6)}{61.47} = 66,632 \text{ LB}$
PERCENT OF INCREASE IN SSME ACTUATOR FORCE CAPABILITY REQUIRED = $\left(\frac{66,632 - 63,093}{63,093} \right) (100) = 5.6\%$
- "INCREASE PRESSURE" MODIFICATION TO ACTUATOR
SSME NOMINAL SUPPLY PRESSURE MUST INCREASE FROM 3,600 X 1.056 = 3,804 PSIG
- "INCREASE AREA" MODIFICATION TO ACTUATOR
NOMINAL PISTON AREA MUST INCREASE FROM 24.83 X 1.056 = 26.24 SQUARE INCHES
NOMINAL PISTON DIAMETER MUST INCREASE FROM 5.62 TO 5.78 INCHES

INSTALLATION WEIGHT PENALTY

- INCREASE IN COMPLIANCE RING WEIGHT FROM LAYOUT DESIGN NO. 2 = 385 LB

MAJOR PROBLEM AREAS

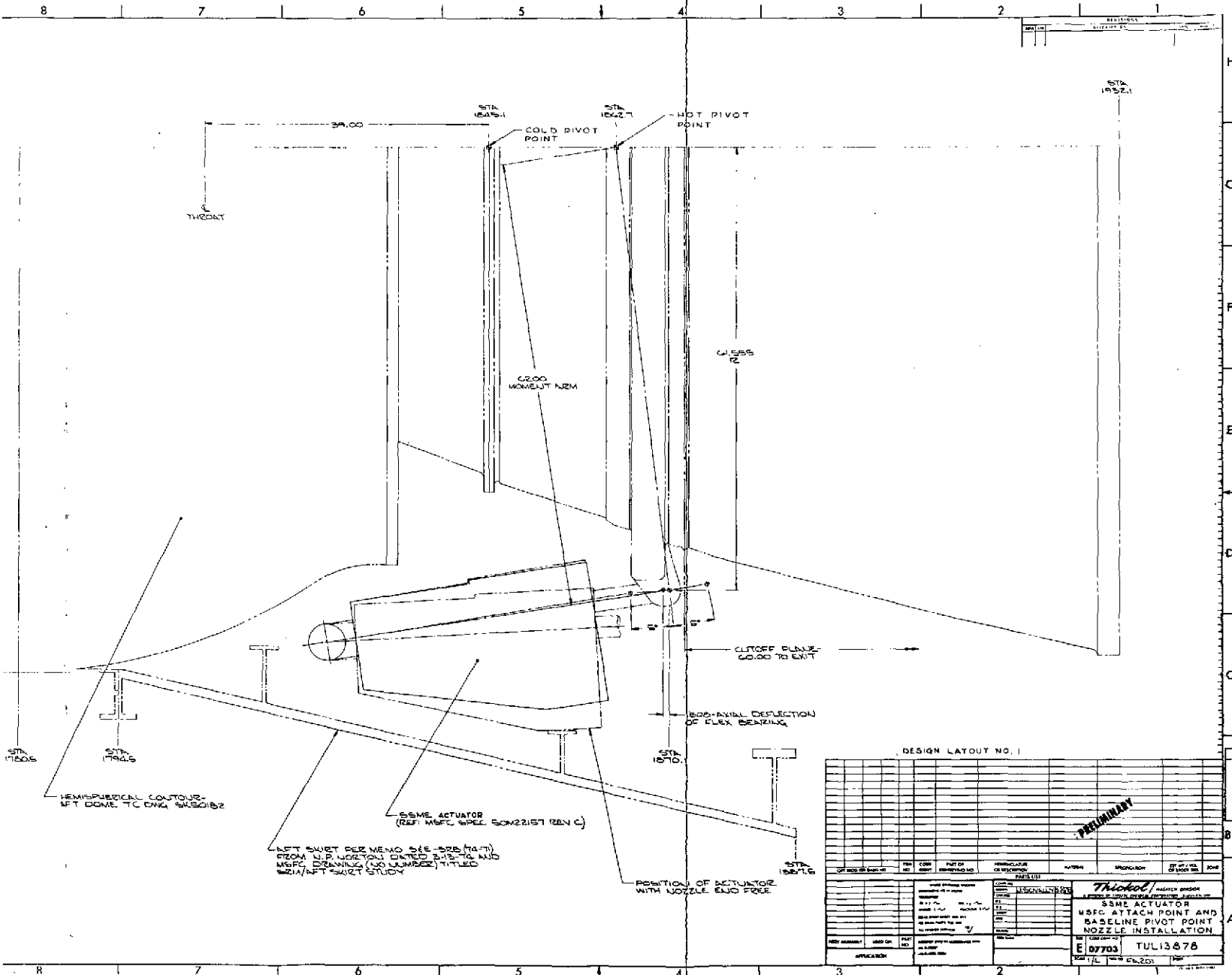
- NO ACTUATOR GROWTH CAPABILITY
- INSUFFICIENT STROKE TO MEET EXISTING REQUIREMENT

SPLASHDOWN CONSIDERATIONS

- ACCEPTABLE - WORST CASE STROKE = 0.88 IN.; WORST CASE VECTOR ANGLE = 1.3 DEGREES

TYPICAL TORQUE CALCULATION

$$T = (F) (MA) = \left[3,600 - \left(3,000 - \frac{48,208}{24.83} \right) \right] (24.83) (61.47) = (3.88) (10^6) \text{ IN-LB}$$



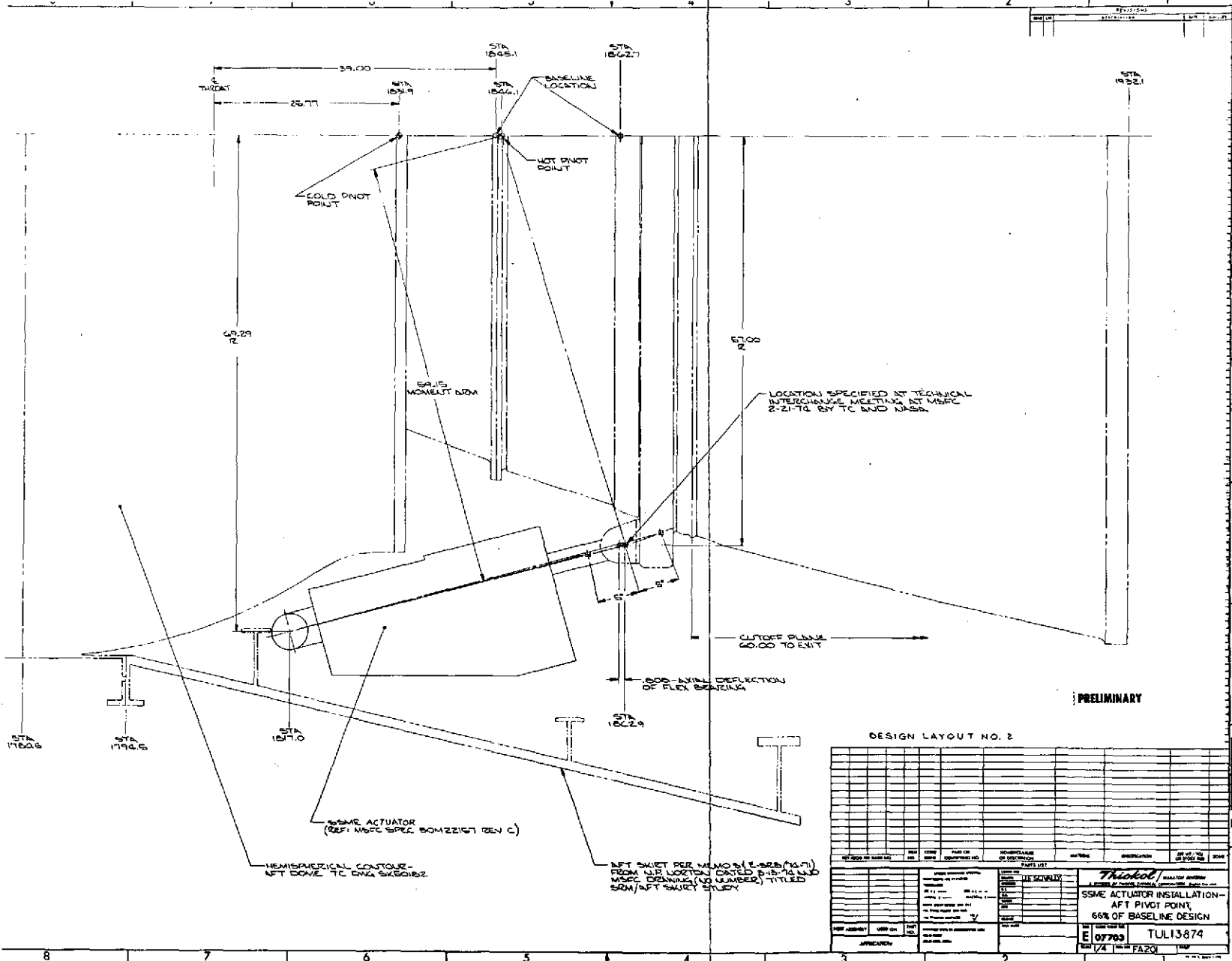
SSME ACTUATOR INSTALLATION STUDY
SRM CONFIGURATION (CONT)

REV B

LAYOUT NUMBER 2 (66% PIVOT POINT)
USE UNMODIFIED SSME ACTUATOR, MSFC SKIRT, AND TC CONFIGURATION 1 AND 2 NOZZLE

ACTUATOR AND NOZZLE DATA	REQUIRED BY DESIGN OR LAYOUT	SSME ACTUATOR CAPABILITIES BASED ON 3,600 PSI	COMMENTS
TORQUE (IN-LB)	(3.61) (10 ⁶)	ACTUATOR TORQUE = (FORCE) (MA) RETRACT TORQUE = (3.74) (10 ⁶) EXTEND TORQUE = (3.73) (10 ⁶)	ACCEPTABLE (ONLY 3.3% GROWTH CAPABILITY)
STROKE (IN.)			
EXTEND	5.17	5.275	
RETRACT	5.18	5.623	ACCEPTABLE
ΔP ALLOWANCE	0.05	--	
CROSSTALK ALLOW	0.03	--	
COMPLIANCE	0.40	--	(ONLY 0.6% GROWTH CAPABILITY)
TOTAL STROKE	10.83	10.90	

- POTENTIAL MODIFICATIONS TO ACTUATOR
 - REQUIRED ACTUATOR FORCE = $\frac{\text{MAX TORQUE}}{\text{MIN MA}} = \frac{(3.61) (10^6)}{59.09} = 61,093 \text{ LB}$ (ACTUATOR FORCE CAPABILITY = 63,093 LB)
PERCENT OF INCREASE IN SSME ACTUATOR FORCE CAPABILITY REQUIRED - NONE
- MAJOR PROBLEM AREAS
 - NO GROWTH ALLOWANCE FOR
 - BASE PRESSURE EFFECTS
 - EXTERNAL AERODYNAMIC LOAD
- PAD CHECKOUT (UNPRESSURIZED)
 - NOZZLE TORQUE (COLD) = (3.34) (10⁶) IN LB
 - ACTUATOR TORQUE CAPABILITY = (63,093) (61.89) = (3.91) (10⁶) IN LB
 - NOZZLE VECTOR CAPABILITY WITH SSME ACTUATOR FORCE = +5 DEGREES
 - NOZZLE VECTOR CAPABILITY WITH SSME ACTUATOR STROKE (11.39 IN. REQUIRED; 10.90 IN. AVAILABLE) = +4.8 DEGREES
- SPLASHDOWN CONSIDERATIONS
 - MARGINAL (WITH FORCE LIMITED TO 110,000 LB)
 - WORST CASE STROKE = 5.2 IN.
 - WORST CASE VECTOR ANGLE = 3.2 DEGREES



74183

was found to be 10.38 inches and the actuator only capable of 10.90 inches. These very marginal functional requirements, plus being marginal at the maximum splash-down load (110,000 pounds) could cause a serious lack of growth capability.

3. TUL 13879-SSME Actuator (Modified) and Baseline Pivot Point Nozzle Installation

This layout is similar to the others except that the SSME actuator was modified to meet the nozzle functional requirements plus provide for adequate growth. It was found that by repositioning the actuator to yield a 55.3 inch lever arm, the stroke reduced to 10.07 inches, therefore not requiring a stroke change to the SSME unit (10.90 inches). However, the effective piston area would have to be increased 15 percent to satisfy the nozzle torque requirements. In effect these new sizing parameters are similar to those of the newer SRB actuator, therefore any advantage in the SSME actuator would be lost during this extensive rework.

4. TUL 13918A-SRB Actuator (Modified) and Configuration 1-1A Nozzle Installation

The Actuator Kinematics for the 1-1A configuration is shown in Layout Drawing TUL 13918A. This layout was approached similar to the other actuator installation except that Thiokol defined the SRB actuator requirements. Starting with a maximum nozzle torque of 4.424×10^6 in. lb (a preliminary estimate for the 4.226×10^6 in. lb now reported) the SRB actuator requirements were defined as follows:

- a. Actuator splash down load 258,000 lb max
- b. Actuator stall force load 102,400 lb
- c. Actuator total stroke (satisfying all conditions)
14.18 in.
- d. Nominal moment arm (hot) 63.2 in.

The original SRB TVC Servoactuator had a 173,000 stall load capability and a total travel of 11.50 inches. Thiokol adjusted the actuator envelope in accordance with the new kinematic requirements.

To satisfy the $\pm 5^\circ$ requirement during ground checkout and all flight conditions the actuator stroke requirements must consider the differences in null lengths

SSME ACTUATOR INSTALLATION STUDY

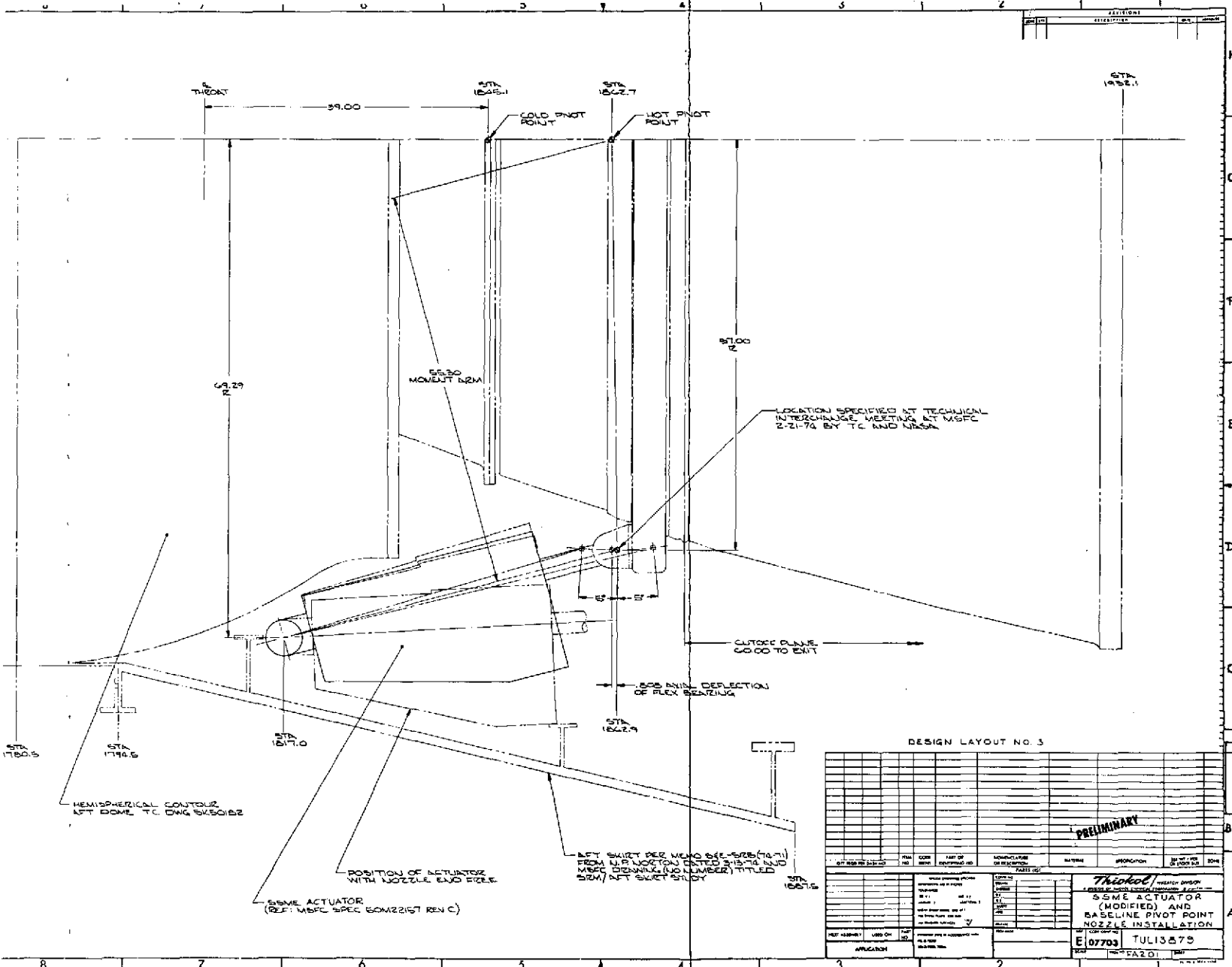
SRM CONFIGURATION (CONT)

REV B

LAYOUT NUMBER 3 (BASELINE PIVOT POINT)
USE MODIFIED SSME ACTUATOR, MSFC SKIRT, AND TC CONFIGURATION 1 AND 2 NOZZLE

ACUTATOR AND NOZZLE DATA	REQUIRED BY DESIGN OR LAYOUT	SSME ACTUATOR CAPABILITIES BASED ON 3,600 PSJ	COMMENTS
TORQUE (IN-LB)	(4.11) (10 ⁶)	ACTUATOR TORQUE = (FORCE) (MA) RETRACT TORQUE = (3.34) (10 ⁶) EXTEND TORQUE = (3.56) (10 ⁶)	NOT ACCEPTABLE
STROKE (IN.)			ACCEPTABLE
EXTEND	4.87	5.275	
RETRACT	4.72	5.623	
ΔP ALLOWANCE	0.05	--	
CROSSTALK ALLOW.	0.03	--	
COMPLIANCE	0.40	--	
TOTAL STROKE	10.07	10.90	

- POTENTIAL MODIFICATIONS TO ACTUATOR
 - REQUIRED ACTUATOR FORCE = $\frac{\text{MAX TORQUE}}{\text{MIN MA}} = \frac{(4.11) (10^6)}{52.94} = 72,635 \text{ LB}$
PERCENT OF INCREASE IN SSME ACTUATOR FORCE CAPABILITY REQUIRED $\frac{72,635 - 63,036}{63,036} (100) = 15.1\%$
 - "INCREASE PRESSURE" MODIFICATION TO ACTUATOR
SSME NOMINAL SUPPLY PRESSURE MUST INCREASE FROM 3,600 X 1.151 = 4,144 PSIG
 - "INCREASE AREA" MODIFICATION TO ACTUATOR
NOMINAL PISTON AREA MUST INCREASE FROM 24.83 X 1.151 = 28.58 SQUARE INCHES
NOMINAL PISTON DIAMETER MUST INCREASE FROM 5.62 TO 6.03 INCHES
- MAJOR PROBLEM AREAS
 - MUST MODIFY SSME OR CREATE NEW ACTUATOR
- SPLASHDOWN CONSIDERATIONS-ACCEPTABLE
 - WORST CASE STROKE = 0.88 IN.
 - WORST CASE VECTOR ANGLE = 1.3 DEGREES



Page intentionally left blank

resulting primarily from the flexible bearing pivot movement and the bearing axial deflections due to SRM internal motor pressure. This results in a stroke increase of 2.41 inches.

Included in this study as in the previous studies were allowances for cross-talk, compliance, and aft polar boss axial movement.

3.3.4 Nozzle Field Joint

The interface between the SRM and the aft skirt may make it necessary to include a field joint in the SRM nozzle. Early in this contract, data were received (NASA Drawing 10A00306) which showed that the clear opening in the aft skirt was approximately 124 inches in diameter. In mid-June, Thiokol received data on a revised aft skirt which has a clear diameter of 132.8 inches. The field joint location is shown on figures 3-31 and 3-32 with the details more clearly shown on figure 3-44. As shown, the upper half of the field joint is an integral part of the exit cone housing. The lower half of the field joint consists of a steel piece secured to the fiberglass structure of the exit cone. Incorporating the field joint into the exit cone housing is an efficient lightweight approach because the joint is at a small diameter. Addition of the field splice as shown adds approximately 300 pounds to the SRM nozzle.

Under consideration at the present time is the possibility of moving the field joint just aft of the compliance ring and incorporating the field joint with the nozzle cutoff device. This concept has not been definitized to the point that weight data are available.

The joint as shown is a technically feasible approach that has the advantage of being incorporated in the exit cone/main structure. If other considerations make it desirable to move the field joint to incorporate it with the compliance ring, it is felt that a feasible concept can be identified. It is expected, however, that because of the larger diameter, the field joint weight penalty would increase. Evaluated from a nozzle manufacturing point of view, the addition of a field joint presents no significant problems.

DESIGN CONSIDERATIONS

- MAX SKIRT CLEARANCE \approx 124 IN. DIA (DWG 10A00306)
- COMPLIANCE RING $>$ 124 IN. DIA
- FIELD JOINT MUST BE ABOVE COMPLIANCE RING
- MINIMUM WEIGHT DESIGN OCCURS IF FIELD JOINT IS AT AFT END OF METAL STRUCTURE

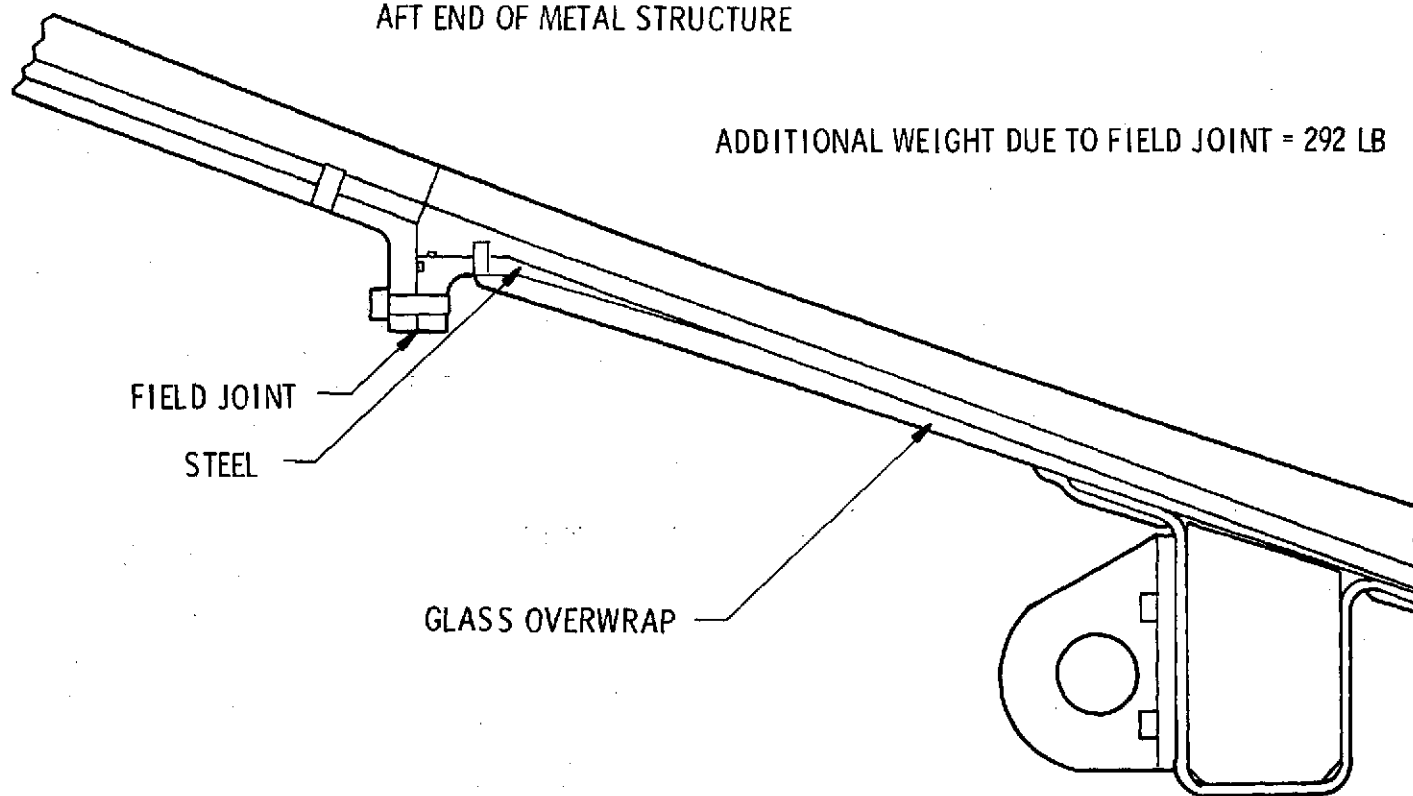


Figure 3-44. Field Joint

3.3.5 Nozzle Cutoff

The water impact loads on the nozzle and actuators can be significantly reduced if the exit cone is cut off prior to water impact and, in fact, the loads data used in the nozzle analyses have assumed that the nozzle cone is off at water impact. Figures 3-31 and 3-32 show a nozzle cutoff device located just aft of the nozzle compliance ring. This location permits maximum amount of nozzle exit cone to be severed and still allows the actuators to remain attached to the nozzle at water impact. The nozzle cutoff device is shown in more detail on figure 3-45.

Data did not exist in industry to define the size of a linear shaped charge (LSC) that would be required to sever the glass/carbon phenolic exit cone. To obtain sizing data to design the nozzle cutoff device, Thiokol conducted tests on subscale samples of glass structure over a carbon phenolic liner.

From these tests, the penetration and cutoff capability of a linear shaped charge as a function of charge size was obtained. These data are presented on figure 3-46. The figure also presents similar data for penetration and cutoff in steel. From figure 3-46, it is apparent that a 300 grain/foot charge will cut through the 1.6 inch thick exit cone wall which remains after motor firing. To provide a safety factor, a tentative charge size selection of 500 ± 100 grains/foot has been selected.

Alternate concepts to reducing the water impact loads on the actuator system are still under consideration. At the present time the two alternates which appear to be the most feasible would both require moving the nozzle field joint to a location just aft of the nozzle compliance ring and incorporating the field joint as part of the compliance ring. The first alternate configuration would use a few small bolts in the exit cone joint. The joint and bolts would be sized so that the bolts would fail and allow the exit cone to shear off before a load sufficient to damage the actuator would be seen. The second alternate configuration uses a Marman clamp on the nozzle cutoff joint to resist longitudinal loads. The joint would be designed with a shear lip or shear pins to react transverse loads. The philosophy is that if the Marman clamp should be inadvertently jettisoned during flight, the axial thrust

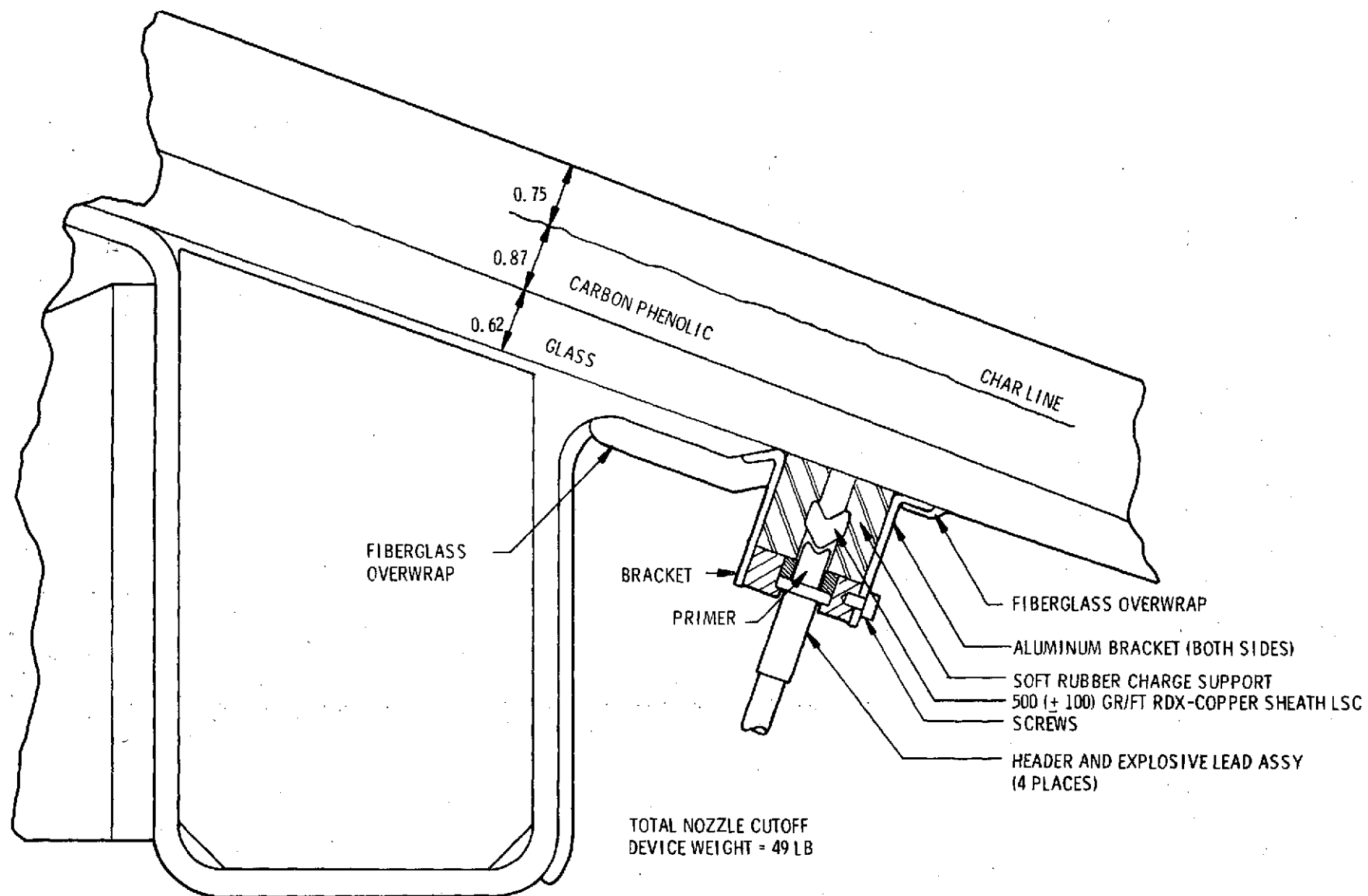


Figure 3-45. Nozzle Cutoff Device

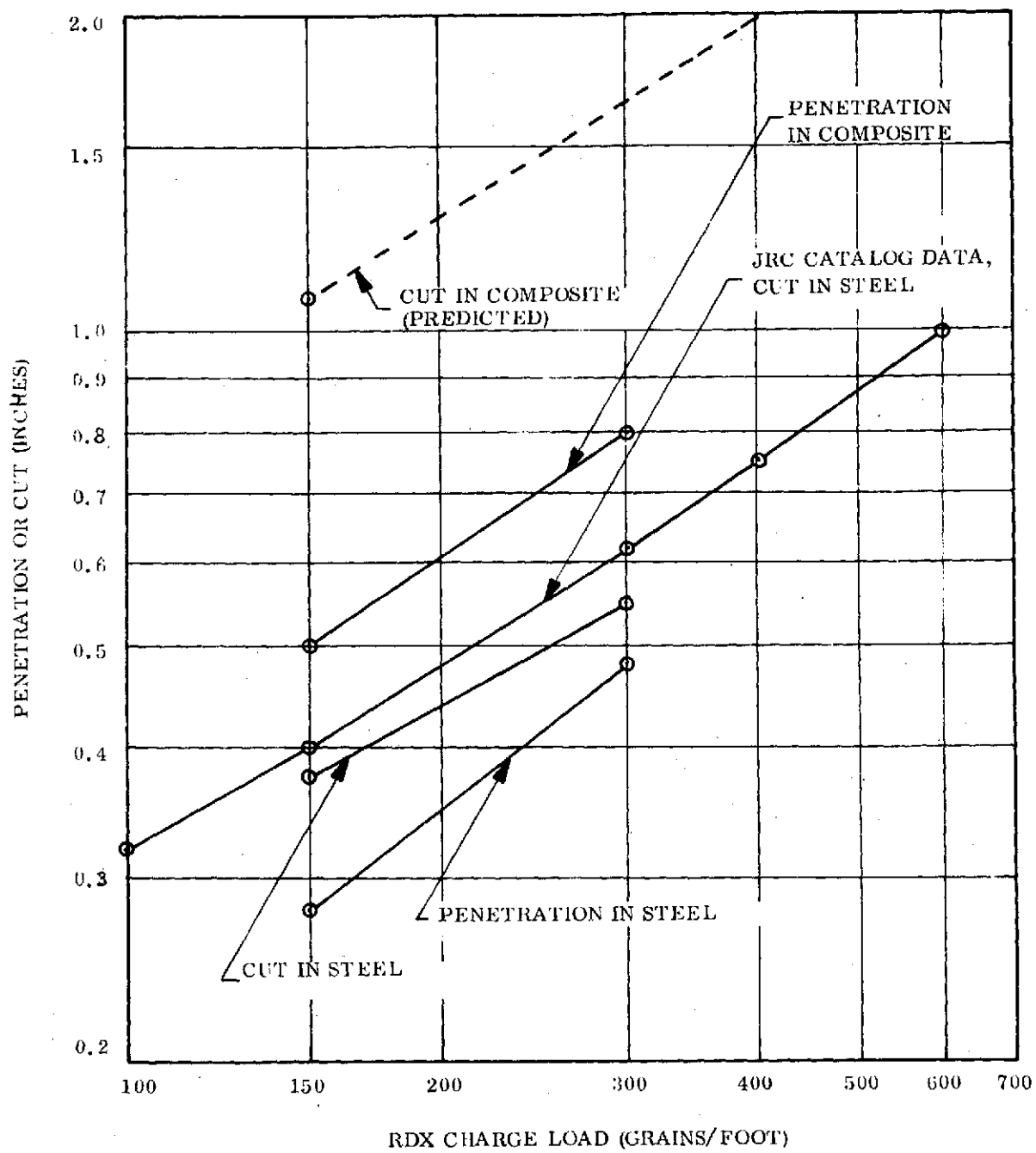


Figure 3-46. Penetration and Cut by RDX Core Copper Sheath LSC

forces in the nozzle would be in a direction to hold the exit cone joint closed, the shear lip or pins would resist transverse loads and the nozzle would hold together.

After motor burnout and prior to water impact, the Marman clamp would be removed by ordnance devices. With the Marman clamp removed and without the thrust forces in the exit cone, the aft portion of the exit cone would fall free and a shortened nozzle would be achieved at water impact.

CONCLUSIONS

It is recognized that further SRB configuration changes will require a continuing update and re-evaluation of the nozzle design. During the contract a considerable number of interim designs have been made, but no significant difficulties have been identified, thus, it is apparent that the nozzle design can be adapted to the motor, aft skirt, actuator, and launch pad interfaces.